

# 6

## Fatigue Failure Resulting from Variable Loading

### Chapter Outline

<b>6-1</b>	Introduction to Fatigue in Metals	<b>258</b>
<b>6-2</b>	Approach to Fatigue Failure in Analysis and Design	<b>264</b>
<b>6-3</b>	Fatigue-Life Methods	<b>265</b>
<b>6-4</b>	The Stress-Life Method	<b>265</b>
<b>6-5</b>	The Strain-Life Method	<b>268</b>
<b>6-6</b>	The Linear-Elastic Fracture Mechanics Method	<b>270</b>
<b>6-7</b>	The Endurance Limit	<b>274</b>
<b>6-8</b>	Fatigue Strength	<b>275</b>
<b>6-9</b>	Endurance Limit Modifying Factors	<b>278</b>
<b>6-10</b>	Stress Concentration and Notch Sensitivity	<b>287</b>
<b>6-11</b>	Characterizing Fluctuating Stresses	<b>292</b>
<b>6-12</b>	Fatigue Failure Criteria for Fluctuating Stress	<b>295</b>
<b>6-13</b>	Torsional Fatigue Strength under Fluctuating Stresses	<b>309</b>
<b>6-14</b>	Combinations of Loading Modes	<b>309</b>
<b>6-15</b>	Varying, Fluctuating Stresses; Cumulative Fatigue Damage	<b>313</b>
<b>6-16</b>	Surface Fatigue Strength	<b>319</b>
<b>6-17</b>	Stochastic Analysis	<b>322</b>
<b>6-18</b>	Road Maps and Important Design Equations for the Stress-Life Method	<b>336</b>

In Chap. 5 we considered the analysis and design of parts subjected to static loading. The behavior of machine parts is entirely different when they are subjected to time-varying loading. In this chapter we shall examine how parts fail under variable loading and how to proportion them to successfully resist such conditions.

## 6-1 Introduction to Fatigue in Metals

In most testing of those properties of materials that relate to the stress-strain diagram, the load is applied gradually, to give sufficient time for the strain to fully develop. Furthermore, the specimen is tested to destruction, and so the stresses are applied only once. Testing of this kind is applicable, to what are known as *static conditions*; such conditions closely approximate the actual conditions to which many structural and machine members are subjected.

The condition frequently arises, however, in which the stresses vary with time or they fluctuate between different levels. For example, a particular fiber on the surface of a rotating shaft subjected to the action of bending loads undergoes both tension and compression for each revolution of the shaft. If the shaft is part of an electric motor rotating at 1725 rev/min, the fiber is stressed in tension and compression 1725 times each minute. If, in addition, the shaft is also axially loaded (as it would be, for example, by a helical or worm gear), an axial component of stress is superposed upon the bending component. In this case, some stress is always present in any one fiber, but now the *level* of stress is fluctuating. These and other kinds of loading occurring in machine members produce stresses that are called *variable, repeated, alternating, or fluctuating stresses*.

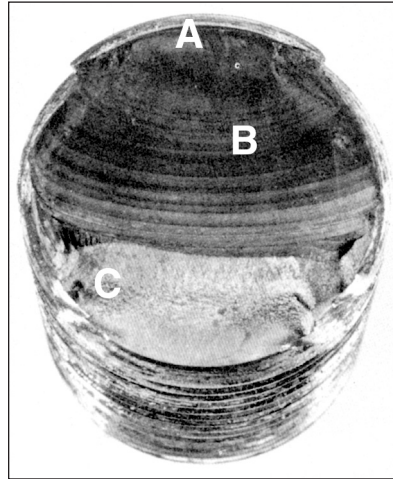
Often, machine members are found to have failed under the action of repeated or fluctuating stresses; yet the most careful analysis reveals that the actual maximum stresses were well below the ultimate strength of the material, and quite frequently even below the yield strength. The most distinguishing characteristic of these failures is that the stresses have been repeated a very large number of times. Hence the failure is called a *fatigue failure*.

When machine parts fail statically, they usually develop a very large deflection, because the stress has exceeded the yield strength, and the part is replaced before fracture actually occurs. Thus many static failures give visible warning in advance. But a fatigue failure gives no warning! It is sudden and total, and hence dangerous. It is relatively simple to design against a static failure, because our knowledge is comprehensive. Fatigue is a much more complicated phenomenon, only partially understood, and the engineer seeking competence must acquire as much knowledge of the subject as possible.

A fatigue failure has an appearance similar to a brittle fracture, as the fracture surfaces are flat and perpendicular to the stress axis with the absence of necking. The fracture features of a fatigue failure, however, are quite different from a static brittle fracture arising from three stages of development. *Stage I* is the initiation of one or more microcracks due to cyclic plastic deformation followed by crystallographic propagation extending from two to five grains about the origin. Stage I cracks are not normally discernible to the naked eye. *Stage II* progresses from microcracks to macrocracks forming parallel plateau-like fracture surfaces separated by longitudinal ridges. The plateaus are generally smooth and normal to the direction of maximum tensile stress. These surfaces can be wavy dark and light bands referred to as *beach marks* or *clamshell marks*, as seen in Fig. 6-1. During cyclic loading, these cracked surfaces open and close, rubbing together, and the beach mark appearance depends on the changes in the level or frequency of loading and the corrosive nature of the environment. *Stage III* occurs during the final stress cycle when the remaining material cannot support the loads, resulting in

**Figure 6-1**

Fatigue failure of a bolt due to repeated unidirectional bending. The failure started at the thread root at A, propagated across most of the cross section shown by the beach marks at B, before final fast fracture at C. (From ASM Handbook, Vol. 12: Fractography, ASM International, Materials Park, OH 44073-0002, fig 50, p. 120. Reprinted by permission of ASM International®, [www.asminternational.org](http://www.asminternational.org).)



a sudden, fast fracture. A stage III fracture can be brittle, ductile, or a combination of both. Quite often the beach marks, if they exist, and possible patterns in the stage III fracture called *chevron lines*, point toward the origins of the initial cracks.

There is a good deal to be learned from the fracture patterns of a fatigue failure.<sup>1</sup> Figure 6-2 shows representations of failure surfaces of various part geometries under differing load conditions and levels of stress concentration. Note that, in the case of rotational bending, even the direction of rotation influences the failure pattern.

Fatigue failure is due to crack formation and propagation. A fatigue crack will typically initiate at a discontinuity in the material where the cyclic stress is a maximum. Discontinuities can arise because of:

- Design of rapid changes in cross section, keyways, holes, etc. where stress concentrations occur as discussed in Secs. 3-13 and 5-2.
- Elements that roll and/or slide against each other (bearings, gears, cams, etc.) under high contact pressure, developing concentrated subsurface contact stresses (Sec. 3-19) that can cause surface pitting or spalling after many cycles of the load.
- Carelessness in locations of stamp marks, tool marks, scratches, and burrs; poor joint design; improper assembly; and other fabrication faults.
- Composition of the material itself as processed by rolling, forging, casting, extrusion, drawing, heat treatment, etc. Microscopic and submicroscopic surface and subsurface discontinuities arise, such as inclusions of foreign material, alloy segregation, voids, hard precipitated particles, and crystal discontinuities.

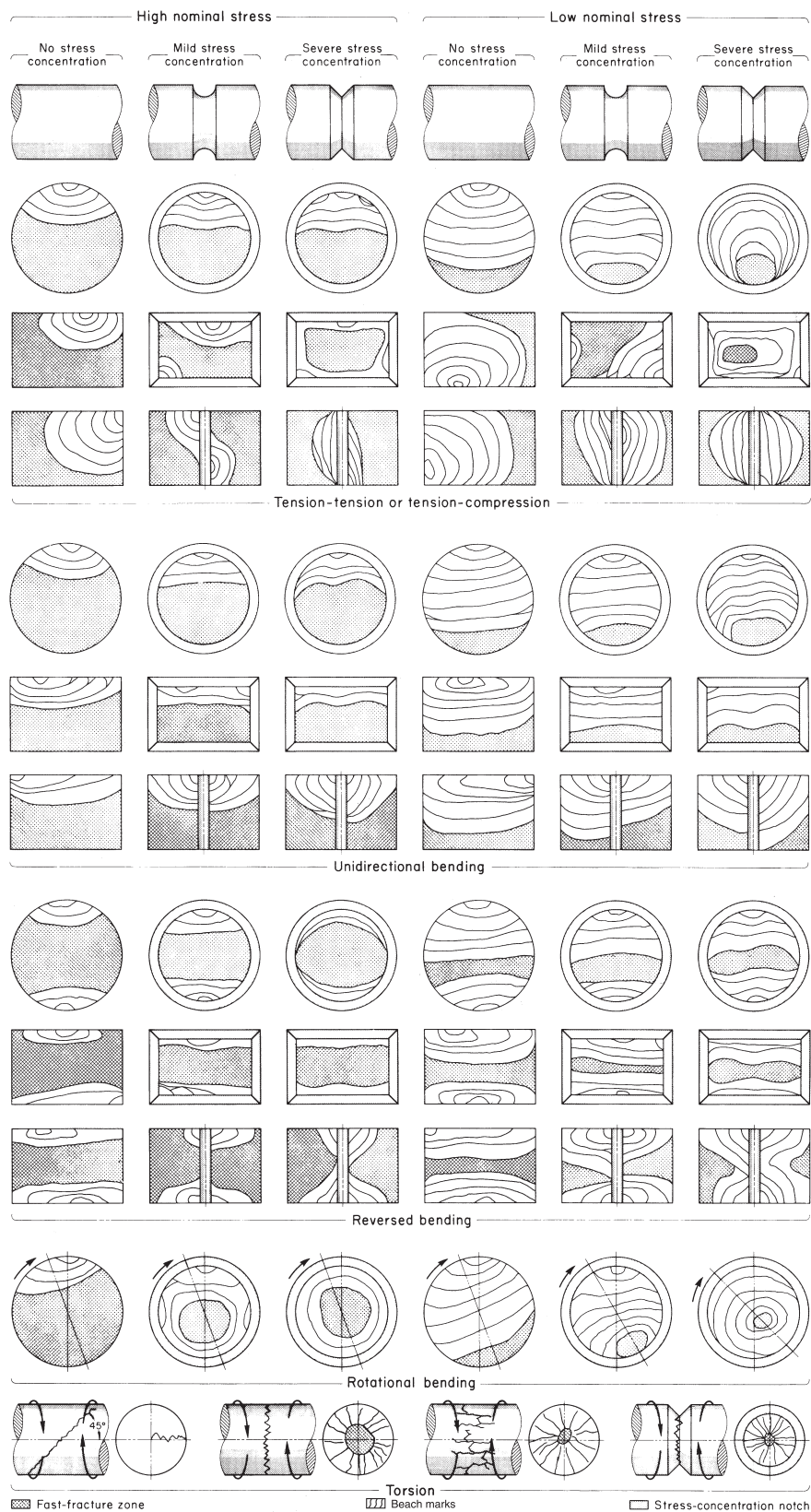
Various conditions that can accelerate crack initiation include residual tensile stresses, elevated temperatures, temperature cycling, a corrosive environment, and high-frequency cycling.

The rate and direction of fatigue crack propagation is primarily controlled by localized stresses and by the structure of the material at the crack. However, as with crack formation, other factors may exert a significant influence, such as environment, temperature, and frequency. As stated earlier, cracks will grow along planes normal to the

<sup>1</sup>See the ASM Handbook, *Fractography*, ASM International, Metals Park, Ohio, vol. 12, 9th ed., 1987.

**Figure 6-2**

Schematics of fatigue fracture surfaces produced in smooth and notched components with round and rectangular cross sections under various loading conditions and nominal stress levels. (From *ASM Handbook, Vol. 11: Failure Analysis and Prevention*, ASM International, Materials Park, OH 44073-0002, fig 18, p. 111. Reprinted by permission of ASM International®, [www.asminternational.org](http://www.asminternational.org).)





maximum tensile stresses. The crack growth process can be explained by fracture mechanics (see Sec. 6–6).

A major reference source in the study of fatigue failure is the 21-volume *ASM Metals Handbook*. Figures 6–1 to 6–8, reproduced with permission from ASM International, are but a minuscule sample of examples of fatigue failures for a great variety of conditions included in the handbook. Comparing Fig. 6–3 with Fig. 6–2, we see that failure occurred by rotating bending stresses, with the direction of rotation being clockwise with respect to the view and with a mild stress concentration and low nominal stress.

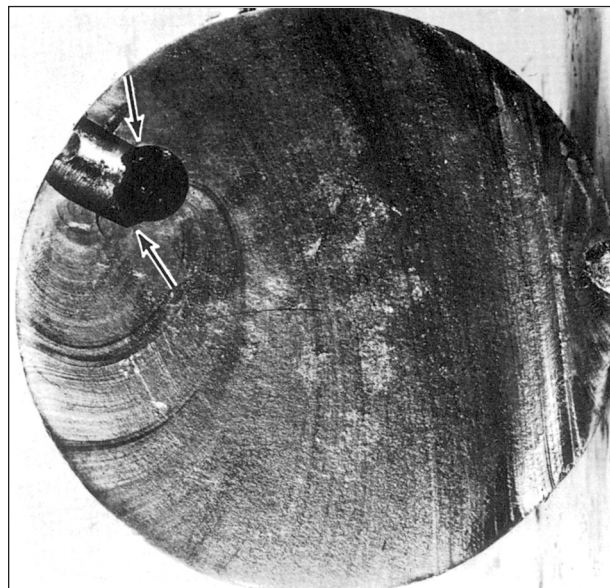
### Figure 6–3

Fatigue fracture of an AISI 4320 drive shaft. The fatigue failure initiated at the end of the keyway at points B and progressed to final rupture at C. The final rupture zone is small, indicating that loads were low. (From ASM Handbook, Vol. 11: Failure Analysis and Prevention, ASM International, Materials Park, OH 44073-0002, fig 18, p. 111. Reprinted by permission of ASM International®, [www.asminternational.org](http://www.asminternational.org).)



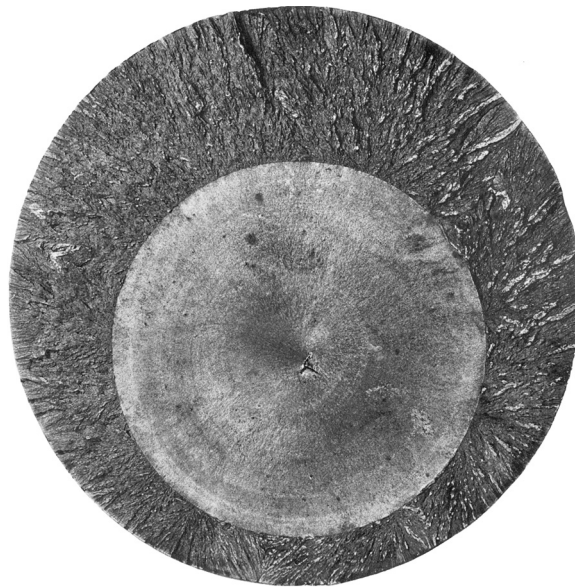
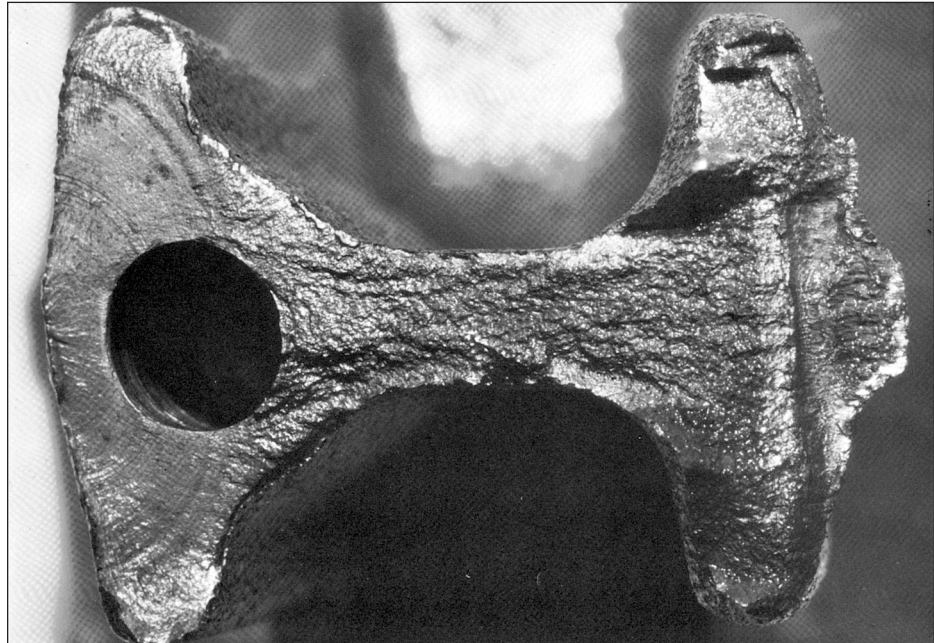
### Figure 6–4

Fatigue fracture surface of an AISI 8640 pin. Sharp corners of the mismatched grease holes provided stress concentrations that initiated two fatigue cracks indicated by the arrows. (From ASM Handbook, Vol. 12: Fractography, ASM International, Materials Park, OH 44073-0002, fig 520, p. 331. Reprinted by permission of ASM International®, [www.asminternational.org](http://www.asminternational.org).)



**Figure 6-5**

Fatigue fracture surface of a forged connecting rod of AISI 8640 steel. The fatigue crack origin is at the left edge, at the flash line of the forging, but no unusual roughness of the flash trim was indicated. The fatigue crack progressed halfway around the oil hole at the left, indicated by the beach marks, before final fracture occurred. Note the pronounced shear lip in the final fracture at the right edge. (From ASM Handbook, Vol. 12: Fractography, ASM International, Materials Park, OH 44073-0002, fig 523, p. 332. Reprinted by permission of ASM International®, [www.asminternational.org](http://www.asminternational.org).)

**Figure 6-6**

Fatigue fracture surface of a 200-mm (8-in) diameter piston rod of an alloy steel steam hammer used for forging. This is an example of a fatigue fracture caused by pure tension where surface stress concentrations are absent and a crack may initiate anywhere in the cross section. In this instance, the initial crack formed at a forging flake slightly below center, grew outward symmetrically, and ultimately produced a brittle fracture without warning. (From ASM Handbook, Vol. 12: Fractography, ASM International, Materials Park, OH 44073-0002, fig 570, p. 342. Reprinted by permission of ASM International®, [www.asminternational.org](http://www.asminternational.org).)



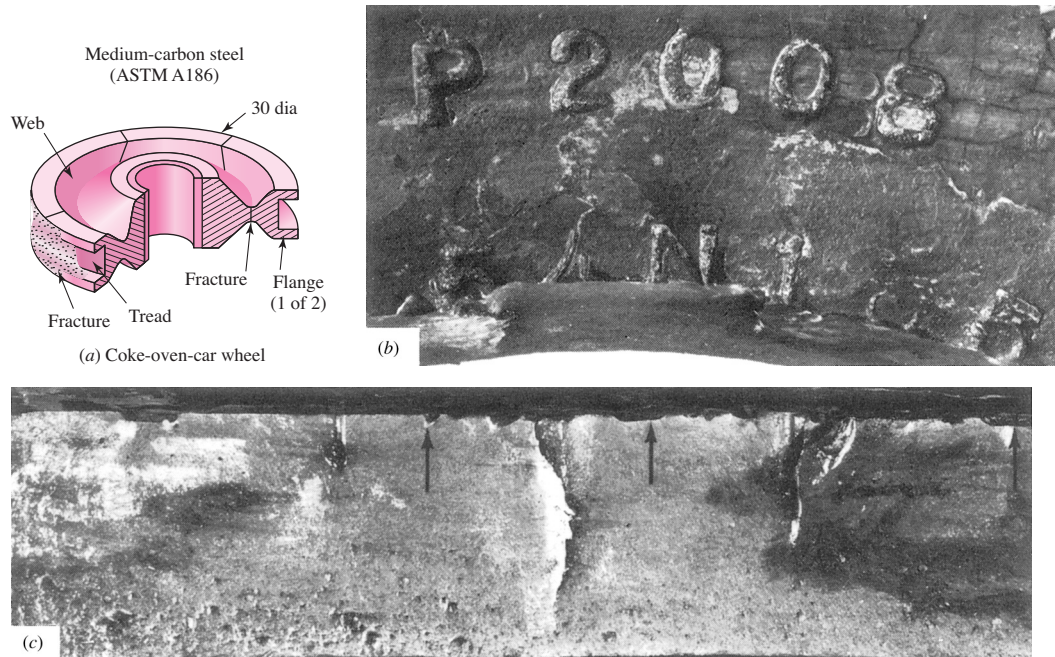
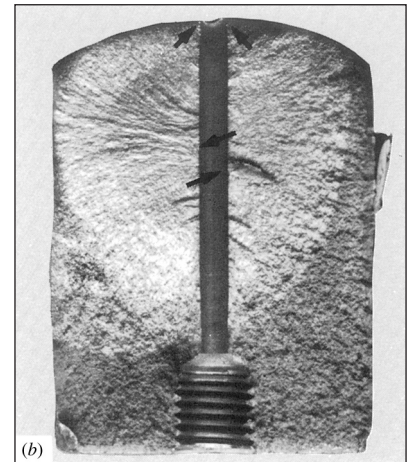
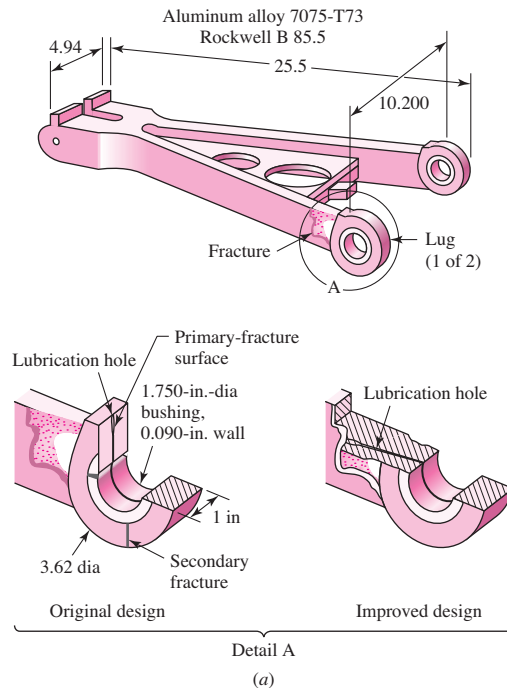


**Figure 6-7**

Fatigue failure of an ASTM A186 steel double-flange trailer wheel caused by stamp marks. (a) Coke-oven car wheel showing position of stamp marks and fractures in the rib and web. (b) Stamp mark showing heavy impression and fracture extending along the base of the lower row of numbers. (c) Notches, indicated by arrows, created from the heavily indented stamp marks from which cracks initiated along the top at the fracture surface. (From ASM Handbook, Vol. 11: Failure Analysis and Prevention, ASM International, Materials Park, OH 44073-0002, fig 51, p. 130. Reprinted by permission of ASM International®, [www.asmtinternational.org](http://www.asmtinternational.org).)

**Figure 6-8**

Aluminum alloy 7075-T73 landing-gear torque-arm assembly redesign to eliminate fatigue fracture at a lubrication hole. (a) Arm configuration, original and improved design (dimensions given in inches). (b) Fracture surface where arrows indicate multiple crack origins. (From ASM Handbook, Vol. 11: Failure Analysis and Prevention, ASM International, Materials Park, OH 44073-0002, fig 23, p. 114. Reprinted by permission of ASM International®, [www.asmtinternational.org](http://www.asmtinternational.org).)



## 6-2 Approach to Fatigue Failure in Analysis and Design

As noted in the previous section, there are a great many factors to be considered, even for very simple load cases. The methods of fatigue failure analysis represent a combination of engineering and science. Often science fails to provide the complete answers that are needed. But the airplane must still be made to fly—safely. And the automobile must be manufactured with a reliability that will ensure a long and troublefree life and at the same time produce profits for the stockholders of the industry. Thus, while science has not yet completely explained the complete mechanism of fatigue, the engineer must still design things that will not fail. In a sense this is a classic example of the true meaning of engineering as contrasted with science. Engineers use science to solve their problems if the science is available. But available or not, the problem must be solved, and whatever form the solution takes under these conditions is called *engineering*.

In this chapter, we will take a structured approach in the design against fatigue failure. As with static failure, we will attempt to relate to test results performed on simply loaded specimens. However, because of the complex nature of fatigue, there is much more to account for. From this point, we will proceed methodically, and in stages. In an attempt to provide some insight as to what follows in this chapter, a brief description of the remaining sections will be given here.

### Fatigue-Life Methods (Secs. 6-3 to 6-6)

Three major approaches used in design and analysis to predict when, if ever, a cyclically loaded machine component will fail in fatigue over a period of time are presented. The premises of each approach are quite different but each adds to our understanding of the mechanisms associated with fatigue. The application, advantages, and disadvantages of each method are indicated. Beyond Sec. 6-6, only one of the methods, the stress-life method, will be pursued for further design applications.

### Fatigue Strength and the Endurance Limit (Secs. 6-7 and 6-8)

The strength-life ( $S$ - $N$ ) diagram provides the fatigue strength  $S_f$  versus cycle life  $N$  of a material. The results are generated from tests using a simple loading of standard laboratory-controlled specimens. The loading often is that of sinusoidally reversing pure bending. The laboratory-controlled specimens are polished without geometric stress concentration at the region of minimum area.

For steel and iron, the  $S$ - $N$  diagram becomes horizontal at some point. The strength at this point is called the *endurance limit*  $S'_e$  and occurs somewhere between  $10^6$  and  $10^7$  cycles. The prime mark on  $S'_e$  refers to the endurance limit of the *controlled laboratory specimen*. For nonferrous materials that do not exhibit an endurance limit, a fatigue strength at a specific number of cycles,  $S'_f$ , may be given, where again, the prime denotes the fatigue strength of the laboratory-controlled specimen.

The strength data are based on many controlled conditions that will not be the same as that for an actual machine part. What follows are practices used to account for the differences between the loading and physical conditions of the specimen and the actual machine part.

### Endurance Limit Modifying Factors (Sec. 6-9)

Modifying factors are defined and used to account for differences between the specimen and the actual machine part with regard to surface conditions, size, loading, temperature, reliability, and miscellaneous factors. Loading is still considered to be simple and reversing.



### **Stress Concentration and Notch Sensitivity (Sec. 6-10)**

The actual part may have a geometric stress concentration by which the fatigue behavior depends on the static stress concentration factor and the component material's sensitivity to fatigue damage.

### **Fluctuating Stresses (Secs. 6-11 to 6-13)**

These sections account for simple stress states from fluctuating load conditions that are not purely sinusoidally reversing axial, bending, or torsional stresses.

### **Combinations of Loading Modes (Sec. 6-14)**

Here a procedure based on the distortion-energy theory is presented for analyzing combined fluctuating stress states, such as combined bending and torsion. Here it is assumed that the levels of the fluctuating stresses are in phase and not time varying.

### **Varying, Fluctuating Stresses; Cumulative Fatigue Damage (Sec. 6-15)**

The fluctuating stress levels on a machine part may be time varying. Methods are provided to assess the fatigue damage on a cumulative basis.

### **Remaining Sections**

The remaining three sections of the chapter pertain to the special topics of surface fatigue strength, stochastic analysis, and roadmaps with important equations.

## **6-3 Fatigue-Life Methods**

The three major fatigue life methods used in design and analysis are the *stress-life method*, the *strain-life method*, and the *linear-elastic fracture mechanics method*. These methods attempt to predict the life in number of cycles to failure,  $N$ , for a specific level of loading. Life of  $1 \leq N \leq 10^3$  cycles is generally classified as *low-cycle fatigue*, whereas *high-cycle fatigue* is considered to be  $N > 10^3$  cycles. The stress-life method, based on stress levels only, is the least accurate approach, especially for low-cycle applications. However, it is the most traditional method, since it is the easiest to implement for a wide range of design applications, has ample supporting data, and represents high-cycle applications adequately.

The strain-life method involves more detailed analysis of the plastic deformation at localized regions where the stresses and strains are considered for life estimates. This method is especially good for low-cycle fatigue applications. In applying this method, several idealizations must be compounded, and so some uncertainties will exist in the results. For this reason, it will be discussed only because of its value in adding to the understanding of the nature of fatigue.

The fracture mechanics method assumes a crack is already present and detected. It is then employed to predict crack growth with respect to stress intensity. It is most practical when applied to large structures in conjunction with computer codes and a periodic inspection program.

## **6-4 The Stress-Life Method**

To determine the strength of materials under the action of fatigue loads, specimens are subjected to repeated or varying forces of specified magnitudes while the cycles or stress reversals are counted to destruction. The most widely used fatigue-testing device

is the R. R. Moore high-speed rotating-beam machine. This machine subjects the specimen to pure bending (no transverse shear) by means of weights. The specimen, shown in Fig. 6-9, is very carefully machined and polished, with a final polishing in an axial direction to avoid circumferential scratches. Other fatigue-testing machines are available for applying fluctuating or reversed axial stresses, torsional stresses, or combined stresses to the test specimens.

To establish the fatigue strength of a material, quite a number of tests are necessary because of the statistical nature of fatigue. For the rotating-beam test, a constant bending load is applied, and the number of revolutions (stress reversals) of the beam required for failure is recorded. The first test is made at a stress that is somewhat under the ultimate strength of the material. The second test is made at a stress that is less than that used in the first. This process is continued, and the results are plotted as an  $S$ - $N$  diagram (Fig. 6-10). This chart may be plotted on semilog paper or on log-log paper. In the case of ferrous metals and alloys, the graph becomes horizontal after the material has been stressed for a certain number of cycles. Plotting on log paper emphasizes the bend in the curve, which might not be apparent if the results were plotted by using Cartesian coordinates.

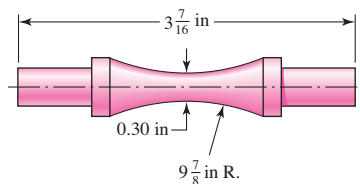


**Figure 6-9**

Testspecimen geometry for the R. R. Moore rotating-beam machine. The bending moment is uniform over the curved at the highest-stressed portion, a valid test of material, whereas a fracture elsewhere (not at the highest-stress level) is grounds for suspicion of material flaw.

**Figure 6-10**

An  $S$ - $N$  diagram plotted from the results of completely reversed axial fatigue tests. Material: UNS G41300 steel, normalized;  $S_{ut} = 116$  kpsi; maximum  $S_{ut} = 125$  kpsi. (Data from NACA Tech. Note 3866, December 1966.)

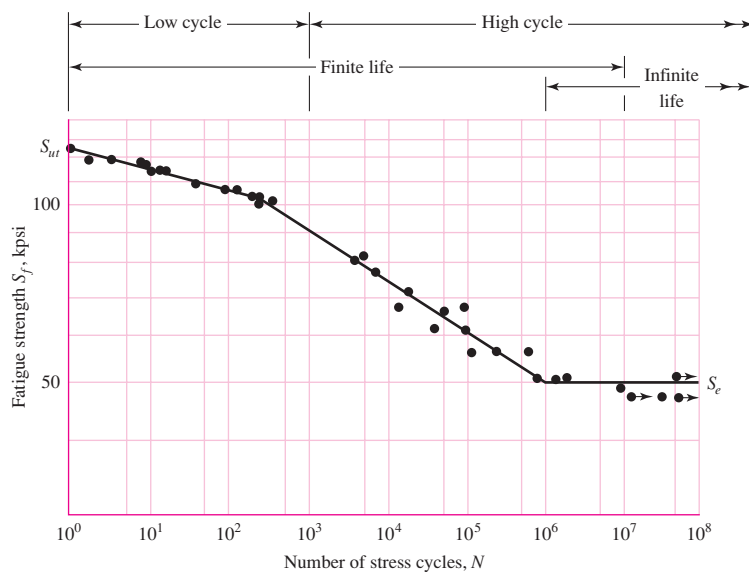
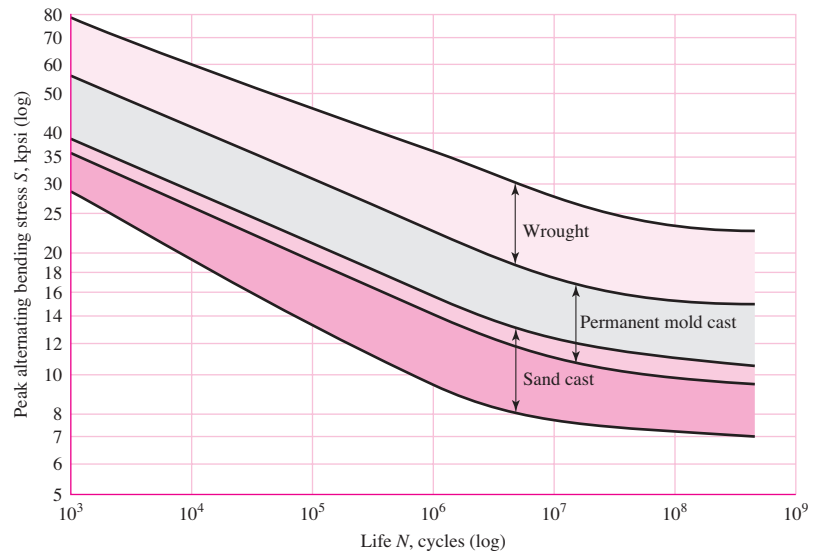


**Figure 6-11**

$S$ - $N$  bands for representative aluminum alloys, excluding wrought alloys with  $S_{ut} < 38$  kpsi. (From R. C. Juvinall, Engineering Considerations of Stress, Strain and Strength. Copyright © 1967 by The McGraw-Hill Companies, Inc. Reprinted by permission.)



The ordinate of the  $S$ - $N$  diagram is called the *fatigue strength*  $S_f$ ; a statement of this strength value must always be accompanied by a statement of the number of cycles  $N$  to which it corresponds.

Soon we shall learn that  $S$ - $N$  diagrams can be determined either for a test specimen or for an actual mechanical element. Even when the material of the test specimen and that of the mechanical element are identical, there will be significant differences between the diagrams for the two.

In the case of the steels, a knee occurs in the graph, and beyond this knee failure will not occur, no matter how great the number of cycles. The strength corresponding to the knee is called the *endurance limit*  $S_e$ , or the *fatigue limit*. The graph of Fig. 6-10 never does become horizontal for nonferrous metals and alloys, and hence these materials do not have an endurance limit. Figure 6-11 shows scatter bands indicating the  $S$ - $N$  curves for most common aluminum alloys excluding wrought alloys having a tensile strength below 38 kpsi. Since aluminum does not have an endurance limit, normally the fatigue strength  $S_f$  is reported at a specific number of cycles, normally  $N = 5(10^8)$  cycles of reversed stress (see Table A-24).

We note that a stress cycle ( $N = 1$ ) constitutes a single application and removal of a load and then another application and removal of the load in the opposite direction. Thus  $N = \frac{1}{2}$  means the load is applied once and then removed, which is the case with the simple tension test.

The body of knowledge available on fatigue failure from  $N = 1$  to  $N = 1000$  cycles is generally classified as *low-cycle fatigue*, as indicated in Fig. 6-10. *High-cycle fatigue*, then, is concerned with failure corresponding to stress cycles greater than  $10^3$  cycles.

We also distinguish a *finite-life region* and an *infinite-life region* in Fig. 6-10. The boundary between these regions cannot be clearly defined except for a specific material; but it lies somewhere between  $10^6$  and  $10^7$  cycles for steels, as shown in Fig. 6-10.

As noted previously, it is always good engineering practice to conduct a testing program on the materials to be employed in design and manufacture. This, in fact, is a requirement, not an option, in guarding against the possibility of a fatigue failure.



*Because of this necessity for testing, it would really be unnecessary for us to proceed any further in the study of fatigue failure except for one important reason: the desire to know why fatigue failures occur so that the most effective method or methods can be used to improve fatigue strength.* Thus our primary purpose in studying fatigue is to understand why failures occur so that we can guard against them in an optimum manner. For this reason, the analytical design approaches presented in this book, or in any other book, for that matter, do not yield absolutely precise results. The results should be taken as a guide, as something that indicates what is important and what is not important in designing against fatigue failure.

As stated earlier, the stress-life method is the least accurate approach especially for low-cycle applications. However, it is the most traditional method, with much published data available. It is the easiest to implement for a wide range of design applications and represents high-cycle applications adequately. For these reasons the stress-life method will be emphasized in subsequent sections of this chapter. However, care should be exercised when applying the method for low-cycle applications, as the method does not account for the true stress-strain behavior when localized yielding occurs.

## 6-5 The Strain-Life Method

The best approach yet advanced to explain the nature of fatigue failure is called by some the *strain-life* method. The approach can be used to estimate fatigue strengths, but when it is so used it is necessary to compound several idealizations, and so some uncertainties will exist in the results. For this reason, the method is presented here only because of its value in explaining the nature of fatigue.

A fatigue failure almost always begins at a local discontinuity such as a notch, crack, or other area of stress concentration. When the stress at the discontinuity exceeds the elastic limit, plastic strain occurs. If a fatigue fracture is to occur, there must exist cyclic plastic strains. Thus we shall need to investigate the behavior of materials subject to cyclic deformation.

In 1910, Bairstow verified by experiment Bauschinger's theory that the elastic limits of iron and steel can be changed, either up or down, by the cyclic variations of stress.<sup>2</sup> In general, the elastic limits of annealed steels are likely to increase when subjected to cycles of stress reversals, while cold-drawn steels exhibit a decreasing elastic limit.

R. W. Landgraf has investigated the low-cycle fatigue behavior of a large number of very high-strength steels, and during his research he made many cyclic stress-strain plots.<sup>3</sup> Figure 6-12 has been constructed to show the general appearance of these plots for the first few cycles of controlled cyclic strain. In this case the strength decreases with stress repetitions, as evidenced by the fact that the reversals occur at ever-smaller stress levels. As previously noted, other materials may be strengthened, instead, by cyclic stress reversals.

The SAE Fatigue Design and Evaluation Steering Committee released a report in 1975 in which the life in reversals to failure is related to the strain amplitude  $\Delta\epsilon/2$ .<sup>4</sup>

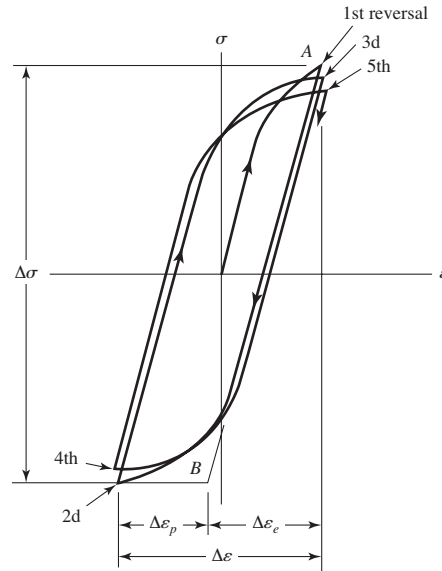
<sup>2</sup>L. Bairstow, "The Elastic Limits of Iron and Steel under Cyclic Variations of Stress," *Philosophical Transactions*, Series A, vol. 210, Royal Society of London, 1910, pp. 35-55.

<sup>3</sup>R. W. Landgraf, *Cyclic Deformation and Fatigue Behavior of Hardened Steels*, Report no. 320, Department of Theoretical and Applied Mechanics, University of Illinois, Urbana, 1968, pp. 84-90.

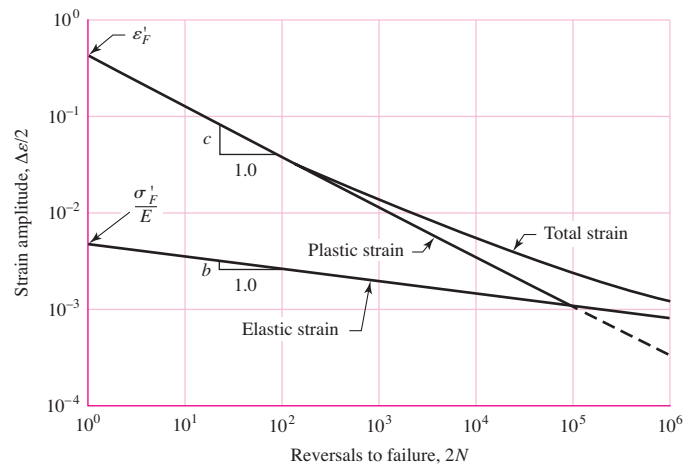
<sup>4</sup>*Technical Report on Fatigue Properties*, SAE J1099, 1975.

**Figure 6-12**

True stress–true strain hysteresis loops showing the first five stress reversals of a cyclic-softening material. The graph is slightly exaggerated for clarity. Note that the slope of the line AB is the modulus of elasticity  $E$ . The stress range is  $\Delta\sigma$ ,  $\Delta\epsilon_p$  is the plastic-strain range, and  $\Delta\epsilon_e$  is the elastic strain range. The total-strain range is  $\Delta\epsilon = \Delta\epsilon_p + \Delta\epsilon_e$ .

**Figure 6-13**

A log-log plot showing how the fatigue life is related to the true-strain amplitude for hotrolled SAE 1020 steel. (Reprinted with permission from SAE J1099\_200208 © 2002 SAE International.)



The report contains a plot of this relationship for SAE 1020 hot-rolled steel; the graph has been reproduced as Fig. 6-13. To explain the graph, we first define the following terms:

- *Fatigue ductility coefficient*  $\epsilon'_F$  is the true strain corresponding to fracture in one reversal (point A in Fig. 6-12). The plastic-strain line begins at this point in Fig. 6-13.
- *Fatigue strength coefficient*  $\sigma'_F$  is the true stress corresponding to fracture in one reversal (point A in Fig. 6-12). Note in Fig. 6-13 that the elastic-strain line begins at  $\sigma'_F/E$ .
- *Fatigue ductility exponent*  $c$  is the slope of the plastic-strain line in Fig. 6-13 and is the power to which the life  $2N$  must be raised to be proportional to the true plastic-strain amplitude. If the number of stress reversals is  $2N$ , then  $N$  is the number of cycles.

- *Fatigue strength exponent  $b$*  is the slope of the elastic-strain line, and is the power to which the life  $2N$  must be raised to be proportional to the true-stress amplitude.

Now, from Fig. 6–12, we see that the total strain is the sum of the elastic and plastic components. Therefore the total strain amplitude is half the total strain range

$$\frac{\Delta \varepsilon}{2} = \frac{\Delta \varepsilon_e}{2} + \frac{\Delta \varepsilon_p}{2} \quad (a)$$

The equation of the plastic-strain line in Fig. 6–13 is

$$\frac{\Delta \varepsilon_p}{2} = \varepsilon'_F (2N)^c \quad (6-1)$$

The equation of the elastic strain line is

$$\frac{\Delta \varepsilon_e}{2} = \frac{\sigma'_F}{E} (2N)^b \quad (6-2)$$

Therefore, from Eq. (a), we have for the total-strain amplitude

$$\frac{\Delta \varepsilon}{2} = \frac{\sigma'_F}{E} (2N)^b + \varepsilon'_F (2N)^c \quad (6-3)$$

which is the Manson-Coffin relationship between fatigue life and total strain.<sup>5</sup> Some values of the coefficients and exponents are listed in Table A–23. Many more are included in the SAE J1099 report.<sup>6</sup>

Though Eq. (6–3) is a perfectly legitimate equation for obtaining the fatigue life of a part when the strain and other cyclic characteristics are given, it appears to be of little use to the designer. The question of how to determine the total strain at the bottom of a notch or discontinuity has not been answered. There are no tables or charts of strain concentration factors in the literature. It is possible that strain concentration factors will become available in research literature very soon because of the increase in the use of finite-element analysis. Moreover, finite element analysis can of itself approximate the strains that will occur at all points in the subject structure.<sup>7</sup>

## 6–6 The Linear-Elastic Fracture Mechanics Method

The first phase of fatigue cracking is designated as stage I fatigue. Crystal slip that extends through several contiguous grains, inclusions, and surface imperfections is presumed to play a role. Since most of this is invisible to the observer, we just say that stage I involves several grains. The second phase, that of crack extension, is called stage II fatigue. The advance of the crack (that is, new crack area is created) does produce evidence that can be observed on micrographs from an electron microscope. The growth of

<sup>5</sup>J. F. Tavernelli and L. F. Coffin, Jr., “Experimental Support for Generalized Equation Predicting Low Cycle Fatigue,” and S. S. Manson, discussion, *Trans. ASME, J. Basic Eng.*, vol. 84, no. 4, pp. 533–537.

<sup>6</sup>See also, Landgraf, *Ibid.*

<sup>7</sup>For further discussion of the strain-life method see N. E. Dowling, *Mechanical Behavior of Materials*, 2nd ed., Prentice-Hall, Englewood Cliffs, N.J., 1999, Chap. 14.



the crack is orderly. Final fracture occurs during stage III fatigue, although fatigue is not involved. When the crack is sufficiently long that  $K_I = K_{Ic}$  for the stress amplitude involved, then  $K_{Ic}$  is the critical stress intensity for the undamaged metal, and there is sudden, catastrophic failure of the remaining cross section in tensile overload (see Sec. 5–12). Stage III fatigue is associated with rapid acceleration of crack growth then fracture.

### Crack Growth

Fatigue cracks nucleate and grow when stresses vary and there is some tension in each stress cycle. Consider the stress to be fluctuating between the limits of  $\sigma_{\min}$  and  $\sigma_{\max}$ , where the stress range is defined as  $\Delta\sigma = \sigma_{\max} - \sigma_{\min}$ . From Eq. (5–37) the stress intensity is given by  $K_I = \beta\sigma\sqrt{\pi a}$ . Thus, for  $\Delta\sigma$ , the stress intensity range per cycle is

$$\Delta K_I = \beta(\sigma_{\max} - \sigma_{\min})\sqrt{\pi a} = \beta\Delta\sigma\sqrt{\pi a} \quad (6-4)$$

To develop fatigue strength data, a number of specimens of the same material are tested at various levels of  $\Delta\sigma$ . Cracks nucleate at or very near a free surface or large discontinuity. Assuming an initial crack length of  $a_i$ , crack growth as a function of the number of stress cycles  $N$  will depend on  $\Delta\sigma$ , that is,  $\Delta K_I$ . For  $\Delta K_I$  below some threshold value  $(\Delta K_I)_{th}$  a crack will not grow. Figure 6–14 represents the crack length  $a$  as a function of  $N$  for three stress levels  $(\Delta\sigma)_3 > (\Delta\sigma)_2 > (\Delta\sigma)_1$ , where  $(\Delta K_I)_3 > (\Delta K_I)_2 > (\Delta K_I)_1$ . Notice the effect of the higher stress range in Fig. 6–14 in the production of longer cracks at a particular cycle count.

When the rate of crack growth per cycle,  $da/dN$  in Fig. 6–14, is plotted as shown in Fig. 6–15, the data from all three stress range levels superpose to give a sigmoidal curve. The three stages of crack development are observable, and the stage II data are linear on log-log coordinates, within the domain of linear elastic fracture mechanics (LEFM) validity. A group of similar curves can be generated by changing the stress ratio  $R = \sigma_{\min}/\sigma_{\max}$  of the experiment.

Here we present a simplified procedure for estimating the remaining life of a cyclically stressed part after discovery of a crack. This requires the assumption that plane strain

**Figure 6–14**

The increase in crack length  $a$  from an initial length of  $a_i$  as a function of cycle count for three stress ranges,  $(\Delta\sigma)_3 > (\Delta\sigma)_2 > (\Delta\sigma)_1$ .

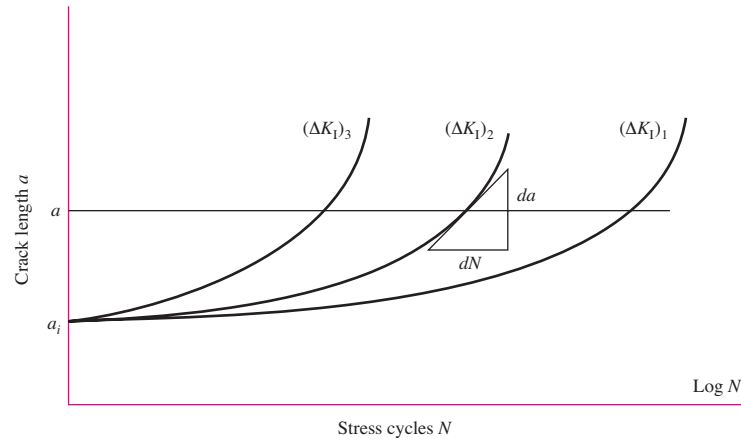


Figure 6-15

When  $da/dN$  is measured in Fig. 6-14 and plotted on loglog coordinates, the data for different stress ranges superpose, giving rise to a sigmoid curve as shown.  $(\Delta K_I)_{th}$  is the threshold value of  $\Delta K_I$ , below which a crack does not grow. From threshold to rupture an aluminum alloy will spend 85-90 percent of life in region I, 5-8 percent in region II, and 1-2 percent in region III.

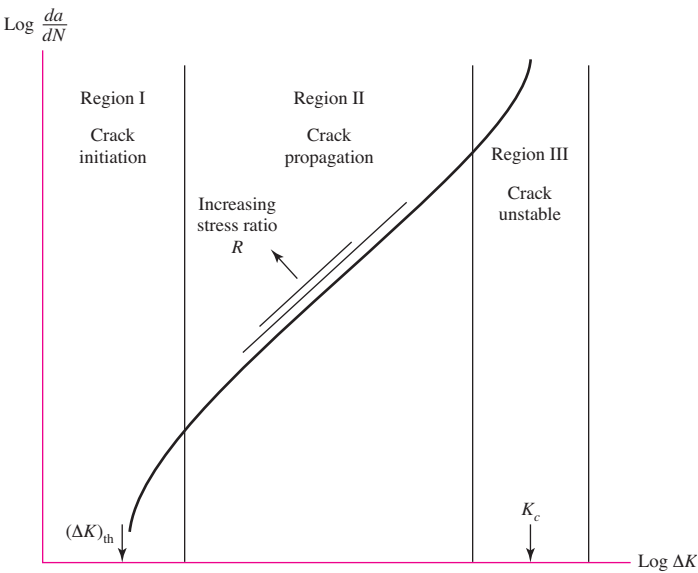


Table 6-1

Conservative Values of Factor C and Exponent m in Eq. (6-5) for Various Forms of Steel ( $R \doteq 0$ )

Material	$C, \frac{\text{m/cycle}}{(\text{MPa}\sqrt{\text{m}})^m}$	$C, \frac{\text{in/cycle}}{(\text{kpsi}\sqrt{\text{in}})^m}$	m
Ferritic-pearlitic steels	$6.89(10^{-12})$	$3.60(10^{-10})$	3.00
Martensitic steels	$1.36(10^{-10})$	$6.60(10^{-9})$	2.25
Austenitic stainless steels	$5.61(10^{-12})$	$3.00(10^{-10})$	3.25

From J.M. Barsom and S.T. Rolfe, *Fatigue and Fracture Control in Structures*, 2nd ed., Prentice Hall, Upper Saddle River, NJ, 1987, pp. 288-291, Copyright ASTM International. Reprinted with permission.

conditions prevail.<sup>8</sup> Assuming a crack is discovered early in stage II, the crack growth in region II of Fig. 6-15 can be approximated by the *Paris equation*, which is of the form

$$\frac{da}{dN} = C(\Delta K_I)^m \tag{6-5}$$

where  $C$  and  $m$  are empirical material constants and  $\Delta K_I$  is given by Eq. (6-4). Representative, but conservative, values of  $C$  and  $m$  for various classes of steels are listed in Table 6-1. Substituting Eq. (6-4) and integrating gives

$$\int_0^{N_f} dN = N_f = \frac{1}{C} \int_{a_i}^{a_f} \frac{da}{(\beta \Delta \sigma \sqrt{\pi a})^m} \tag{6-6}$$

Here  $a_i$  is the initial crack length,  $a_f$  is the final crack length corresponding to failure, and  $N_f$  is the estimated number of cycles to produce a failure *after* the initial crack is formed. Note that  $\beta$  may vary in the integration variable (e.g., see Figs. 5-25 to 5-30).

<sup>8</sup>Recommended references are: Dowling, op. cit.; J. A. Collins, *Failure of Materials in Mechanical Design*, John Wiley & Sons, New York, 1981; H. O. Fuchs and R. I. Stephens, *Metal Fatigue in Engineering*, John Wiley & Sons, New York, 1980; and Harold S. Reemsnyder, "Constant Amplitude Fatigue Life Assessment Models," *SAE Trans.* 820688, vol. 91, Nov. 1983.

If this should happen, then Reemsnyder<sup>9</sup> suggests the use of numerical integration employing the algorithm

$$\begin{aligned}\delta a_j &= C(\Delta K_I)_j^m (\delta N)_j \\ a_{j+1} &= a_j + \delta a_j \\ N_{j+1} &= N_j + \delta N_j \\ N_f &= \sum \delta N_j\end{aligned}\tag{6-7}$$

Here  $\delta a_j$  and  $\delta N_j$  are increments of the crack length and the number of cycles. The procedure is to select a value of  $\delta N_j$ , using  $a_i$  determine  $\beta$  and compute  $\Delta K_I$ , determine  $\delta a_j$ , and then find the next value of  $a$ . Repeat the procedure until  $a = a_f$ .

The following example is highly simplified with  $\beta$  constant in order to give some understanding of the procedure. Normally, one uses fatigue crack growth computer programs such as NASA/FLAGRO 2.0 with more comprehensive theoretical models to solve these problems.

<sup>9</sup>Op. cit.

### EXAMPLE 6-1

The bar shown in Fig. 6-16 is subjected to a repeated moment  $0 \leq M \leq 1200 \text{ lbf} \cdot \text{in}$ . The bar is AISI 4430 steel with  $S_{ut} = 185 \text{ kpsi}$ ,  $S_y = 170 \text{ kpsi}$ , and  $K_{Ic} = 73 \text{ kpsi}\sqrt{\text{in}}$ . Material tests on various specimens of this material with identical heat treatment indicate worst-case constants of  $C = 3.8(10^{-11})(\text{in/cycle})/(\text{kpsi}\sqrt{\text{in}})^m$  and  $m = 3.0$ . As shown, a nick of size 0.004 in has been discovered on the bottom of the bar. Estimate the number of cycles of life remaining.

#### Solution

The stress range  $\Delta\sigma$  is always computed by using the nominal (uncracked) area. Thus

$$\frac{I}{c} = \frac{bh^2}{6} = \frac{0.25(0.5)^2}{6} = 0.01042 \text{ in}^3$$

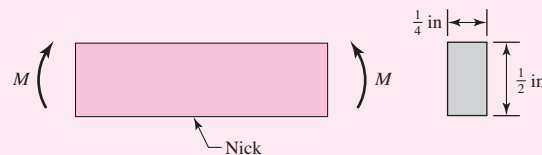
Therefore, before the crack initiates, the stress range is

$$\Delta\sigma = \frac{\Delta M}{I/c} = \frac{1200}{0.01042} = 115.2(10^3) \text{ psi} = 115.2 \text{ kpsi}$$

which is below the yield strength. As the crack grows, it will eventually become long enough such that the bar will completely yield or undergo a brittle fracture. For the ratio of  $S_y/S_{ut}$  it is highly unlikely that the bar will reach complete yield. For brittle fracture, designate the crack length as  $a_f$ . If  $\beta = 1$ , then from Eq. (5-37) with  $K_I = K_{Ic}$ , we approximate  $a_f$  as

$$a_f = \frac{1}{\pi} \left( \frac{K_{Ic}}{\beta\sigma_{\max}} \right)^2 = \frac{1}{\pi} \left( \frac{73}{115.2} \right)^2 = 0.1278 \text{ in}$$

| Figure 6-16





From Fig. 5–27, we compute the ratio  $a_f/h$  as

$$\frac{a_f}{h} = \frac{0.1278}{0.5} = 0.256$$

Thus  $a_f/h$  varies from near zero to approximately 0.256. From Fig. 5–27, for this range  $\beta$  is nearly constant at approximately 1.07. We will assume it to be so, and re-evaluate  $a_f$  as

$$a_f = \frac{1}{\pi} \left( \frac{73}{1.07(115.2)} \right)^2 = 0.112 \text{ in}$$

Thus, from Eq. (6–6), the estimated remaining life is

$$\begin{aligned} N_f &= \frac{1}{C} \int_{a_i}^{a_f} \frac{da}{(\beta \Delta \sigma \sqrt{\pi a})^m} = \frac{1}{3.8(10^{-11})} \int_{0.004}^{0.112} \frac{da}{[1.07(115.2)\sqrt{\pi a}]^3} \\ &= -\frac{5.047(10^3)}{\sqrt{a}} \Big|_{0.004}^{0.112} = 64.7 (10^3) \text{ cycles} \end{aligned}$$

## 6–7 The Endurance Limit

The determination of endurance limits by fatigue testing is now routine, though a lengthy procedure. Generally, stress testing is preferred to strain testing for endurance limits.

For preliminary and prototype design and for some failure analysis as well, a quick method of estimating endurance limits is needed. There are great quantities of data in the literature on the results of rotating-beam tests and simple tension tests of specimens taken from the same bar or ingot. By plotting these as in Fig. 6–17, it is possible to see whether there is any correlation between the two sets of results. The graph appears to suggest that the endurance limit ranges from about 40 to 60 percent of the tensile strength for steels up to about 210 kpsi (1450 MPa). Beginning at about  $S_{ut} = 210$  kpsi (1450 MPa), the scatter appears to increase, but the trend seems to level off, as suggested by the dashed horizontal line at  $S'_e = 105$  kpsi.

We wish now to present a method for estimating endurance limits. Note that estimates obtained from quantities of data obtained from many sources probably have a large spread and might deviate significantly from the results of actual laboratory tests of the mechanical properties of specimens obtained through strict purchase-order specifications. Since the area of uncertainty is greater, compensation must be made by employing larger design factors than would be used for static design.

For steels, simplifying our observation of Fig. 6–17, we will estimate the endurance limit as

$$S'_e = \begin{cases} 0.5S_{ut} & S_{ut} \leq 200 \text{ kpsi (1400 MPa)} \\ 100 \text{ kpsi} & S_{ut} > 200 \text{ kpsi} \\ 700 \text{ MPa} & S_{ut} > 1400 \text{ MPa} \end{cases} \quad (6-8)$$

where  $S_{ut}$  is the *minimum* tensile strength. The prime mark on  $S'_e$  in this equation refers to the *rotating-beam specimen* itself. We wish to reserve the unprimed symbol  $S_e$  for the endurance limit of any particular machine element subjected to any kind of loading. Soon we shall learn that the two strengths may be quite different.

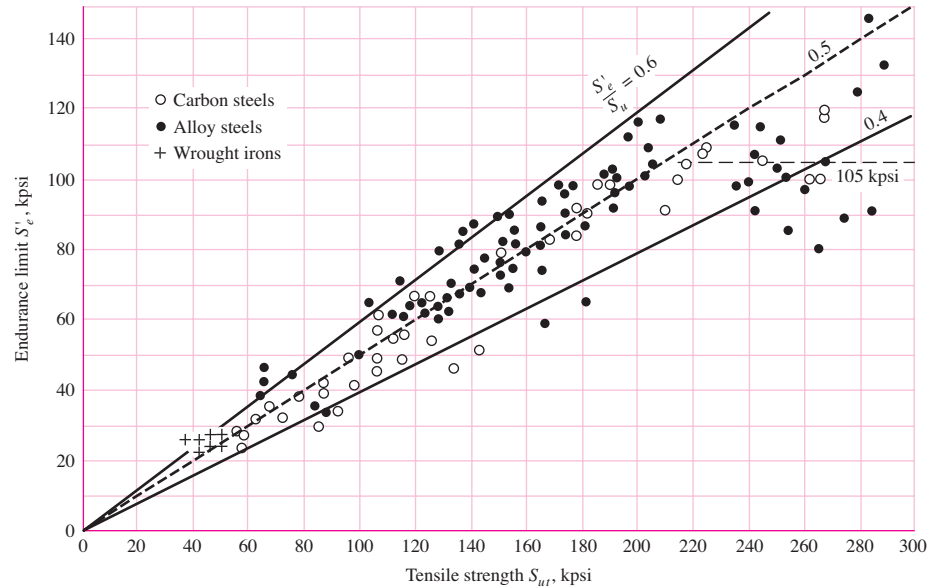


**Figure 6-17**

Graph of endurance limits versus tensile strengths from actual test results for a large number of wrought irons and steels. Ratios of  $S'_e/S_{ut}$  of 0.60, 0.50, and 0.40 are shown by the solid and dashed lines. Note also the horizontal dashed line for  $S'_e = 105$  kpsi. Points shown having a tensile strength greater than 210 kpsi have a mean endurance limit of  $S'_e = 105$  kpsi and a standard deviation of 13.5 kpsi. (Collated from data compiled by H. J. Grover, S. A. Gordon, and L. R. Jackson in *Fatigue of Metals and Structures*, Bureau of Naval Weapons Document NAVWEPS 00-25-534, 1960; and from *Fatigue Design Handbook*, SAE, 1968, p. 42.)

Steels treated to give different microstructures have different  $S'_e/S_{ut}$  ratios. It appears that the more ductile microstructures have a higher ratio. Martensite has a very brittle nature and is highly susceptible to fatigue-induced cracking; thus the ratio is low. When designs include detailed heat-treating specifications to obtain specific microstructures, it is possible to use an estimate of the endurance limit based on test data for the particular microstructure; such estimates are much more reliable and indeed should be used.

The endurance limits for various classes of cast irons, polished or machined, are given in Table A-24. Aluminum alloys do not have an endurance limit. The fatigue strengths of some aluminum alloys at  $5(10^8)$  cycles of reversed stress are given in Table A-24.

## 6-8 Fatigue Strength

As shown in Fig. 6-10, a region of low-cycle fatigue extends from  $N = 1$  to about  $10^3$  cycles. In this region the fatigue strength  $S_f$  is only slightly smaller than the tensile strength  $S_{ut}$ . An analytical approach has been given by Mischke<sup>10</sup> for both

<sup>10</sup>J. E. Shigley, C. R. Mischke, and T. H. Brown, Jr., *Standard Handbook of Machine Design*, 3rd ed., McGraw-Hill, New York, 2004, pp. 29.25–29.27.

high-cycle and low-cycle regions, requiring the parameters of the Manson-Coffin equation plus the strain-strengthening exponent  $m$ . Engineers often have to work with less information.

Figure 6–10 indicates that the high-cycle fatigue domain extends from  $10^3$  cycles for steels to the endurance limit life  $N_e$ , which is about  $10^6$  to  $10^7$  cycles. The purpose of this section is to develop methods of approximation of the  $S$ - $N$  diagram in the high-cycle region, when information may be as sparse as the results of a simple tension test. Experience has shown high-cycle fatigue data are rectified by a logarithmic transform to both stress and cycles-to-failure. Equation (6–2) can be used to determine the fatigue strength at  $10^3$  cycles. Defining the specimen fatigue strength at a specific number of cycles as  $(S'_f)_N = E \Delta \varepsilon_e / 2$ , write Eq. (6–2) as

$$(S'_f)_N = \sigma'_F (2N)^b \quad (6-9)$$

At  $10^3$  cycles,

$$(S'_f)10^3 = \sigma'_F (2 \cdot 10^3)^b = f S_{ut}$$

where  $f$  is the fraction of  $S_{ut}$  represented by  $(S'_f)_{10^3 \text{ cycles}}$ . Solving for  $f$  gives

$$f = \frac{\sigma'_F}{S_{ut}} (2 \cdot 10^3)^b \quad (6-10)$$

Now, from Eq. (2–11),  $\sigma'_F = \sigma_0 \varepsilon^m$ , with  $\varepsilon = \varepsilon'_F$ . If this true-stress–true-strain equation is not known, the SAE approximation<sup>11</sup> for steels with  $H_B \leq 500$  may be used:

$$\sigma'_F = S_{ut} + 50 \text{ kpsi} \quad \text{or} \quad \sigma'_F = S_{ut} + 345 \text{ MPa} \quad (6-11)$$

To find  $b$ , substitute the endurance strength and corresponding cycles,  $S'_e$  and  $N_e$ , respectively into Eq. (6–9) and solving for  $b$

$$b = -\frac{\log(\sigma'_F/S'_e)}{\log(2N_e)} \quad (6-12)$$

Thus, the equation  $S'_f = \sigma'_F (2N)^b$  is known. For example, if  $S_{ut} = 105$  kpsi and  $S'_e = 52.5$  kpsi at failure,

$$\text{Eq. (6-11)} \quad \sigma'_F = 105 + 50 = 155 \text{ kpsi}$$

$$\text{Eq. (6-12)} \quad b = -\frac{\log(155/52.5)}{\log(2 \cdot 10^6)} = -0.0746$$

$$\text{Eq. (6-10)} \quad f = \frac{155}{105} (2 \cdot 10^3)^{-0.0746} = 0.837$$

and for Eq. (6–9), with  $S'_f = (S'_f)_N$ ,

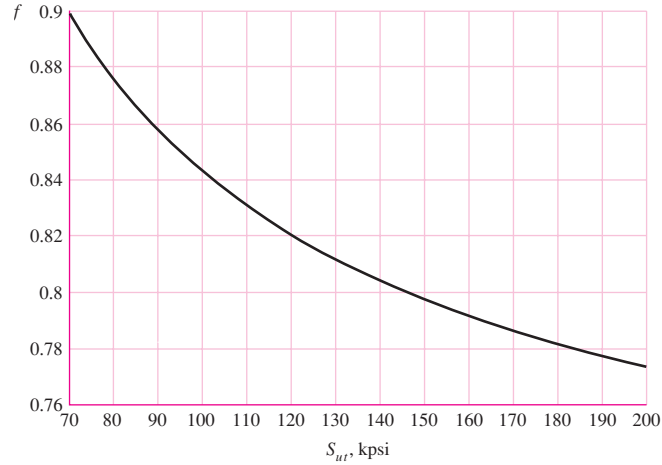
$$S'_f = 155(2N)^{-0.0746} = 147 N^{-0.0746} \quad (a)$$

<sup>11</sup>*Fatigue Design Handbook*, vol. 4, Society of Automotive Engineers, New York, 1958, p. 27.



**Figure 6-18**

Fatigue strength fraction,  $f$ , of  $S_{ut}$  at  $10^3$  cycles for  $S_e = S'_e = 0.5 S_{ut}$ .



The process given for finding  $f$  can be repeated for various ultimate strengths. Figure 6-18 is a plot of  $f$  for  $70 \leq S_{ut} \leq 200$  kpsi. To be conservative, for  $S_{ut} < 70$  kpsi, let  $f = 0.9$ .

For an actual mechanical component,  $S'_e$  is reduced to  $S_e$  (see Sec. 6-9) which is less than  $0.5 S_{ut}$ . However, unless actual data is available, we recommend using the value of  $f$  found from Fig. 6-18. Equation (a), for the actual mechanical component, can be written in the form

$$S_f = a N^b \quad (6-13)$$

where  $N$  is cycles to failure and the constants  $a$  and  $b$  are defined by the points  $10^3$ ,  $(S_f)_{10^3}$  and  $10^6$ ,  $S_e$  with  $(S_f)_{10^3} = f S_{ut}$ . Substituting these two points in Eq. (6-13) gives

$$a = \frac{(f S_{ut})^2}{S_e} \quad (6-14)$$

$$b = -\frac{1}{3} \log \left( \frac{f S_{ut}}{S_e} \right) \quad (6-15)$$

If a completely reversed stress  $\sigma_a$  is given, setting  $S_f = \sigma_a$  in Eq. (6-13), the number of cycles-to-failure can be expressed as

$$N = \left( \frac{\sigma_a}{a} \right)^{1/b} \quad (6-16)$$

Low-cycle fatigue is often defined (see Fig. 6-10) as failure that occurs in a range of  $1 \leq N \leq 10^3$  cycles. On a loglog plot such as Fig. 6-10 the failure locus in this range is nearly linear below  $10^3$  cycles. A straight line between  $10^3$ ,  $f S_{ut}$  and 1,  $S_{ut}$  (transformed) is conservative, and it is given by

$$S_f \geq S_{ut} N^{(\log f)/3} \quad 1 \leq N \leq 10^3 \quad (6-17)$$

**EXAMPLE 6-2**

Given a 1050 HR steel, *estimate*

- (a) the rotating-beam endurance limit at  $10^6$  cycles.
- (b) the endurance strength of a polished rotating-beam specimen corresponding to  $10^4$  cycles to failure
- (c) the expected life of a polished rotating-beam specimen under a completely reversed stress of 55 kpsi.

**Solution** (a) From Table A-20,  $S_{ut} = 90$  kpsi. From Eq. (6-8),

**Answer** 
$$S'_e = 0.5(90) = 45 \text{ kpsi}$$

(b) From Fig. 6-18, for  $S_{ut} = 90$  kpsi,  $f \doteq 0.86$ . From Eq. (6-14),

$$a = \frac{[0.86(90)^2]}{45} = 133.1 \text{ kpsi}$$

From Eq. (6-15),

$$b = -\frac{1}{3} \log \left[ \frac{0.86(90)}{45} \right] = -0.0785$$

Thus, Eq. (6-13) is

$$S'_f = 133.1 N^{-0.0785}$$

**Answer** For  $10^4$  cycles to failure,  $S'_f = 133.1(10^4)^{-0.0785} = 64.6$  kpsi

(c) From Eq. (6-16), with  $\sigma_a = 55$  kpsi,

**Answer** 
$$N = \left( \frac{55}{133.1} \right)^{1/-0.0785} = 77\,500 = 7.75(10^4) \text{ cycles}$$

Keep in mind that these are only *estimates*. So expressing the answers using three-place accuracy is a little misleading.

**6-9****Endurance Limit Modifying Factors**

We have seen that the rotating-beam specimen used in the laboratory to determine endurance limits is prepared very carefully and tested under closely controlled conditions. It is unrealistic to expect the endurance limit of a mechanical or structural member to match the values obtained in the laboratory. Some differences include

- *Material*: composition, basis of failure, variability
- *Manufacturing*: method, heat treatment, fretting corrosion, surface condition, stress concentration
- *Environment*: corrosion, temperature, stress state, relaxation times
- *Design*: size, shape, life, stress state, stress concentration, speed, fretting, galling

Marin<sup>12</sup> identified factors that quantified the effects of surface condition, size, loading, temperature, and miscellaneous items. The question of whether to adjust the endurance limit by subtractive corrections or multiplicative corrections was resolved by an extensive statistical analysis of a 4340 (electric furnace, aircraft quality) steel, in which a correlation coefficient of 0.85 was found for the multiplicative form and 0.40 for the additive form. A Marin equation is therefore written as

$$S_e = k_a k_b k_c k_d k_e k_f S'_e \quad (6-18)$$

where  $k_a$  = surface condition modification factor  
 $k_b$  = size modification factor  
 $k_c$  = load modification factor  
 $k_d$  = temperature modification factor  
 $k_e$  = reliability factor<sup>13</sup>  
 $k_f$  = miscellaneous-effects modification factor  
 $S'_e$  = rotary-beam test specimen endurance limit  
 $S_e$  = endurance limit at the critical location of a machine part in the geometry and condition of use

When endurance tests of parts are not available, estimations are made by applying Marin factors to the endurance limit.

### Surface Factor $k_a$

The surface of a rotating-beam specimen is highly polished, with a final polishing in the axial direction to smooth out any circumferential scratches. The surface modification factor depends on the quality of the finish of the actual part surface and on the tensile strength of the part material. To find quantitative expressions for common finishes of machine parts (ground, machined, or cold-drawn, hot-rolled, and as-forged), the coordinates of data points were recaptured from a plot of endurance limit versus ultimate tensile strength of data gathered by Lipson and Noll and reproduced by Horger.<sup>14</sup> The data can be represented by

$$k_a = a S_{ut}^b \quad (6-19)$$

where  $S_{ut}$  is the minimum tensile strength and  $a$  and  $b$  are to be found in Table 6-2.

<sup>12</sup>Joseph Marin, *Mechanical Behavior of Engineering Materials*, Prentice-Hall, Englewood Cliffs, N.J., 1962, p. 224.

<sup>13</sup>Complete stochastic analysis is presented in Sec. 6-17. Until that point the presentation here is one of a deterministic nature. However, we must take care of the known scatter in the fatigue data. This means that we will not carry out a true reliability analysis at this time but will attempt to answer the question: What is the probability that a *known* (assumed) stress will exceed the strength of a randomly selected component made from this material population?

<sup>14</sup>C. J. Noll and C. Lipson, "Allowable Working Stresses," *Society for Experimental Stress Analysis*, vol. 3, no. 2, 1946, p. 29. Reproduced by O. J. Horger (ed.), *Metals Engineering Design ASME Handbook*, McGraw-Hill, New York, 1953, p. 102.

**Table 6-2**

Parameters for Marin  
Surface Modification  
Factor, Eq. (6-19)

Surface Finish	Factor $a$		Exponent $b$
	$S_{UT}$ kpsi	$S_{UT}$ MPa	
Ground	1.34	1.58	-0.085
Machined or cold-drawn	2.70	4.51	-0.265
Hot-rolled	14.4	57.7	-0.718
As-forged	39.9	272.	-0.995

From C.J. Noll and C. Lipson, "Allowable Working Stresses," *Society for Experimental Stress Analysis*, vol. 3, no. 2, 1946 p. 29. Reproduced by O.J. Horger (ed.) *Metals Engineering Design ASME Handbook*, McGraw-Hill, New York. Copyright © 1953 by The McGraw-Hill Companies, Inc. Reprinted by permission.

**EXAMPLE 6-3**

A steel has a minimum ultimate strength of 520 MPa and a machined surface. Estimate  $k_a$ .

**Solution**

From Table 6-2,  $a = 4.51$  and  $b = -0.265$ . Then, from Eq. (6-19)

**Answer**

$$k_a = 4.51(520)^{-0.265} = 0.860$$

Again, it is important to note that this is an approximation as the data is typically quite scattered. Furthermore, this is not a correction to take lightly. For example, if in the previous example the steel was forged, the correction factor would be 0.540, a significant reduction of strength.

**Size Factor  $k_b$** 

The size factor has been evaluated using 133 sets of data points.<sup>15</sup> The results for bending and torsion may be expressed as

$$k_b = \begin{cases} (d/0.3)^{-0.107} = 0.879d^{-0.107} & 0.11 \leq d \leq 2 \text{ in} \\ 0.91d^{-0.157} & 2 < d \leq 10 \text{ in} \\ (d/7.62)^{-0.107} = 1.24d^{-0.107} & 2.79 \leq d \leq 51 \text{ mm} \\ 1.51d^{-0.157} & 51 < d \leq 254 \text{ mm} \end{cases} \quad (6-20)$$

For axial loading there is no size effect, so

$$k_b = 1 \quad (6-21)$$

but see  $k_c$ .

One of the problems that arises in using Eq. (6-20) is what to do when a round bar in bending is not rotating, or when a noncircular cross section is used. For example, what is the size factor for a bar 6 mm thick and 40 mm wide? The approach to be used

<sup>15</sup>Charles R. Mischke, "Prediction of Stochastic Endurance Strength," *Trans. of ASME, Journal of Vibration, Acoustics, Stress, and Reliability in Design*, vol. 109, no. 1, January 1987, Table 3.

here employs an *effective dimension*  $d_e$  obtained by equating the volume of material stressed at and above 95 percent of the maximum stress to the same volume in the rotating-beam specimen.<sup>16</sup> It turns out that when these two volumes are equated, the lengths cancel, and so we need only consider the areas. For a rotating round section, the 95 percent stress area is the area in a ring having an outside diameter  $d$  and an inside diameter of  $0.95d$ . So, designating the 95 percent stress area  $A_{0.95\sigma}$ , we have

$$A_{0.95\sigma} = \frac{\pi}{4}[d^2 - (0.95d)^2] = 0.0766d^2 \quad (6-22)$$

This equation is also valid for a rotating hollow round. For nonrotating solid or hollow rounds, the 95 percent stress area is twice the area outside of two parallel chords having a spacing of  $0.95d$ , where  $d$  is the diameter. Using an exact computation, this is

$$A_{0.95\sigma} = 0.01046d^2 \quad (6-23)$$

with  $d_e$  in Eq. (6-22), setting Eqs. (6-22) and (6-23) equal to each other enables us to solve for the effective diameter. This gives

$$d_e = 0.370d \quad (6-24)$$

as the effective size of a round corresponding to a nonrotating solid or hollow round.

A rectangular section of dimensions  $h \times b$  has  $A_{0.95\sigma} = 0.05hb$ . Using the same approach as before,

$$d_e = 0.808(hb)^{1/2} \quad (6-25)$$

Table 6-3 provides  $A_{0.95\sigma}$  areas of common structural shapes undergoing non-rotating bending.

<sup>16</sup>See R. Kuguel, "A Relation between Theoretical Stress Concentration Factor and Fatigue Notch Factor Deduced from the Concept of Highly Stressed Volume," *Proc. ASTM*, vol. 61, 1961, pp. 732-748.

### EXAMPLE 6-4

A steel shaft loaded in bending is 32 mm in diameter, abutting a filleted shoulder 38 mm in diameter. The shaft material has a mean ultimate tensile strength of 690 MPa. Estimate the Marin size factor  $k_b$  if the shaft is used in

- (a) A rotating mode.
- (b) A nonrotating mode.

**Solution** (a) From Eq. (6-20)

$$\text{Answer} \quad k_b = \left(\frac{d}{7.62}\right)^{-0.107} = \left(\frac{32}{7.62}\right)^{-0.107} = 0.858$$

(b) From Table 6-3,

$$d_e = 0.37d = 0.37(32) = 11.84 \text{ mm}$$

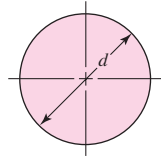
From Eq. (6-20),

$$\text{Answer} \quad k_b = \left(\frac{11.84}{7.62}\right)^{-0.107} = 0.954$$



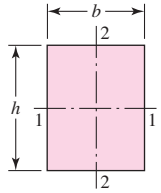
**Table 6-3**

$A_{0.95\sigma}$  Areas of  
Common Nonrotating  
Structural Shapes



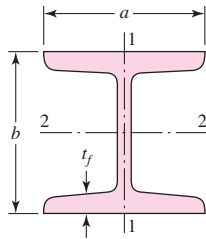
$$A_{0.95\sigma} = 0.01046d^2$$

$$d_e = 0.370d$$

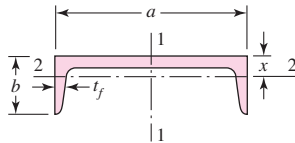


$$A_{0.95\sigma} = 0.05hb$$

$$d_e = 0.808\sqrt{hb}$$



$$A_{0.95\sigma} = \begin{cases} 0.10at_f & \text{axis 1-1} \\ 0.05ba & \text{axis 2-2} \end{cases} \quad t_f > 0.025a$$



$$A_{0.95\sigma} = \begin{cases} 0.05ab & \text{axis 1-1} \\ 0.052xa + 0.1t_f(b-x) & \text{axis 2-2} \end{cases}$$

### Loading Factor $k_c$

When fatigue tests are carried out with rotating bending, axial (push-pull), and torsional loading, the endurance limits differ with  $S_{ut}$ . This is discussed further in Sec. 6-17. Here, we will specify average values of the load factor as

$$k_c = \begin{cases} 1 & \text{bending} \\ 0.85 & \text{axial} \\ 0.59 & \text{torsion}^{17} \end{cases} \quad (6-26)$$

### Temperature Factor $k_d$

When operating temperatures are below room temperature, brittle fracture is a strong possibility and should be investigated first. When the operating temperatures are higher than room temperature, yielding should be investigated first because the yield strength drops off so rapidly with temperature; see Fig. 2-9. Any stress will induce creep in a material operating at high temperatures; so this factor must be considered too.

<sup>17</sup>Use this only for pure torsional fatigue loading. When torsion is combined with other stresses, such as bending,  $k_c = 1$  and the combined loading is managed by using the effective von Mises stress as in Sec. 5-5. Note: For pure torsion, the distortion energy predicts that  $(k_c)_{\text{torsion}} = 0.577$ .

**Table 6-4**

Effect of Operating Temperature on the Tensile Strength of Steel.\* ( $S_T$  = tensile strength at operating temperature;  $S_{RT}$  = tensile strength at room temperature;  $0.099 \leq \hat{\sigma} \leq 0.110$ )

Temperature, °C	$S_T/S_{RT}$	Temperature, °F	$S_T/S_{RT}$
20	1.000	70	1.000
50	1.010	100	1.008
100	1.020	200	1.020
150	1.025	300	1.024
200	1.020	400	1.018
250	1.000	500	0.995
300	0.975	600	0.963
350	0.943	700	0.927
400	0.900	800	0.872
450	0.843	900	0.797
500	0.768	1000	0.698
550	0.672	1100	0.567
600	0.549		

\*Data source: Fig. 2-9.

Finally, it may be true that there is no fatigue limit for materials operating at high temperatures. Because of the reduced fatigue resistance, the failure process is, to some extent, dependent on time.

The limited amount of data available show that the endurance limit for steels increases slightly as the temperature rises and then begins to fall off in the 400 to 700°F range, not unlike the behavior of the tensile strength shown in Fig. 2-9. For this reason it is probably true that the endurance limit is related to tensile strength at elevated temperatures in the same manner as at room temperature.<sup>18</sup> It seems quite logical, therefore, to employ the same relations to predict endurance limit at elevated temperatures as are used at room temperature, at least until more comprehensive data become available. At the very least, this practice will provide a useful standard against which the performance of various materials can be compared.

Table 6-4 has been obtained from Fig. 2-9 by using only the tensile-strength data. Note that the table represents 145 tests of 21 different carbon and alloy steels. A fourth-order polynomial curve fit to the data underlying Fig. 2-9 gives

$$k_d = 0.975 + 0.432(10^{-3})T_F - 0.115(10^{-5})T_F^2 + 0.104(10^{-8})T_F^3 - 0.595(10^{-12})T_F^4 \quad (6-27)$$

where  $70 \leq T_F \leq 1000^\circ\text{F}$ .

Two types of problems arise when temperature is a consideration. If the rotating-beam endurance limit is known at room temperature, then use

$$k_d = \frac{S_T}{S_{RT}} \quad (6-28)$$

<sup>18</sup>For more, see Table 2 of ANSI/ASME B106. 1M-1985 shaft standard, and E. A. Brandes (ed.), *Smithell's Metals Reference Book*, 6th ed., Butterworth, London, 1983, pp. 22-134 to 22-136, where endurance limits from 100 to 650°C are tabulated.

from Table 6–4 or Eq. (6–27) and proceed as usual. If the rotating-beam endurance limit is not given, then compute it using Eq. (6–8) and the temperature-corrected tensile strength obtained by using the factor from Table 6–4. Then use  $k_d = 1$ .

### EXAMPLE 6–5

A 1035 steel has a tensile strength of 70 kpsi and is to be used for a part that sees 450°F in service. Estimate the Marin temperature modification factor and  $(S_e)_{450^\circ}$  if  
(a) The room-temperature endurance limit by test is  $(S'_e)_{70^\circ} = 39.0$  kpsi.  
(b) Only the tensile strength at room temperature is known.

#### Solution

(a) First, from Eq. (6–27),

$$k_d = 0.975 + 0.432(10^{-3})(450) - 0.115(10^{-5})(450^2) \\ + 0.104(10^{-8})(450^3) - 0.595(10^{-12})(450^4) = 1.007$$

Thus,

#### Answer

$$(S_e)_{450^\circ} = k_d(S'_e)_{70^\circ} = 1.007(39.0) = 39.3 \text{ kpsi}$$

(b) Interpolating from Table 6–4 gives

$$(S_T/S_{RT})_{450^\circ} = 1.018 + (0.995 - 1.018) \frac{450 - 400}{500 - 400} = 1.007$$

Thus, the tensile strength at 450°F is estimated as

$$(S_{ut})_{450^\circ} = (S_T/S_{RT})_{450^\circ} (S_{ut})_{70^\circ} = 1.007(70) = 70.5 \text{ kpsi}$$

From Eq. (6–8) then,

#### Answer

$$(S_e)_{450^\circ} = 0.5 (S_{ut})_{450^\circ} = 0.5(70.5) = 35.2 \text{ kpsi}$$

Part *a* gives the better estimate due to actual testing of the particular material.

### Reliability Factor $k_e$

The discussion presented here accounts for the scatter of data such as shown in Fig. 6–17 where the mean endurance limit is shown to be  $S'_e/S_{ut} \doteq 0.5$ , or as given by Eq. (6–8). Most endurance strength data are reported as mean values. Data presented by Haugen and Wirching<sup>19</sup> show standard deviations of endurance strengths of less than 8 percent. Thus the reliability modification factor to account for this can be written as

$$k_e = 1 - 0.08 z_a \quad (6-29)$$

where  $z_a$  is defined by Eq. (20–16) and values for any desired reliability can be determined from Table A–10. Table 6–5 gives reliability factors for some standard specified reliabilities.

For a more comprehensive approach to reliability, see Sec. 6–17.

<sup>19</sup>E. B. Haugen and P. H. Wirching, “Probabilistic Design,” *Machine Design*, vol. 47, no. 12, 1975, pp. 10–14.

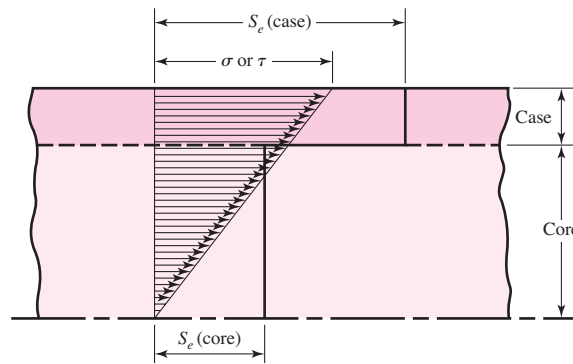
**Table 6-5**

Reliability Factors  $k_e$   
Corresponding to  
8 Percent Standard  
Deviation of the  
Endurance Limit

Reliability, %	Transformation Variate $z_a$	Reliability Factor $k_e$
50	0	1.000
90	1.288	0.897
95	1.645	0.868
99	2.326	0.814
99.9	3.091	0.753
99.99	3.719	0.702
99.999	4.265	0.659
99.9999	4.753	0.620

**Figure 6-19**

The failure of a case-hardened part in bending or torsion. In this example, failure occurs in the core.



### Miscellaneous-Effects Factor $k_f$

Though the factor  $k_f$  is intended to account for the reduction in endurance limit due to all other effects, it is really intended as a reminder that these must be accounted for, because actual values of  $k_f$  are not always available.

*Residual stresses* may either improve the endurance limit or affect it adversely. Generally, if the residual stress in the surface of the part is compression, the endurance limit is improved. Fatigue failures appear to be tensile failures, or at least to be caused by tensile stress, and so anything that reduces tensile stress will also reduce the possibility of a fatigue failure. Operations such as shot peening, hammering, and cold rolling build compressive stresses into the surface of the part and improve the endurance limit significantly. Of course, the material must not be worked to exhaustion.

The endurance limits of parts that are made from rolled or drawn sheets or bars, as well as parts that are forged, may be affected by the so-called *directional characteristics* of the operation. Rolled or drawn parts, for example, have an endurance limit in the transverse direction that may be 10 to 20 percent less than the endurance limit in the longitudinal direction.

Parts that are case-hardened may fail at the surface or at the maximum core radius, depending upon the stress gradient. Figure 6-19 shows the typical triangular stress distribution of a bar under bending or torsion. Also plotted as a heavy line in this figure are the endurance limits  $S_e$  for the case and core. For this example the endurance limit of the core rules the design because the figure shows that the stress  $\sigma$  or  $\tau$ , whichever applies, at the outer core radius, is appreciably larger than the core endurance limit.

Of course, if stress concentration is also present, the stress gradient is much steeper, and hence failure in the core is unlikely.

### Corrosion

It is to be expected that parts that operate in a corrosive atmosphere will have a lowered fatigue resistance. This is, of course, true, and it is due to the roughening or pitting of the surface by the corrosive material. But the problem is not so simple as the one of finding the endurance limit of a specimen that has been corroded. The reason for this is that the corrosion and the stressing occur at the same time. Basically, this means that in time any part will fail when subjected to repeated stressing in a corrosive atmosphere. There is no fatigue limit. Thus the designer's problem is to attempt to minimize the factors that affect the fatigue life; these are:

- Mean or static stress
- Alternating stress
- Electrolyte concentration
- Dissolved oxygen in electrolyte
- Material properties and composition
- Temperature
- Cyclic frequency
- Fluid flow rate around specimen
- Local crevices

### Electrolytic Plating

Metallic coatings, such as chromium plating, nickel plating, or cadmium plating, reduce the endurance limit by as much as 50 percent. In some cases the reduction by coatings has been so severe that it has been necessary to eliminate the plating process. Zinc plating does not affect the fatigue strength. Anodic oxidation of light alloys reduces bending endurance limits by as much as 39 percent but has no effect on the torsional endurance limit.

### Metal Spraying

Metal spraying results in surface imperfections that can initiate cracks. Limited tests show reductions of 14 percent in the fatigue strength.

### Cyclic Frequency

If, for any reason, the fatigue process becomes time-dependent, then it also becomes frequency-dependent. Under normal conditions, fatigue failure is independent of frequency. But when corrosion or high temperatures, or both, are encountered, the cyclic rate becomes important. The slower the frequency and the higher the temperature, the higher the crack propagation rate and the shorter the life at a given stress level.

### Fretage Corrosion

The phenomenon of fretage corrosion is the result of microscopic motions of tightly fitting parts or structures. Bolted joints, bearing-race fits, wheel hubs, and any set of tightly fitted parts are examples. The process involves surface discoloration, pitting, and eventual fatigue. The fretage factor  $k_f$  depends upon the material of the mating pairs and ranges from 0.24 to 0.90.



## 6-10 Stress Concentration and Notch Sensitivity

In Sec. 3-13 it was pointed out that the existence of irregularities or discontinuities, such as holes, grooves, or notches, in a part increases the theoretical stresses significantly in the immediate vicinity of the discontinuity. Equation (3-48) defined a stress concentration factor  $K_t$  (or  $K_{ts}$ ), which is used with the nominal stress to obtain the maximum resulting stress due to the irregularity or defect. It turns out that some materials are not fully sensitive to the presence of notches and hence, for these, a reduced value of  $K_t$  can be used. For these materials, the maximum stress is, in fact,

$$\sigma_{\max} = K_f \sigma_0 \quad \text{or} \quad \tau_{\max} = K_{fs} \tau_0 \quad (6-30)$$

where  $K_f$  is a reduced value of  $K_t$  and  $\sigma_0$  is the nominal stress. The factor  $K_f$  is commonly called a *fatigue stress-concentration factor*, and hence the subscript  $f$ . So it is convenient to think of  $K_f$  as a stress-concentration factor reduced from  $K_t$  because of lessened sensitivity to notches. The resulting factor is defined by the equation

$$K_f = \frac{\text{maximum stress in notched specimen}}{\text{stress in notch-free specimen}} \quad (a)$$

Notch sensitivity  $q$  is defined by the equation

$$q = \frac{K_f - 1}{K_t - 1} \quad \text{or} \quad q_{\text{shear}} = \frac{K_{fs} - 1}{K_{ts} - 1} \quad (6-31)$$

where  $q$  is usually between zero and unity. Equation (6-31) shows that if  $q = 0$ , then  $K_f = 1$ , and the material has no sensitivity to notches at all. On the other hand, if  $q = 1$ , then  $K_f = K_t$ , and the material has full notch sensitivity. In analysis or design work, find  $K_t$  first, from the geometry of the part. Then specify the material, find  $q$ , and solve for  $K_f$  from the equation

$$K_f = 1 + q(K_t - 1) \quad \text{or} \quad K_{fs} = 1 + q_{\text{shear}}(K_{ts} - 1) \quad (6-32)$$

For steels and 2024 aluminum alloys, use Fig. 6-20 to find  $q$  for bending and axial loading. For shear loading, use Fig. 6-21. In using these charts it is well to know that the actual test results from which the curves were derived exhibit a large amount of

**Figure 6-20**

Notch-sensitivity charts for steels and UNS A92024-T wrought aluminum alloys subjected to reversed bending or reversed axial loads. For larger notch radii, use the values of  $q$  corresponding to the  $r = 0.16$ -in (4-mm) ordinate. (From George Sines and J. L. Waisman (eds.), *Metal Fatigue*, McGraw-Hill, New York. Copyright © 1969 by The McGraw-Hill Companies, Inc. Reprinted by permission.)

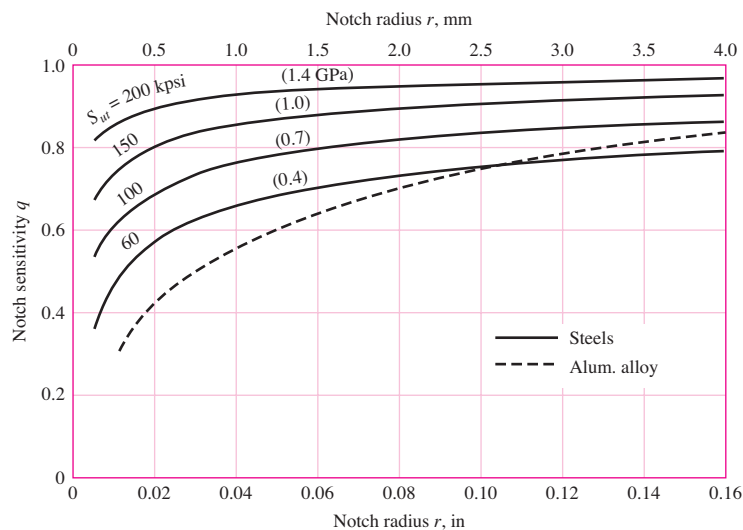
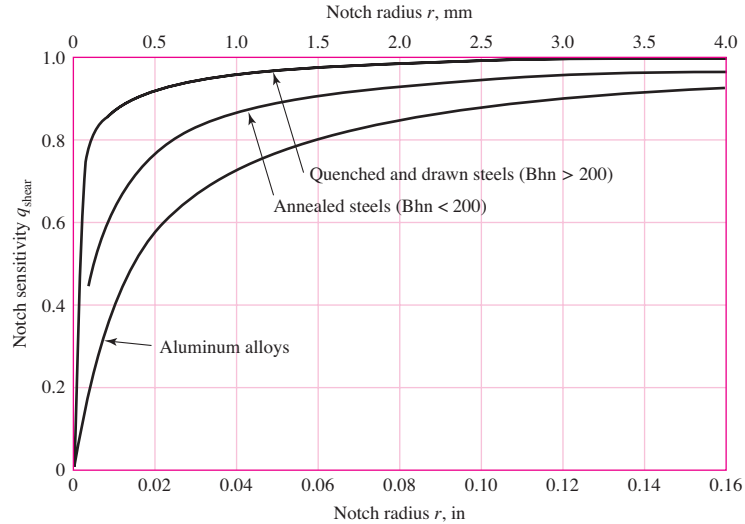


**Figure 6-21**

Notch-sensitivity curves for materials in reversed torsion. For larger notch radii, use the values of  $q_{\text{shear}}$  corresponding to  $r = 0.16$  in (4 mm).



scatter. Because of this scatter it is always safe to use  $K_f = K_t$  if there is any doubt about the true value of  $q$ . Also, note that  $q$  is not far from unity for large notch radii.

The notch sensitivity of the cast irons is very low, varying from 0 to about 0.20, depending upon the tensile strength. To be on the conservative side, it is recommended that the value  $q = 0.20$  be used for all grades of cast iron.

Figure 6-20 has as its basis the *Neuber equation*, which is given by

$$K_f = 1 + \frac{K_t - 1}{1 + \sqrt{a/r}} \quad (6-33)$$

where  $\sqrt{a}$  is defined as the *Neuber constant* and is a material constant. Equating Eqs. (6-31) and (6-33) yields the notch sensitivity equation

$$q = \frac{1}{1 + \frac{\sqrt{a}}{\sqrt{r}}} \quad (6-34)$$

For steel, with  $S_{ut}$  in *kpsi*, the Neuber constant can be approximated by a third-order polynomial fit of data as

$$\begin{aligned} \sqrt{a} = & 0.245\,799 - 0.307\,794(10^{-2})S_{ut} \\ & + 0.150\,874(10^{-4})S_{ut}^2 - 0.266\,978(10^{-7})S_{ut}^3 \end{aligned} \quad (6-35)$$

To use Eq. (6-33) or (6-34) for torsion for low-alloy steels, increase the ultimate strength by 20 *kpsi* in Eq. (6-35) and apply this value of  $\sqrt{a}$ .

### EXAMPLE 6-6

A steel shaft in bending has an ultimate strength of 690 MPa and a shoulder with a fillet radius of 3 mm connecting a 32-mm diameter with a 38-mm diameter. Estimate  $K_f$  using:

- Figure 6-20.
- Equations (6-33) and (6-35).

**Solution** From Fig. A-15-9, using  $D/d = 38/32 = 1.1875$ ,  $r/d = 3/32 = 0.09375$ , we read the graph to find  $K_t \doteq 1.65$ .

(a) From Fig. 6-20, for  $S_{ut} = 690$  MPa and  $r = 3$  mm,  $q \doteq 0.84$ . Thus, from Eq. (6-32)

**Answer** 
$$K_f = 1 + q(K_t - 1) \doteq 1 + 0.84(1.65 - 1) = 1.55$$

(b) From Eq. (6-35) with  $S_{ut} = 690$  MPa = 100 kpsi,  $\sqrt{a} = 0.0622\sqrt{\text{in}} = 0.313\sqrt{\text{mm}}$ . Substituting this into Eq. (6-33) with  $r = 3$  mm gives

**Answer** 
$$K_f = 1 + \frac{K_t - 1}{1 + \sqrt{a}/r} \doteq 1 + \frac{1.65 - 1}{1 + \frac{0.313}{\sqrt{3}}} = 1.55$$

For simple loading, it is acceptable to reduce the endurance limit by either dividing the unnotched specimen endurance limit by  $K_f$  or multiplying the reversing stress by  $K_f$ . However, in dealing with combined stress problems that may involve more than one value of fatigue-concentration factor, the stresses are multiplied by  $K_f$ .

### EXAMPLE 6-7

Consider an unnotched specimen with an endurance limit of 55 kpsi. If the specimen was notched such that  $K_f = 1.6$ , what would be the factor of safety against failure for  $N > 10^6$  cycles at a reversing stress of 30 kpsi?

(a) Solve by reducing  $S'_e$ .

(b) Solve by increasing the applied stress.

**Solution** (a) The endurance limit of the notched specimen is given by

$$S_e = \frac{S'_e}{K_f} = \frac{55}{1.6} = 34.4 \text{ kpsi}$$

and the factor of safety is

**Answer** 
$$n = \frac{S_e}{\sigma_a} = \frac{34.4}{30} = 1.15$$

(b) The maximum stress can be written as

$$(\sigma_a)_{\max} = K_f \sigma_a = 1.6(30) = 48.0 \text{ kpsi}$$

and the factor of safety is

**Answer** 
$$n = \frac{S'_e}{K_f \sigma_a} = \frac{55}{48} = 1.15$$

Up to this point, examples illustrated each factor in Marin's equation and stress concentrations alone. Let us consider a number of factors occurring simultaneously.

**EXAMPLE 6-8**

A 1015 hot-rolled steel bar has been machined to a diameter of 1 in. It is to be placed in reversed axial loading for 70 000 cycles to failure in an operating environment of 550°F. Using ASTM minimum properties, and a reliability of 99 percent, estimate the endurance limit and fatigue strength at 70 000 cycles.

**Solution**

From Table A-20,  $S_{ut} = 50$  kpsi at 70°F. Since the rotating-beam specimen endurance limit is not known at room temperature, we determine the ultimate strength at the elevated temperature first, using Table 6-4. From Table 6-4,

$$\left( \frac{S_T}{S_{RT}} \right)_{550^\circ} = \frac{0.995 + 0.963}{2} = 0.979$$

The ultimate strength at 550°F is then

$$(S_{ut})_{550^\circ} = (S_T/S_{RT})_{550^\circ} (S_{ut})_{70^\circ} = 0.979(50) = 49.0 \text{ kpsi}$$

The rotating-beam specimen endurance limit at 550°F is then estimated from Eq. (6-8) as

$$S'_e = 0.5(49) = 24.5 \text{ kpsi}$$

Next, we determine the Marin factors. For the machined surface, Eq. (6-19) with Table 6-2 gives

$$k_a = aS_{ut}^b = 2.70(49^{-0.265}) = 0.963$$

For axial loading, from Eq. (6-21), the size factor  $k_b = 1$ , and from Eq. (6-26) the loading factor is  $k_c = 0.85$ . The temperature factor  $k_d = 1$ , since we accounted for the temperature in modifying the ultimate strength and consequently the endurance limit. For 99 percent reliability, from Table 6-5,  $k_e = 0.814$ . Finally, since no other conditions were given, the miscellaneous factor is  $k_f = 1$ . The endurance limit for the part is estimated by Eq. (6-18) as

$$\begin{aligned} S_e &= k_a k_b k_c k_d k_e k_f S'_e \\ &= 0.963(1)(0.85)(1)(0.814)(1)24.5 = 16.3 \text{ kpsi} \end{aligned}$$

**Answer**

For the fatigue strength at 70 000 cycles we need to construct the  $S$ - $N$  equation. From p. 277, since  $S_{ut} = 49 < 70$  kpsi, then  $f = 0.9$ . From Eq. (6-14)

$$a = \frac{(f S_{ut})^2}{S_e} = \frac{[0.9(49)]^2}{16.3} = 119.3 \text{ kpsi}$$

and Eq. (6-15)

$$b = -\frac{1}{3} \log \left( \frac{f S_{ut}}{S_e} \right) = -\frac{1}{3} \log \left[ \frac{0.9(49)}{16.3} \right] = -0.1441$$

Finally, for the fatigue strength at 70 000 cycles, Eq. (6-13) gives

**Answer**

$$S_f = a N^b = 119.3(70\,000)^{-0.1441} = 23.9 \text{ kpsi}$$

**EXAMPLE 6-9**

Figure 6-22*a* shows a rotating shaft simply supported in ball bearings at *A* and *D* and loaded by a nonrotating force *F* of 6.8 kN. Using ASTM “minimum” strengths, estimate the life of the part.

**Solution**

From Fig. 6-22*b* we learn that failure will probably occur at *B* rather than at *C* or at the point of maximum moment. Point *B* has a smaller cross section, a higher bending moment, and a higher stress-concentration factor than *C*, and the location of maximum moment has a larger size and no stress-concentration factor.

We shall solve the problem by first estimating the strength at point *B*, since the strength will be different elsewhere, and comparing this strength with the stress at the same point.

From Table A-20 we find  $S_{ut} = 690$  MPa and  $S_y = 580$  MPa. The endurance limit  $S'_e$  is estimated as

$$S'_e = 0.5(690) = 345 \text{ MPa}$$

From Eq. (6-19) and Table 6-2,

$$k_a = 4.51(690)^{-0.265} = 0.798$$

From Eq. (6-20),

$$k_b = (32/7.62)^{-0.107} = 0.858$$

Since  $k_c = k_d = k_e = k_f = 1$ ,

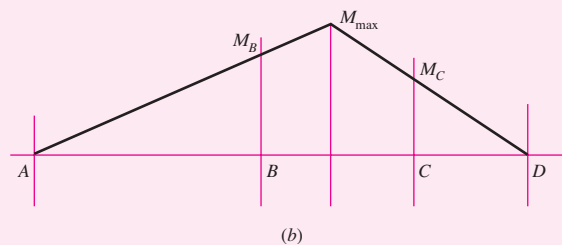
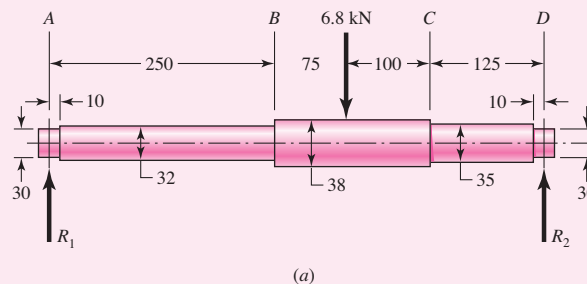
$$S_e = 0.798(0.858)345 = 236 \text{ MPa}$$

To find the geometric stress-concentration factor  $K_t$  we enter Fig. A-15-9 with  $D/d = 38/32 = 1.1875$  and  $r/d = 3/32 = 0.09375$  and read  $K_t \doteq 1.65$ . Substituting  $S_{ut} = 690/6.89 = 100$  kpsi into Eq. (6-35) yields  $\sqrt{a} = 0.0622 \sqrt{\text{in}} = 0.313 \sqrt{\text{mm}}$ . Substituting this into Eq. (6-33) gives

$$K_f = 1 + \frac{K_t - 1}{1 + \sqrt{a}/r} = 1 + \frac{1.65 - 1}{1 + 0.313/\sqrt{3}} = 1.55$$

**Figure 6-22**

(*a*) Shaft drawing showing all dimensions in millimeters; all fillets 3-mm radius. The shaft rotates and the load is stationary; material is machined from AISI 1050 cold-drawn steel. (*b*) Bending-moment diagram.





The next step is to estimate the bending stress at point  $B$ . The bending moment is

$$M_B = R_1 x = \frac{225F}{550} 250 = \frac{225(6.8)}{550} 250 = 695.5 \text{ N} \cdot \text{m}$$

Just to the left of  $B$  the section modulus is  $I/c = \pi d^3/32 = \pi 32^3/32 = 3.217 (10^3) \text{ mm}^3$ . The reversing bending stress is, assuming infinite life,

$$\sigma = K_f \frac{M_B}{I/c} = 1.55 \frac{695.5}{3.217} (10)^{-6} = 335.1 (10^6) \text{ Pa} = 335.1 \text{ MPa}$$

This stress is greater than  $S_e$  and less than  $S_y$ . This means we have both finite life and no yielding on the first cycle.

For finite life, we will need to use Eq. (6-16). The ultimate strength,  $S_{ut} = 690 \text{ MPa} = 100 \text{ kpsi}$ . From Fig. 6-18,  $f = 0.844$ . From Eq. (6-14)

$$a = \frac{(f S_{ut})^2}{S_e} = \frac{[0.844(690)]^2}{236} = 1437 \text{ MPa}$$

and from Eq. (6-15)

$$b = -\frac{1}{3} \log \left( \frac{f S_{ut}}{S_e} \right) = -\frac{1}{3} \log \left[ \frac{0.844(690)}{236} \right] = -0.1308$$

From Eq. (6-16),

**Answer**

$$N = \left( \frac{\sigma_a}{a} \right)^{1/b} = \left( \frac{335.1}{1437} \right)^{-1/0.1308} = 68(10^3) \text{ cycles}$$

## 6-11 Characterizing Fluctuating Stresses

Fluctuating stresses in machinery often take the form of a sinusoidal pattern because of the nature of some rotating machinery. However, other patterns, some quite irregular, do occur. It has been found that in periodic patterns exhibiting a single maximum and a single minimum of force, the shape of the wave is not important, but the peaks on both the high side (maximum) and the low side (minimum) are important. Thus  $F_{\max}$  and  $F_{\min}$  in a cycle of force can be used to characterize the force pattern. It is also true that ranging above and below some baseline can be equally effective in characterizing the force pattern. If the largest force is  $F_{\max}$  and the smallest force is  $F_{\min}$ , then a steady component and an alternating component can be constructed as follows:

$$F_m = \frac{F_{\max} + F_{\min}}{2} \quad F_a = \left| \frac{F_{\max} - F_{\min}}{2} \right|$$

where  $F_m$  is the midrange steady component of force, and  $F_a$  is the amplitude of the alternating component of force.

**Figure 6-23**

Some stress-time relations:  
 (a) fluctuating stress with high-frequency ripple;  
 (b and c) nonsinusoidal fluctuating stress;  
 (d) sinusoidal fluctuating stress;  
 (e) repeated stress;  
 (f) completely reversed sinusoidal stress.

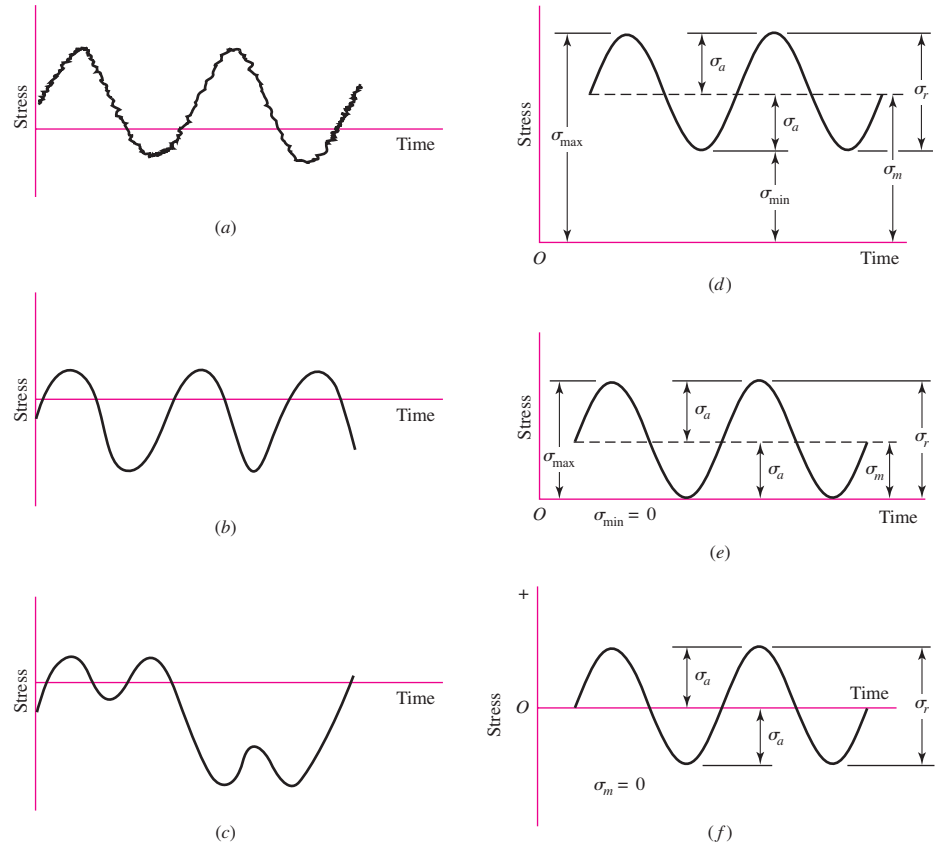


Figure 6-23 illustrates some of the various stress-time traces that occur. The components of stress, some of which are shown in Fig. 6-23d, are

$\sigma_{\min}$ = minimum stress	$\sigma_m$ = midrange component
$\sigma_{\max}$ = maximum stress	$\sigma_r$ = range of stress
$\sigma_a$ = amplitude component	$\sigma_s$ = static or steady stress

The steady, or static, stress is *not* the same as the midrange stress; in fact, it may have any value between  $\sigma_{\min}$  and  $\sigma_{\max}$ . The steady stress exists because of a fixed load or preload applied to the part, and it is usually independent of the varying portion of the load. A helical compression spring, for example, is always loaded into a space shorter than the free length of the spring. The stress created by this initial compression is called the steady, or static, component of the stress. It is not the same as the midrange stress.

We shall have occasion to apply the subscripts of these components to shear stresses as well as normal stresses.

The following relations are evident from Fig. 6-23:

$$\sigma_m = \frac{\sigma_{\max} + \sigma_{\min}}{2}$$

$$\sigma_a = \left| \frac{\sigma_{\max} - \sigma_{\min}}{2} \right| \quad (6-36)$$

In addition to Eq. (6–36), the *stress ratio*

$$R = \frac{\sigma_{\min}}{\sigma_{\max}} \quad (6-37)$$

and the *amplitude ratio*

$$A = \frac{\sigma_a}{\sigma_m} \quad (6-38)$$

are also defined and used in connection with fluctuating stresses.

Equations (6–36) utilize symbols  $\sigma_a$  and  $\sigma_m$  as the stress components at the location under scrutiny. This means, in the absence of a notch,  $\sigma_a$  and  $\sigma_m$  are equal to the nominal stresses  $\sigma_{ao}$  and  $\sigma_{mo}$  induced by loads  $F_a$  and  $F_m$ , respectively; in the presence of a notch they are  $K_f\sigma_{ao}$  and  $K_f\sigma_{mo}$ , respectively, as long as the material remains without plastic strain. In other words, the fatigue stress concentration factor  $K_f$  is applied to *both* components.

When the steady stress component is high enough to induce localized notch yielding, the designer has a problem. The first-cycle local yielding produces plastic strain and strain-strengthening. This is occurring at the location where fatigue crack nucleation and growth are most likely. The material properties ( $S_y$  and  $S_{ut}$ ) are new and difficult to quantify. The prudent engineer controls the concept, material and condition of use, and geometry so that no plastic strain occurs. There are discussions concerning possible ways of quantifying what is occurring under localized and general yielding in the presence of a notch, referred to as the *nominal mean stress* method, *residual stress* method, and the like.<sup>20</sup> The nominal mean stress method (set  $\sigma_a = K_f\sigma_{ao}$  and  $\sigma_m = \sigma_{mo}$ ) gives roughly comparable results to the residual stress method, but both are *approximations*.

There is the method of Dowling<sup>21</sup> for ductile materials, which, for materials with a pronounced yield point and approximated by an elastic–perfectly plastic behavior model, quantitatively expresses the steady stress component stress-concentration factor  $K_{fm}$  as

$$\begin{aligned} K_{fm} &= K_f & K_f|\sigma_{\max,o}| &< S_y \\ K_{fm} &= \frac{S_y - K_f\sigma_{ao}}{|\sigma_{mo}|} & K_f|\sigma_{\max,o}| &> S_y \\ K_{fm} &= 0 & K_f|\sigma_{\max,o} - \sigma_{\min,o}| &> 2S_y \end{aligned} \quad (6-39)$$

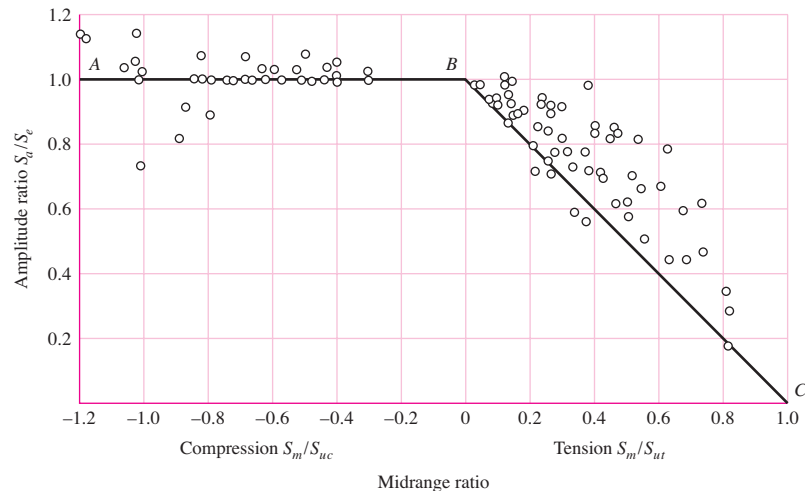
For the purposes of this book, for ductile materials in fatigue,

- Avoid localized plastic strain at a notch. Set  $\sigma_a = K_f\sigma_{ao}$  and  $\sigma_m = K_f\sigma_{mo}$ .
- When plastic strain at a notch cannot be avoided, use Eqs. (6–39); or conservatively, set  $\sigma_a = K_f\sigma_{ao}$  and use  $K_{fm} = 1$ , that is,  $\sigma_m = \sigma_{mo}$ .

<sup>20</sup>R. C. Juvinall, *Stress, Strain, and Strength*, McGraw-Hill, New York, 1967, articles 14.9–14.12; R. C. Juvinall and K. M. Marshek, *Fundamentals of Machine Component Design*, 4th ed., Wiley, New York, 2006, Sec. 8.11; M. E. Dowling, *Mechanical Behavior of Materials*, 2nd ed., Prentice Hall, Englewood Cliffs, N.J., 1999, Secs. 10.3–10.5.

<sup>21</sup>Dowling, op. cit., p. 437–438.

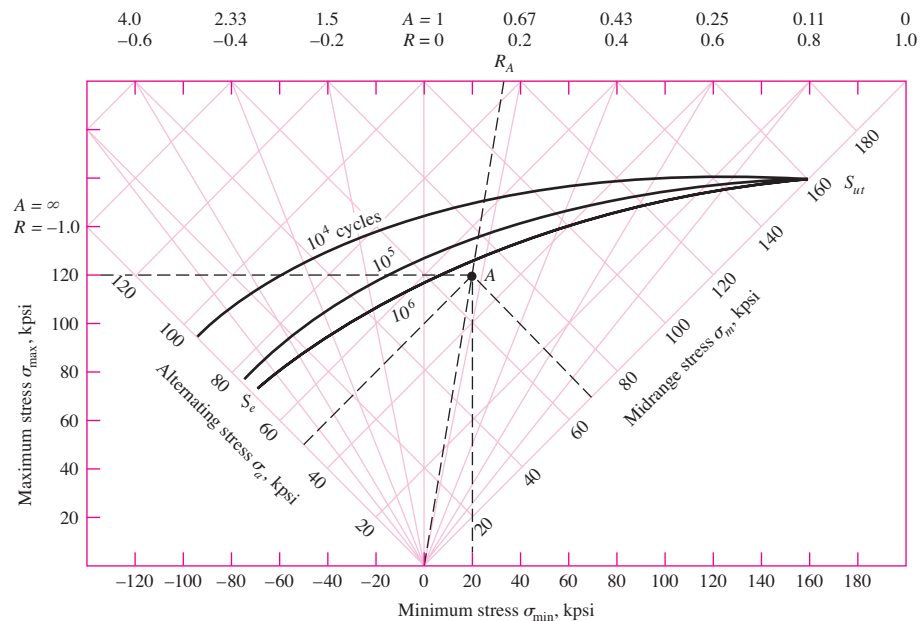


**Figure 6-25**

Plot of fatigue failures for midrange stresses in both tensile and compressive regions. Normalizing the data by using the ratio of steady strength component to tensile strength  $S_m/S_{ut}$ , steady strength component to compressive strength  $S_m/S_{uc}$  and strength amplitude component to endurance limit  $S_a/S'_e$  enables a plot of experimental results for a variety of steels. [Data source: Thomas J. Dolan, "Stress Range," Sec. 6.2 in O. J. Horger (ed.), ASME Handbook—Metals Engineering Design, McGraw-Hill, New York, 1953.]

**Figure 6-26**

Master fatigue diagram created for AISI 4340 steel having  $S_{ut} = 158$  and  $S_y = 147$  kpsi. The stress components at A are  $\sigma_{\min} = 20$ ,  $\sigma_{\max} = 120$ ,  $\sigma_m = 70$ , and  $\sigma_a = 50$ , all in kpsi. (Source: H. J. Grover, Fatigue of Aircraft Structures, U.S. Government Printing Office, Washington, D.C., 1966, pp. 317, 322. See also J. A. Collins, Failure of Materials in Mechanical Design, Wiley, New York, 1981, p. 216.)

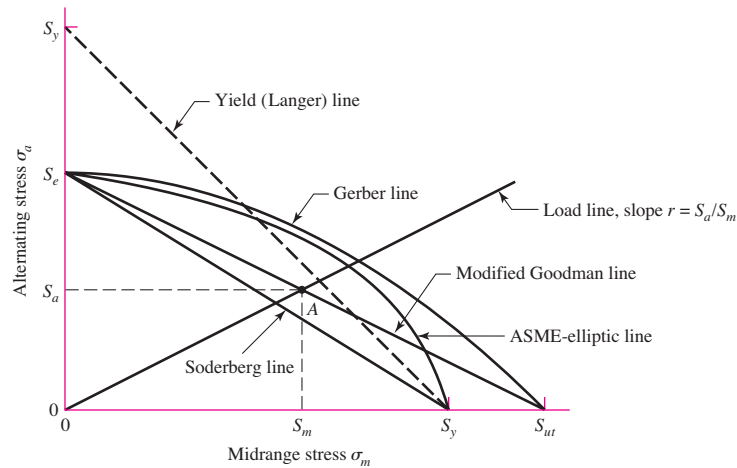


have been drawn too. Any stress state, such as the one at A, can be described by the minimum and maximum components, or by the midrange and alternating components. And safety is indicated whenever the point described by the stress components lies below the constant-life line.



**Figure 6-27**

Fatigue diagram showing various criteria of failure. For each criterion, points on or “above” the respective line indicate failure. Some point A on the Goodman line, for example, gives the strength  $S_m$  as the limiting value of  $\sigma_m$  corresponding to the strength  $S_a$ , which, paired with  $\sigma_m$ , is the limiting value of  $\sigma_a$ .



When the midrange stress is compression, failure occurs whenever  $\sigma_a = S_e$  or whenever  $\sigma_{\max} = S_{yc}$ , as indicated by the left-hand side of Fig. 6-25. Neither a fatigue diagram nor any other failure criteria need be developed.

In Fig. 6-27, the tensile side of Fig. 6-25 has been redrawn in terms of strengths, instead of strength ratios, with the same modified Goodman criterion together with four additional criteria of failure. Such diagrams are often constructed for analysis and design purposes; they are easy to use and the results can be scaled off directly.

The early viewpoint expressed on a  $\sigma_a\sigma_m$  diagram was that there existed a locus which divided safe from unsafe combinations of  $\sigma_a$  and  $\sigma_m$ . Ensuing proposals included the parabola of Gerber (1874), the Goodman (1890)<sup>22</sup> (straight) line, and the Soderberg (1930) (straight) line. As more data were generated it became clear that a fatigue criterion, rather than being a “fence,” was more like a zone or band wherein the probability of failure could be estimated. We include the failure criterion of Goodman because

- It is a straight line and the algebra is linear and easy.
- It is easily graphed, every time for every problem.
- It reveals subtleties of insight into fatigue problems.
- Answers can be scaled from the diagrams as a check on the algebra.

We also caution that it is deterministic and the phenomenon is not. It is biased and we cannot quantify the bias. It is not conservative. It is a stepping-stone to understanding; it is history; and to read the work of other engineers and to have meaningful oral exchanges with them, it is necessary that you understand the Goodman approach should it arise.

Either the fatigue limit  $S_e$  or the finite-life strength  $S_f$  is plotted on the ordinate of Fig. 6-27. These values will have already been corrected using the Marin factors of Eq. (6-18). Note that the yield strength  $S_y$  is plotted on the ordinate too. This serves as a reminder that first-cycle yielding rather than fatigue might be the criterion of failure.

The midrange-stress axis of Fig. 6-27 has the yield strength  $S_y$  and the tensile strength  $S_{ut}$  plotted along it.

<sup>22</sup>It is difficult to date Goodman’s work because it went through several modifications and was never published.

Five criteria of failure are diagrammed in Fig. 6–27: the Soderberg, the modified Goodman, the Gerber, the ASME-elliptic, and yielding. The diagram shows that only the Soderberg criterion guards against any yielding, but is biased low.

Considering the modified Goodman line as a criterion, point *A* represents a limiting point with an alternating strength  $S_a$  and midrange strength  $S_m$ . The slope of the load line shown is defined as  $r = S_a/S_m$ .

The criterion equation for the Soderberg line is

$$\frac{S_a}{S_e} + \frac{S_m}{S_y} = 1 \quad (6-40)$$

Similarly, we find the modified Goodman relation to be

$$\frac{S_a}{S_e} + \frac{S_m}{S_{ut}} = 1 \quad (6-41)$$

Examination of Fig. 6–25 shows that both a parabola and an ellipse have a better opportunity to pass among the midrange tension data and to permit quantification of the probability of failure. The Gerber failure criterion is written as

$$\frac{S_a}{S_e} + \left( \frac{S_m}{S_{ut}} \right)^2 = 1 \quad (6-42)$$

and the ASME-elliptic is written as

$$\left( \frac{S_a}{S_e} \right)^2 + \left( \frac{S_m}{S_y} \right)^2 = 1 \quad (6-43)$$

The *Langer* first-cycle-yielding criterion is used in connection with the fatigue curve:

$$S_a + S_m = S_y \quad (6-44)$$

The stresses  $n\sigma_a$  and  $n\sigma_m$  can replace  $S_a$  and  $S_m$ , where  $n$  is the design factor or factor of safety. Then, Eq. (6–40), the Soderberg line, becomes

$$\text{Soderberg} \quad \frac{\sigma_a}{S_e} + \frac{\sigma_m}{S_y} = \frac{1}{n} \quad (6-45)$$

Equation (6–41), the modified Goodman line, becomes

$$\text{mod-Goodman} \quad \frac{\sigma_a}{S_e} + \frac{\sigma_m}{S_{ut}} = \frac{1}{n} \quad (6-46)$$

Equation (6–42), the Gerber line, becomes

$$\text{Gerber} \quad \frac{n\sigma_a}{S_e} + \left( \frac{n\sigma_m}{S_{ut}} \right)^2 = 1 \quad (6-47)$$

Equation (6–43), the ASME-elliptic line, becomes

$$\text{ASME-elliptic} \quad \left( \frac{n\sigma_a}{S_e} \right)^2 + \left( \frac{n\sigma_m}{S_y} \right)^2 = 1 \quad (6-48)$$

We will emphasize the Gerber and ASME-elliptic for fatigue failure criterion and the Langer for first-cycle yielding. However, conservative designers often use the modified Goodman criterion, so we will continue to include it in our discussions. The design equation for the Langer first-cycle-yielding is

$$\text{Langer static yield} \quad \sigma_a + \sigma_m = \frac{S_y}{n} \quad (6-49)$$

The failure criteria are used in conjunction with a load line,  $r = S_a/S_m = \sigma_a/\sigma_m$ . Principal intersections are tabulated in Tables 6–6 to 6–8. Formal expressions for fatigue factor of safety are given in the lower panel of Tables 6–6 to 6–8. The first row of each table corresponds to the fatigue criterion, the second row is the static Langer criterion, and the third row corresponds to the intersection of the static and fatigue

**Table 6–6**

Amplitude and Steady  
Coordinates of Strength  
and Important  
Intersections in First  
Quadrant for Modified  
Goodman and Langer  
Failure Criteria

Intersecting Equations	Intersection Coordinates
$\frac{S_a}{S_e} + \frac{S_m}{S_{ut}} = 1$	$S_a = \frac{r S_e S_{ut}}{r S_{ut} + S_e}$
Load line $r = \frac{S_a}{S_m}$	$S_m = \frac{S_a}{r}$
$\frac{S_a}{S_y} + \frac{S_m}{S_y} = 1$	$S_a = \frac{r S_y}{1 + r}$
Load line $r = \frac{S_a}{S_m}$	$S_m = \frac{S_y}{1 + r}$
$\frac{S_a}{S_e} + \frac{S_m}{S_{ut}} = 1$	$S_m = \frac{(S_y - S_e) S_{ut}}{S_{ut} - S_e}$
$\frac{S_a}{S_y} + \frac{S_m}{S_y} = 1$	$S_a = S_y - S_m, r_{crit} = S_a/S_m$

Fatigue factor of safety

$$n_f = \frac{1}{\frac{\sigma_a}{S_e} + \frac{\sigma_m}{S_{ut}}}$$

**Table 6–7**

Amplitude and Steady  
Coordinates of Strength  
and Important  
Intersections in First  
Quadrant for Gerber  
and Langer Failure  
Criteria

Intersecting Equations	Intersection Coordinates
$\frac{S_a}{S_e} + \left(\frac{S_m}{S_{ut}}\right)^2 = 1$	$S_a = \frac{r^2 S_{ut}^2}{2 S_e} \left[ -1 + \sqrt{1 + \left(\frac{2 S_e}{r S_{ut}}\right)^2} \right]$
Load line $r = \frac{S_a}{S_m}$	$S_m = \frac{S_a}{r}$
$\frac{S_a}{S_y} + \frac{S_m}{S_y} = 1$	$S_a = \frac{r S_y}{1 + r}$
Load line $r = \frac{S_a}{S_m}$	$S_m = \frac{S_y}{1 + r}$
$\frac{S_a}{S_e} + \left(\frac{S_m}{S_{ut}}\right)^2 = 1$	$S_m = \frac{S_{ut}^2}{2 S_e} \left[ 1 - \sqrt{1 + \left(\frac{2 S_e}{S_{ut}}\right)^2 \left(1 - \frac{S_y}{S_e}\right)} \right]$
$\frac{S_a}{S_y} + \frac{S_m}{S_y} = 1$	$S_a = S_y - S_m, r_{crit} = S_a/S_m$

Fatigue factor of safety

$$n_f = \frac{1}{2} \left( \frac{S_{ut}}{\sigma_m} \right)^2 \frac{\sigma_a}{S_e} \left[ -1 + \sqrt{1 + \left( \frac{2 \sigma_m S_e}{S_{ut} \sigma_a} \right)^2} \right] \quad \sigma_m > 0$$

**Table 6-8**

Amplitude and Steady Coordinates of Strength and Important Intersections in First Quadrant for ASME-Elliptic and Langer Failure Criteria

Intersecting Equations	Intersection Coordinates
$\left(\frac{S_a}{S_e}\right)^2 + \left(\frac{S_m}{S_y}\right)^2 = 1$ <p>Load line <math>r = S_a/S_m</math></p>	$S_a = \sqrt{\frac{r^2 S_e^2 S_y^2}{S_e^2 + r^2 S_y^2}}$ $S_m = \frac{S_a}{r}$
$\frac{S_a}{S_y} + \frac{S_m}{S_y} = 1$ <p>Load line <math>r = S_a/S_m</math></p>	$S_a = \frac{r S_y}{1 + r}$ $S_m = \frac{S_y}{1 + r}$
$\left(\frac{S_a}{S_e}\right)^2 + \left(\frac{S_m}{S_y}\right)^2 = 1$ $\frac{S_a}{S_y} + \frac{S_m}{S_y} = 1$	$S_a = 0, \frac{2 S_y S_e^2}{S_e^2 + S_y^2}$ $S_m = S_y - S_a, r_{crit} = S_a/S_m$
<p>Fatigue factor of safety</p> $n_f = \sqrt{\frac{1}{(\sigma_a/S_e)^2 + (\sigma_m/S_y)^2}}$	

criteria. The first column gives the intersecting equations and the second column the intersection coordinates.

There are two ways to proceed with a typical analysis. One method is to assume that fatigue occurs first and use one of Eqs. (6-45) to (6-48) to determine  $n$  or size, depending on the task. Most often fatigue is the governing failure mode. Then follow with a static check. If static failure governs then the analysis is repeated using Eq. (6-49).

Alternatively, one could use the tables. Determine the load line and establish which criterion the load line intersects first and use the corresponding equations in the tables.

Some examples will help solidify the ideas just discussed.

**EXAMPLE 6-10**

A 1.5-in-diameter bar has been machined from an AISI 1050 cold-drawn bar. This part is to withstand a fluctuating tensile load varying from 0 to 16 kip. Because of the ends, and the fillet radius, a fatigue stress-concentration factor  $K_f$  is 1.85 for  $10^6$  or larger life. Find  $S_a$  and  $S_m$  and the factor of safety guarding against fatigue and first-cycle yielding, using (a) the Gerber fatigue line and (b) the ASME-elliptic fatigue line.

**Solution**

We begin with some preliminaries. From Table A-20,  $S_{ut} = 100$  kpsi and  $S_y = 84$  kpsi. Note that  $F_a = F_m = 8$  kip. The Marin factors are, deterministically,

$$k_a = 2.70(100)^{-0.265} = 0.797; \text{ Eq. (6-19), Table 6-2, p. 279}$$

$$k_b = 1 \text{ (axial loading, see } k_c \text{)}$$

$k_c = 0.85$ : Eq. (6-26), p. 282

$k_d = k_e = k_f = 1$

$S_e = 0.797(1)0.850(1)(1)(1)0.5(100) = 33.9$  kpsi: Eqs. (6-8), (6-18), p. 274, p. 279

The nominal axial stress components  $\sigma_{ao}$  and  $\sigma_{mo}$  are

$$\sigma_{ao} = \frac{4F_a}{\pi d^2} = \frac{4(8)}{\pi 1.5^2} = 4.53 \text{ kpsi} \quad \sigma_{mo} = \frac{4F_m}{\pi d^2} = \frac{4(8)}{\pi 1.5^2} = 4.53 \text{ kpsi}$$

Applying  $K_f$  to both components  $\sigma_{ao}$  and  $\sigma_{mo}$  constitutes a prescription of no notch yielding:

$$\sigma_a = K_f \sigma_{ao} = 1.85(4.53) = 8.38 \text{ kpsi} = \sigma_m$$

(a) Let us calculate the factors of safety first. From the bottom panel from Table 6-7 the factor of safety for fatigue is

Answer 
$$n_f = \frac{1}{2} \left( \frac{100}{8.38} \right)^2 \left( \frac{8.38}{33.9} \right) \left\{ -1 + \sqrt{1 + \left[ \frac{2(8.38)33.9}{100(8.38)} \right]^2} \right\} = 3.66$$

From Eq. (6-49) the factor of safety guarding against first-cycle yield is

Answer 
$$n_y = \frac{S_y}{\sigma_a + \sigma_m} = \frac{84}{8.38 + 8.38} = 5.01$$

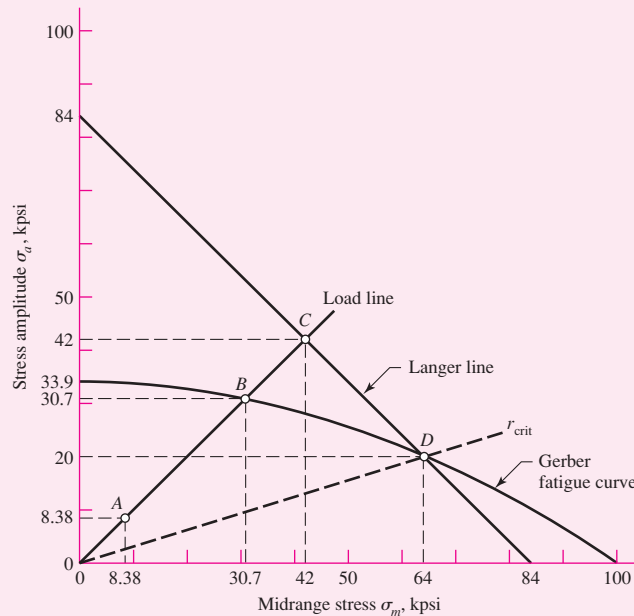
Thus, we see that fatigue will occur first and the factor of safety is 3.68. This can be seen in Fig. 6-28 where the load line intersects the Gerber fatigue curve first at point  $B$ . If the plots are created to true scale it would be seen that  $n_f = OB/OA$ .

From the first panel of Table 6-7,  $r = \sigma_a/\sigma_m = 1$ ,

Answer 
$$S_a = \frac{(1)^2 100^2}{2(33.9)} \left\{ -1 + \sqrt{1 + \left[ \frac{2(33.9)}{(1)100} \right]^2} \right\} = 30.7 \text{ kpsi}$$

**Figure 6-28**

Principal points  $A$ ,  $B$ ,  $C$ , and  $D$  on the designer's diagram drawn for Gerber, Langer, and load line.



Answer

$$S_m = \frac{S_a}{r} = \frac{30.7}{1} = 30.7 \text{ kpsi}$$

As a check on the previous result,  $n_f = OB/OA = S_a/\sigma_a = S_m/\sigma_m = 30.7/8.38 = 3.66$  and we see total agreement.

We could have detected that fatigue failure would occur first without drawing Fig. 6–28 by calculating  $r_{crit}$ . From the third row third column panel of Table 6–7, the intersection point between fatigue and first-cycle yield is

$$S_m = \frac{100^2}{2(33.9)} \left[ 1 - \sqrt{1 + \left( \frac{2(33.9)}{100} \right)^2 \left( 1 - \frac{84}{33.9} \right)} \right] = 64.0 \text{ kpsi}$$

$$S_a = S_y - S_m = 84 - 64 = 20 \text{ kpsi}$$

The critical slope is thus

$$r_{crit} = \frac{S_a}{S_m} = \frac{20}{64} = 0.312$$

which is less than the actual load line of  $r = 1$ . This indicates that fatigue occurs before first-cycle-yield.

(b) Repeating the same procedure for the ASME-elliptic line, for fatigue

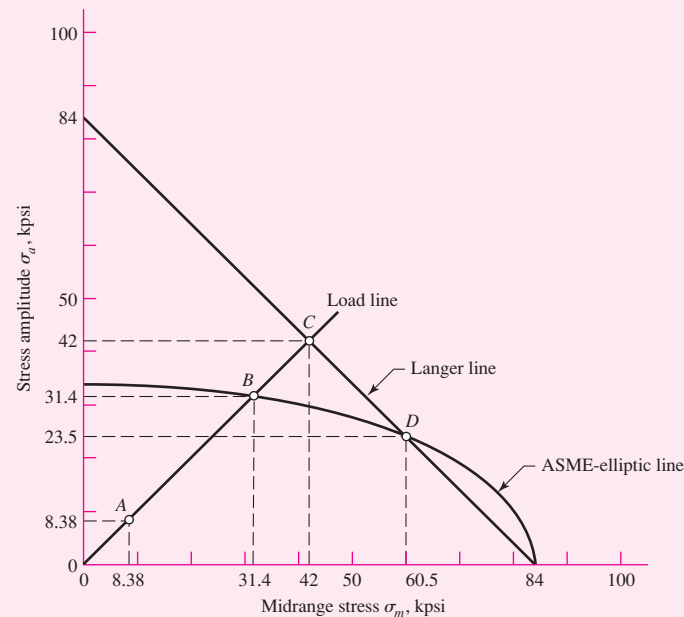
Answer

$$n_f = \sqrt{\frac{1}{(8.38/33.9)^2 + (8.38/84)^2}} = 3.75$$

Again, this is less than  $n_y = 5.01$  and fatigue is predicted to occur first. From the first row second column panel of Table 6–8, with  $r = 1$ , we obtain the coordinates  $S_a$  and  $S_m$  of point  $B$  in Fig. 6–29 as

**Figure 6–29**

Principal points  $A$ ,  $B$ ,  $C$ , and  $D$  on the designer's diagram drawn for ASME-elliptic, Langer, and load lines.



**Answer**

$$S_a = \sqrt{\frac{(1)^2 33.9^2 (84)^2}{33.9^2 + (1)^2 84^2}} = 31.4 \text{ kpsi}, \quad S_m = \frac{S_a}{r} = \frac{31.4}{1} = 31.4 \text{ kpsi}$$

To verify the fatigue factor of safety,  $n_f = S_a/\sigma_a = 31.4/8.38 = 3.75$ .

As before, let us calculate  $r_{\text{crit}}$ . From the third row second column panel of Table 6-8,

$$S_a = \frac{2(84)33.9^2}{33.9^2 + 84^2} = 23.5 \text{ kpsi}, \quad S_m = S_y - S_a = 84 - 23.5 = 60.5 \text{ kpsi}$$

$$r_{\text{crit}} = \frac{S_a}{S_m} = \frac{23.5}{60.5} = 0.388$$

which again is less than  $r = 1$ , verifying that fatigue occurs first with  $n_f = 3.75$ .

The Gerber and the ASME-elliptic fatigue failure criteria are very close to each other and are used interchangeably. The ANSI/ASME Standard B106.1M-1985 uses ASME-elliptic for shafting.

**EXAMPLE 6-11**

A flat-leaf spring is used to retain an oscillating flat-faced follower in contact with a plate cam. The follower range of motion is 2 in and fixed, so the alternating component of force, bending moment, and stress is fixed, too. The spring is preloaded to adjust to various cam speeds. The preload must be increased to prevent follower float or jump. For lower speeds the preload should be decreased to obtain longer life of cam and follower surfaces. The spring is a steel cantilever 32 in long, 2 in wide, and  $\frac{1}{4}$  in thick, as seen in Fig. 6-30a. The spring strengths are  $S_{ut} = 150$  kpsi,  $S_y = 127$  kpsi, and  $S_e = 28$  kpsi fully corrected. The total cam motion is 2 in. The designer wishes to preload the spring by deflecting it 2 in for low speed and 5 in for high speed.

(a) Plot the Gerber-Langer failure lines with the load line.

(b) What are the strength factors of safety corresponding to 2 in and 5 in preload?

**Solution**

We begin with preliminaries. The second area moment of the cantilever cross section is

$$I = \frac{bh^3}{12} = \frac{2(0.25)^3}{12} = 0.00260 \text{ in}^4$$

Since, from Table A-9, beam 1, force  $F$  and deflection  $y$  in a cantilever are related by  $F = 3EIy/l^3$ , then stress  $\sigma$  and deflection  $y$  are related by

$$\sigma = \frac{Mc}{I} = \frac{32Fc}{I} = \frac{32(3EIy)c}{l^3 I} = \frac{96Ecy}{l^3} = Ky$$

$$\text{where } K = \frac{96Ec}{l^3} = \frac{96(30 \cdot 10^6)(0.125)}{32^3} = 10.99(10^3) \text{ psi/in} = 10.99 \text{ kpsi/in}$$

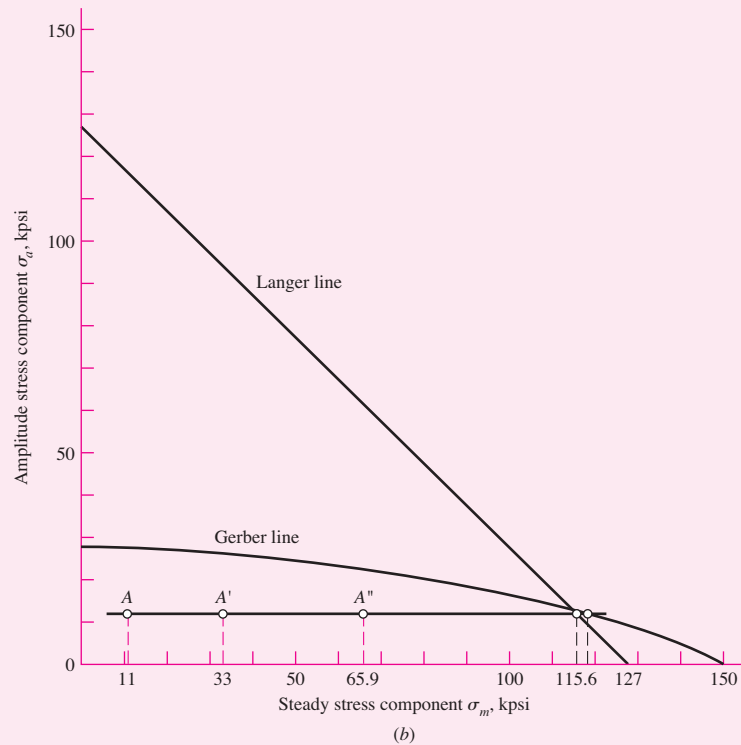
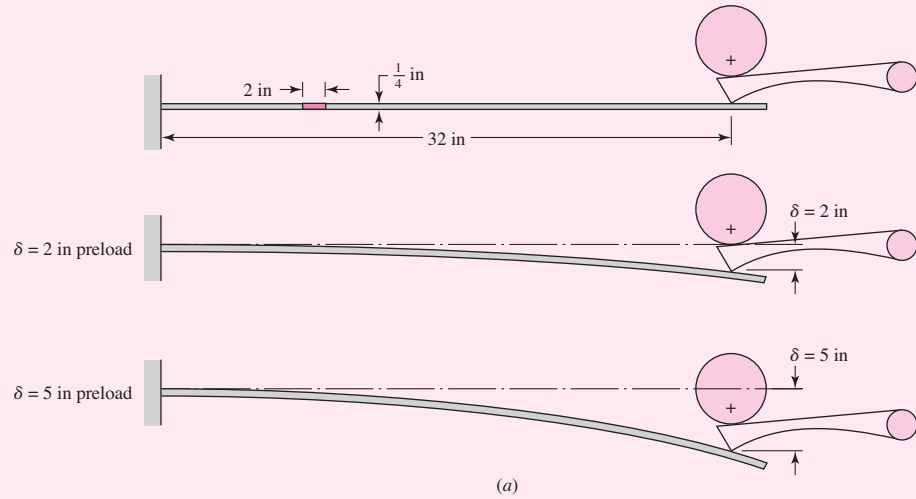
Now the minimums and maximums of  $y$  and  $\sigma$  can be defined by

$$\begin{aligned} y_{\min} &= \delta & y_{\max} &= 2 + \delta \\ \sigma_{\min} &= K\delta & \sigma_{\max} &= K(2 + \delta) \end{aligned}$$



**Figure 6-30**

Cam follower retaining spring.  
 (a) Geometry; (b) designer's  
 fatigue diagram for Ex. 6-11.



The stress components are thus

$$\sigma_a = \frac{K(2 + \delta) - K\delta}{2} = K = 10.99 \text{ kpsi}$$

$$\sigma_m = \frac{K(2 + \delta) + K\delta}{2} = K(1 + \delta) = 10.99(1 + \delta)$$

$$\text{For } \delta = 0, \quad \sigma_a = \sigma_m = 10.99 = 11 \text{ kpsi}$$

$$\text{For } \delta = 2 \text{ in,} \quad \sigma_a = 11 \text{ kpsi, } \sigma_m = 10.99(1 + 2) = 33 \text{ kpsi}$$

$$\text{For } \delta = 5 \text{ in,} \quad \sigma_a = 11 \text{ kpsi, } \sigma_m = 10.99(1 + 5) = 65.9 \text{ kpsi}$$

(a) A plot of the Gerber and Langer criteria is shown in Fig. 6–30b. The three preload deflections of 0, 2, and 5 in are shown as points A, A', and A''. Note that since  $\sigma_a$  is constant at 11 kpsi, the load line is horizontal and does not contain the origin. The intersection between the Gerber line and the load line is found from solving Eq. (6–42) for  $S_m$  and substituting 11 kpsi for  $S_a$ :

$$S_m = S_{ut} \sqrt{1 - \frac{S_a}{S_e}} = 150 \sqrt{1 - \frac{11}{28}} = 116.9 \text{ kpsi}$$

The intersection of the Langer line and the load line is found from solving Eq. (6–44) for  $S_m$  and substituting 11 kpsi for  $S_a$ :

$$S_m = S_y - S_a = 127 - 11 = 116 \text{ kpsi}$$

The threats from fatigue and first-cycle yielding are approximately equal.

(b) For  $\delta = 2 \text{ in}$ ,

Answer 
$$n_f = \frac{S_m}{\sigma_m} = \frac{116.9}{33} = 3.54 \quad n_y = \frac{116}{33} = 3.52$$

and for  $\delta = 5 \text{ in}$ ,

Answer 
$$n_f = \frac{116.9}{65.9} = 1.77 \quad n_y = \frac{116}{65.9} = 1.76$$

### EXAMPLE 6–12

A steel bar undergoes cyclic loading such that  $\sigma_{\max} = 60 \text{ kpsi}$  and  $\sigma_{\min} = -20 \text{ kpsi}$ . For the material,  $S_{ut} = 80 \text{ kpsi}$ ,  $S_y = 65 \text{ kpsi}$ , a fully corrected endurance limit of  $S_e = 40 \text{ kpsi}$ , and  $f = 0.9$ . Estimate the number of cycles to a fatigue failure using:

(a) Modified Goodman criterion.

(b) Gerber criterion.

Solution From the given stresses,

$$\sigma_a = \frac{60 - (-20)}{2} = 40 \text{ kpsi} \quad \sigma_m = \frac{60 + (-20)}{2} = 20 \text{ kpsi}$$

From the material properties, Eqs. (6–14) to (6–16), p. 277, give

$$a = \frac{(f S_{ut})^2}{S_e} = \frac{[0.9(80)]^2}{40} = 129.6 \text{ kpsi}$$

$$b = -\frac{1}{3} \log \left( \frac{f S_{ut}}{S_e} \right) = -\frac{1}{3} \log \left[ \frac{0.9(80)}{40} \right] = -0.0851$$

$$N = \left( \frac{S_f}{a} \right)^{1/b} = \left( \frac{S_f}{129.6} \right)^{-1/0.0851} \quad (1)$$

where  $S_f$  replaced  $\sigma_a$  in Eq. (6–16).

(a) The modified Goodman line is given by Eq. (6-46), p. 298, where the endurance limit  $S_e$  is used for infinite life. For finite life at  $S_f > S_e$ , replace  $S_e$  with  $S_f$  in Eq. (6-46) and rearrange giving

$$S_f = \frac{\sigma_a}{1 - \frac{\sigma_m}{S_{ut}}} = \frac{40}{1 - \frac{20}{80}} = 53.3 \text{ kpsi}$$

Substituting this into Eq. (1) yields

Answer 
$$N = \left( \frac{53.3}{129.6} \right)^{-1/0.0851} \doteq 3.4(10^4) \text{ cycles}$$

(b) For Gerber, similar to part (a), from Eq. (6-47),

$$S_f = \frac{\sigma_a}{1 - \left( \frac{\sigma_m}{S_{ut}} \right)^2} = \frac{40}{1 - \left( \frac{20}{80} \right)^2} = 42.7 \text{ kpsi}$$

Again, from Eq. (1),

Answer 
$$N = \left( \frac{42.7}{129.6} \right)^{-1/0.0851} \doteq 4.6(10^5) \text{ cycles}$$

Comparing the answers, we see a large difference in the results. Again, the modified Goodman criterion is conservative as compared to Gerber for which the moderate difference in  $S_f$  is then magnified by a logarithmic  $S, N$  relationship.

For many *brittle* materials, the first quadrant fatigue failure criteria follows a concave upward Smith-Dolan locus represented by

$$\frac{S_a}{S_e} = \frac{1 - S_m/S_{ut}}{1 + S_m/S_{ut}} \quad (6-50)$$

or as a design equation,

$$\frac{n\sigma_a}{S_e} = \frac{1 - n\sigma_m/S_{ut}}{1 + n\sigma_m/S_{ut}} \quad (6-51)$$

For a radial load line of slope  $r$ , we substitute  $S_a/r$  for  $S_m$  in Eq. (6-50) and solve for  $S_a$ , obtaining

$$S_a = \frac{r S_{ut} + S_e}{2} \left[ -1 + \sqrt{1 + \frac{4r S_{ut} S_e}{(r S_{ut} + S_e)^2}} \right] \quad (6-52)$$

The fatigue diagram for a brittle material differs markedly from that of a ductile material because:

- Yielding is not involved since the material may not have a yield strength.
- Characteristically, the compressive ultimate strength exceeds the ultimate tensile strength severalfold.

- First-quadrant fatigue failure locus is concave-upward (Smith-Dolan), for example, and as flat as Goodman. Brittle materials are more sensitive to midrange stress, being lowered, but compressive midrange stresses are beneficial.
- Not enough work has been done on brittle fatigue to discover insightful generalities, so we stay in the first and a bit of the second quadrant.

The most likely domain of designer use is in the range from  $-S_{ut} \leq \sigma_m \leq S_{ut}$ . The locus in the first quadrant is Goodman, Smith-Dolan, or something in between. The portion of the second quadrant that is used is represented by a straight line between the points  $-S_{ut}$ ,  $S_{ut}$  and  $0$ ,  $S_e$ , which has the equation

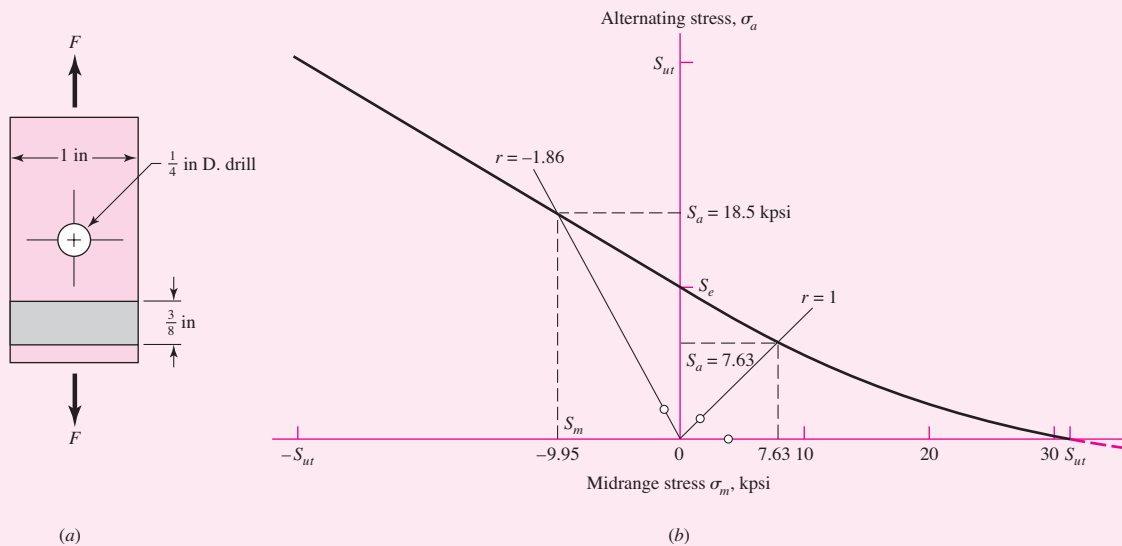
$$S_a = S_e + \left( \frac{S_e}{S_{ut}} - 1 \right) S_m \quad -S_{ut} \leq S_m \leq 0 \quad (\text{for cast iron}) \quad (6-53)$$

Table A-24 gives properties of gray cast iron. The endurance limit stated is really  $k_a k_b S'_e$  and only corrections  $k_c$ ,  $k_d$ ,  $k_e$ , and  $k_f$  need be made. The average  $k_c$  for axial and torsional loading is 0.9.

### EXAMPLE 6-13

A grade 30 gray cast iron is subjected to a load  $F$  applied to a 1 by  $\frac{3}{8}$ -in cross-section link with a  $\frac{1}{4}$ -in-diameter hole drilled in the center as depicted in Fig. 6-31a. The surfaces are machined. In the neighborhood of the hole, what is the factor of safety guarding against failure under the following conditions:

- The load  $F = 1000$  lbf tensile, steady.
  - The load is 1000 lbf repeatedly applied.
  - The load fluctuates between  $-1000$  lbf and 300 lbf without column action.
- Use the Smith-Dolan fatigue locus.



**Figure 6-31**

The grade 30 cast-iron part in axial fatigue with (a) its geometry displayed and (b) its designer's fatigue diagram for the circumstances of Ex. 6-13.

**Solution** Some preparatory work is needed. From Table A-24,  $S_{ut} = 31$  kpsi,  $S_{uc} = 109$  kpsi,  $k_a k_b S'_e = 14$  kpsi. Since  $k_c$  for axial loading is 0.9, then  $S_e = (k_a k_b S'_e) k_c = 14(0.9) = 12.6$  kpsi. From Table A-15-1,  $A = t(w - d) = 0.375(1 - 0.25) = 0.281$  in<sup>2</sup>,  $d/w = 0.25/1 = 0.25$ , and  $K_t = 2.45$ . The notch sensitivity for cast iron is 0.20 (see p. 288), so

$$K_f = 1 + q(K_t - 1) = 1 + 0.20(2.45 - 1) = 1.29$$

$$(a) \quad \sigma_a = \frac{K_f F_a}{A} = \frac{1.29(0)}{0.281} = 0 \quad \sigma_m = \frac{K_f F_m}{A} = \frac{1.29(1000)}{0.281}(10^{-3}) = 4.59 \text{ kpsi}$$

and

$$\text{Answer} \quad n = \frac{S_{ut}}{\sigma_m} = \frac{31.0}{4.59} = 6.75$$

$$(b) \quad F_a = F_m = \frac{F}{2} = \frac{1000}{2} = 500 \text{ lbf}$$

$$\sigma_a = \sigma_m = \frac{K_f F_a}{A} = \frac{1.29(500)}{0.281}(10^{-3}) = 2.30 \text{ kpsi}$$

$$r = \frac{\sigma_a}{\sigma_m} = 1$$

From Eq. (6-52),

$$S_a = \frac{(1)31 + 12.6}{2} \left[ -1 + \sqrt{1 + \frac{4(1)31(12.6)}{[(1)31 + 12.6]^2}} \right] = 7.63 \text{ kpsi}$$

$$\text{Answer} \quad n = \frac{S_a}{\sigma_a} = \frac{7.63}{2.30} = 3.32$$

$$(c) \quad F_a = \frac{1}{2}|300 - (-1000)| = 650 \text{ lbf} \quad \sigma_a = \frac{1.29(650)}{0.281}(10^{-3}) = 2.98 \text{ kpsi}$$

$$F_m = \frac{1}{2}[300 + (-1000)] = -350 \text{ lbf} \quad \sigma_m = \frac{1.29(-350)}{0.281}(10^{-3}) = -1.61 \text{ kpsi}$$

$$r = \frac{\sigma_a}{\sigma_m} = \frac{3.0}{-1.61} = -1.86$$

From Eq. (6-53),  $S_a = S_e + (S_e/S_{ut} - 1)S_m$  and  $S_m = S_a/r$ . It follows that

$$S_a = \frac{S_e}{1 - \frac{1}{r} \left( \frac{S_e}{S_{ut}} - 1 \right)} = \frac{12.6}{1 - \frac{1}{-1.86} \left( \frac{12.6}{31} - 1 \right)} = 18.5 \text{ kpsi}$$

$$\text{Answer} \quad n = \frac{S_a}{\sigma_a} = \frac{18.5}{2.98} = 6.20$$

Figure 6-31b shows the portion of the designer's fatigue diagram that was constructed.

### 6-13 Torsional Fatigue Strength under Fluctuating Stresses

Extensive tests by Smith<sup>23</sup> provide some very interesting results on pulsating torsional fatigue. Smith's first result, based on 72 tests, shows that the existence of a torsional steady-stress component not more than the torsional yield strength has no effect on the torsional endurance limit, provided the material is *ductile, polished, notch-free, and cylindrical*.

Smith's second result applies to materials with stress concentration, notches, or surface imperfections. In this case, he finds that the torsional fatigue limit decreases monotonically with torsional steady stress. Since the great majority of parts will have surfaces that are less than perfect, this result indicates Gerber, ASME-elliptic, and other approximations are useful. Joerres of Associated Spring-Barnes Group, confirms Smith's results and recommends the use of the modified Goodman relation for pulsating torsion. In constructing the Goodman diagram, Joerres uses

$$S_{su} = 0.67S_{ut} \quad (6-54)$$

Also, from Chap. 5,  $S_{sy} = 0.577S_{yt}$  from distortion-energy theory, and the mean load factor  $k_c$  is given by Eq. (6-26), or 0.577. This is discussed further in Chap. 10.

### 6-14 Combinations of Loading Modes

It may be helpful to think of fatigue problems as being in three categories:

- Completely reversing simple loads
- Fluctuating simple loads
- *Combinations of loading modes*

The simplest category is that of a completely reversed single stress which is handled with the  $S$ - $N$  diagram, relating the alternating stress to a life. Only one type of loading is allowed here, and the midrange stress must be zero. The next category incorporates general fluctuating loads, using a criterion to relate midrange and alternating stresses (modified Goodman, Gerber, ASME-elliptic, or Soderberg). Again, only *one* type of loading is allowed at a time. The third category, which we will develop in this section, involves cases where there are combinations of different types of loading, such as combined bending, torsion, and axial.

In Sec. 6-9 we learned that a load factor  $k_c$  is used to obtain the endurance limit, and hence the result is dependent on whether the loading is axial, bending, or torsion. In this section we want to answer the question, "How do we proceed when the loading is a *mixture* of, say, axial, bending, and torsional loads?" This type of loading introduces a few complications in that there may now exist combined normal and shear stresses, each with alternating and midrange values, and several of the factors used in determining the endurance limit depend on the type of loading. There may also be multiple stress-concentration factors, one for each mode of loading. The problem of how to deal with combined stresses was encountered when developing static failure theories. The distortion energy failure theory proved to be a satisfactory method of combining the

<sup>23</sup>James O. Smith, "The Effect of Range of Stress on the Fatigue Strength of Metals," *Univ. of Ill. Eng. Exp. Sta. Bull.* 334, 1942.

multiple stresses on a stress element into a single equivalent von Mises stress. The same approach will be used here.

The first step is to generate *two* stress elements—one for the alternating stresses and one for the midrange stresses. Apply the appropriate fatigue stress concentration factors to each of the stresses; i.e., apply  $(K_f)_{\text{bending}}$  for the bending stresses,  $(K_{fs})_{\text{torsion}}$  for the torsional stresses, and  $(K_f)_{\text{axial}}$  for the axial stresses. Next, calculate an equivalent von Mises stress for each of these two stress elements,  $\sigma'_a$  and  $\sigma'_m$ . Finally, select a fatigue failure criterion (modified Goodman, Gerber, ASME-elliptic, or Soderberg) to complete the fatigue analysis. For the endurance limit,  $S_e$ , use the endurance limit modifiers,  $k_a$ ,  $k_b$ , and  $k_c$ , for bending. The torsional load factor,  $k_c = 0.59$  should not be applied as it is already accounted for in the von Mises stress calculation (see footnote 17 on page 282). The load factor for the axial load can be accounted for by dividing the alternating axial stress by the axial load factor of 0.85. For example, consider the common case of a shaft with bending stresses, torsional shear stresses, and axial stresses. For this case, the von Mises stress is of the form  $\sigma' = (\sigma_x^2 + 3\tau_{xy}^2)^{1/2}$ . Considering that the bending, torsional, and axial stresses have alternating and midrange components, the von Mises stresses for the two stress elements can be written as

$$\sigma'_a = \left\{ \left[ (K_f)_{\text{bending}}(\sigma_a)_{\text{bending}} + (K_f)_{\text{axial}} \frac{(\sigma_a)_{\text{axial}}}{0.85} \right]^2 + 3 \left[ (K_{fs})_{\text{torsion}}(\tau_a)_{\text{torsion}} \right]^2 \right\}^{1/2} \quad (6-55)$$

$$\sigma'_m = \left\{ \left[ (K_f)_{\text{bending}}(\sigma_m)_{\text{bending}} + (K_f)_{\text{axial}}(\sigma_m)_{\text{axial}} \right]^2 + 3 \left[ (K_{fs})_{\text{torsion}}(\tau_m)_{\text{torsion}} \right]^2 \right\}^{1/2} \quad (6-56)$$

For first-cycle localized yielding, the maximum von Mises stress is calculated. This would be done by first adding the axial and bending alternating and midrange stresses to obtain  $\sigma_{\text{max}}$  and adding the alternating and midrange shear stresses to obtain  $\tau_{\text{max}}$ . Then substitute  $\sigma_{\text{max}}$  and  $\tau_{\text{max}}$  into the equation for the von Mises stress. A simpler and more conservative method is to add Eq. (6-55) and Eq. (6-56). That is, let  $\sigma'_{\text{max}} \doteq \sigma'_a + \sigma'_m$ .

If the stress components are not in phase but have the same frequency, the maxima can be found by expressing each component in trigonometric terms, using phase angles, and then finding the sum. If two or more stress components have differing frequencies, the problem is difficult; one solution is to assume that the two (or more) components often reach an in-phase condition, so that their magnitudes are additive.

### EXAMPLE 6-14

A rotating shaft is made of 42- × 4-mm AISI 1018 cold-drawn steel tubing and has a 6-mm-diameter hole drilled transversely through it. Estimate the factor of safety guarding against fatigue and static failures using the Gerber and Langer failure criteria for the following loading conditions:

- The shaft is subjected to a completely reversed torque of 120 N · m in phase with a completely reversed bending moment of 150 N · m.
- The shaft is subjected to a pulsating torque fluctuating from 20 to 160 N · m and a steady bending moment of 150 N · m.

### Solution

Here we follow the procedure of estimating the strengths and then the stresses, followed by relating the two.



From Table A-20 we find the minimum strengths to be  $S_{ut} = 440$  MPa and  $S_y = 370$  MPa. The endurance limit of the rotating-beam specimen is  $0.5(440) = 220$  MPa. The surface factor, obtained from Eq. (6-19) and Table 6-2, p. 279 is

$$k_a = 4.51 S_{ut}^{-0.265} = 4.51(440)^{-0.265} = 0.899$$

From Eq. (6-20) the size factor is

$$k_b = \left( \frac{d}{7.62} \right)^{-0.107} = \left( \frac{42}{7.62} \right)^{-0.107} = 0.833$$

The remaining Marin factors are all unity, so the modified endurance strength  $S_e$  is

$$S_e = 0.899(0.833)220 = 165 \text{ MPa}$$

(a) Theoretical stress-concentration factors are found from Table A-16. Using  $a/D = 6/42 = 0.143$  and  $d/D = 34/42 = 0.810$ , and using linear interpolation, we obtain  $A = 0.798$  and  $K_t = 2.366$  for bending; and  $A = 0.89$  and  $K_{ts} = 1.75$  for torsion. Thus, for bending,

$$Z_{\text{net}} = \frac{\pi A}{32D} (D^4 - d^4) = \frac{\pi(0.798)}{32(42)} [(42)^4 - (34)^4] = 3.31 (10^3) \text{ mm}^3$$

and for torsion

$$J_{\text{net}} = \frac{\pi A}{32} (D^4 - d^4) = \frac{\pi(0.89)}{32} [(42)^4 - (34)^4] = 155 (10^3) \text{ mm}^4$$

Next, using Figs. 6-20 and 6-21, pp. 287-288, with a notch radius of 3 mm we find the notch sensitivities to be 0.78 for bending and 0.96 for torsion. The two corresponding fatigue stress-concentration factors are obtained from Eq. (6-32) as

$$K_f = 1 + q(K_t - 1) = 1 + 0.78(2.366 - 1) = 2.07$$

$$K_{fs} = 1 + 0.96(1.75 - 1) = 1.72$$

The alternating bending stress is now found to be

$$\sigma_{xa} = K_f \frac{M}{Z_{\text{net}}} = 2.07 \frac{150}{3.31(10^{-6})} = 93.8(10^6) \text{ Pa} = 93.8 \text{ MPa}$$

and the alternating torsional stress is

$$\tau_{xya} = K_{fs} \frac{TD}{2J_{\text{net}}} = 1.72 \frac{120(42)(10^{-3})}{2(155)(10^{-9})} = 28.0(10^6) \text{ Pa} = 28.0 \text{ MPa}$$

The midrange von Mises component  $\sigma'_m$  is zero. The alternating component  $\sigma'_a$  is given by

$$\sigma'_a = (\sigma_{xa}^2 + 3\tau_{xya}^2)^{1/2} = [93.8^2 + 3(28^2)]^{1/2} = 105.6 \text{ MPa}$$

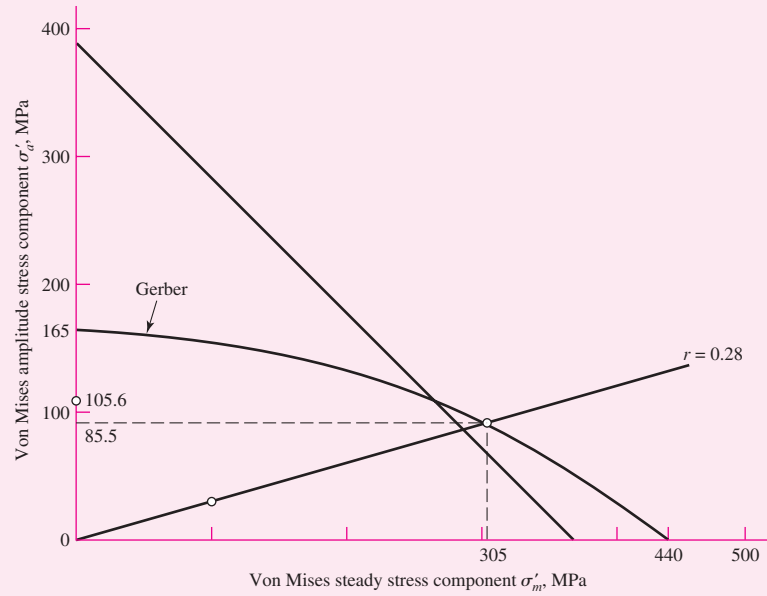
Since  $S_e = S_a$ , the fatigue factor of safety  $n_f$  is

$$n_f = \frac{S_a}{\sigma'_a} = \frac{165}{105.6} = 1.56$$

Answer

**Figure 6-32**

Designer's fatigue diagram for  
Ex. 6-14.



The first-cycle yield factor of safety is

**Answer**

$$n_y = \frac{S_y}{\sigma'_a} = \frac{370}{105.6} = 3.50$$

There is no localized yielding; the threat is from fatigue. See Fig. 6-32.

(b) This part asks us to find the factors of safety when the alternating component is due to pulsating torsion, and a steady component is due to both torsion and bending. We have  $T_a = (160 - 20)/2 = 70 \text{ N} \cdot \text{m}$  and  $T_m = (160 + 20)/2 = 90 \text{ N} \cdot \text{m}$ . The corresponding amplitude and steady-stress components are

$$\tau_{xya} = K_{fs} \frac{T_a D}{2J_{\text{net}}} = 1.72 \frac{70(42)(10^{-3})}{2(155)(10^{-9})} = 16.3(10^6) \text{ Pa} = 16.3 \text{ MPa}$$

$$\tau_{xym} = K_{fs} \frac{T_m D}{2J_{\text{net}}} = 1.72 \frac{90(42)(10^{-3})}{2(155)(10^{-9})} = 21.0(10^6) \text{ Pa} = 21.0 \text{ MPa}$$

The steady bending stress component  $\sigma_{xm}$  is

$$\sigma_{xm} = K_f \frac{M_m}{Z_{\text{net}}} = 2.07 \frac{150}{3.31(10^{-6})} = 93.8(10^6) \text{ Pa} = 93.8 \text{ MPa}$$

The von Mises components  $\sigma'_a$  and  $\sigma'_m$  are

$$\sigma'_a = [3(16.3)^2]^{1/2} = 28.2 \text{ MPa}$$

$$\sigma'_m = [93.8^2 + 3(21)^2]^{1/2} = 100.6 \text{ MPa}$$

From Table 6-7, p. 299, the fatigue factor of safety is

**Answer**

$$n_f = \frac{1}{2} \left( \frac{440}{100.6} \right)^2 \frac{28.2}{165} \left\{ -1 + \sqrt{1 + \left[ \frac{2(100.6)(165)}{440(28.2)} \right]^2} \right\} = 3.03$$

From the same table, with  $r = \sigma'_a / \sigma'_m = 28.2 / 100.6 = 0.280$ , the strengths can be shown to be  $S_a = 85.5$  MPa and  $S_m = 305$  MPa. See the plot in Fig. 6–32.

The first-cycle yield factor of safety  $n_y$  is

Answer

$$n_y = \frac{S_y}{\sigma'_a + \sigma'_m} = \frac{370}{28.2 + 100.6} = 2.87$$

There is no notch yielding. The likelihood of failure may first come from first-cycle yielding at the notch. See the plot in Fig. 6–32.

## 6–15 Varying, Fluctuating Stresses; Cumulative Fatigue Damage

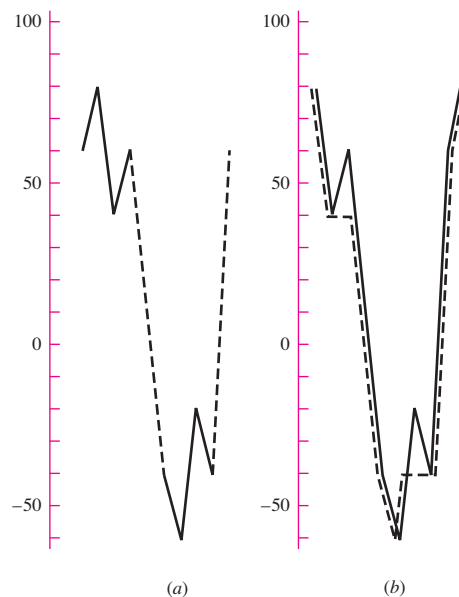
Instead of a single fully reversed stress history block composed of  $n$  cycles, suppose a machine part, at a critical location, is subjected to

- A fully reversed stress  $\sigma_1$  for  $n_1$  cycles,  $\sigma_2$  for  $n_2$  cycles, . . . , or
- A “wiggly” time line of stress exhibiting many and different peaks and valleys.

What stresses are significant, what counts as a cycle, and what is the measure of damage incurred? Consider a fully reversed cycle with stresses varying 60, 80, 40, and 60 kpsi and a second fully reversed cycle  $-40, -60, -20$ , and  $-40$  kpsi as depicted in Fig. 6–33*a*. First, it is clear that to impose the pattern of stress in Fig. 6–33*a* on a part it is necessary that the time trace look like the solid line plus the dashed line in Fig. 6–33*a*. Figure 6–33*b* moves the snapshot to exist beginning with 80 kpsi and ending with 80 kpsi. Acknowledging the existence of a single stress-time trace is to discover a “hidden” cycle shown as the dashed line in Fig. 6–33*b*. If there are 100 applications of the all-positive stress cycle, then 100 applications of the all-negative stress cycle, the

**Figure 6–33**

Variable stress diagram prepared for assessing cumulative damage.



hidden cycle is applied but once. If the all-positive stress cycle is applied alternately with the all-negative stress cycle, the hidden cycle is applied 100 times.

To ensure that the hidden cycle is not lost, begin on the snapshot with the largest (or smallest) stress and add previous history to the right side, as was done in Fig. 6-33*b*. Characterization of a cycle takes on a max–min–same max (or min–max–same min) form. We identify the hidden cycle first by moving along the dashed-line trace in Fig. 6-33*b* identifying a cycle with an 80-kpsi max, a 60-kpsi min, and returning to 80 kpsi. Mentally deleting the used part of the trace (the dashed line) leaves a 40, 60, 40 cycle and a –40, –20, –40 cycle. Since failure loci are expressed in terms of stress amplitude component  $\sigma_a$  and steady component  $\sigma_m$ , we use Eq. (6-36) to construct the table below:

Cycle Number	$\sigma_{\max}$	$\sigma_{\min}$	$\sigma_a$	$\sigma_m$
1	80	–60	70	10
2	60	40	10	50
3	–20	–40	10	–30

The most damaging cycle is number 1. It could have been lost.

Methods for counting cycles include:

- Number of tensile peaks to failure.
- All maxima above the waveform mean, all minima below.
- The global maxima between crossings above the mean and the global minima between crossings below the mean.
- All positive slope crossings of levels above the mean, and all negative slope crossings of levels below the mean.
- A modification of the preceding method with only one count made between successive crossings of a level associated with each counting level.
- Each local maxi-min excursion is counted as a half-cycle, and the associated amplitude is half-range.
- The preceding method plus consideration of the local mean.
- Rain-flow counting technique.

The method used here amounts to a variation of the *rain-flow counting technique*.

The *Palmgren-Miner*<sup>24</sup> *cycle-ratio summation rule*, also called *Miner's rule*, is written

$$\sum \frac{n_i}{N_i} = c \quad (6-57)$$

where  $n_i$  is the number of cycles at stress level  $\sigma_i$  and  $N_i$  is the number of cycles to failure at stress level  $\sigma_i$ . The parameter  $c$  has been determined by experiment; it is usually found in the range  $0.7 < c < 2.2$  with an average value near unity.

<sup>24</sup>A. Palmgren, "Die Lebensdauer von Kugellagern," *ZVDI*, vol. 68, pp. 339–341, 1924; M. A. Miner, "Cumulative Damage in Fatigue," *J. Appl. Mech.*, vol. 12, *Trans. ASME*, vol. 67, pp. A159–A164, 1945.

Using the deterministic formulation as a linear damage rule we write

$$D = \sum \frac{n_i}{N_i} \quad (6-58)$$

where  $D$  is the accumulated damage. When  $D = c = 1$ , failure ensues.

### EXAMPLE 6-15

Given a part with  $S_{ut} = 151$  kpsi and at the critical location of the part,  $S_e = 67.5$  kpsi. For the loading of Fig. 6-33, estimate the number of repetitions of the stress-time block in Fig. 6-33 that can be made before failure.

### Solution

From Fig. 6-18, p. 277, for  $S_{ut} = 151$  kpsi,  $f = 0.795$ . From Eq. (6-14),

$$a = \frac{(f S_{ut})^2}{S_e} = \frac{[0.795(151)]^2}{67.5} = 213.5 \text{ kpsi}$$

From Eq. (6-15),

$$b = -\frac{1}{3} \log \left( \frac{f S_{ut}}{S_e} \right) = -\frac{1}{3} \log \left[ \frac{0.795(151)}{67.5} \right] = -0.0833$$

So,

$$S_f = 213.5 N^{-0.0833} \quad N = \left( \frac{S_f}{213.5} \right)^{-1/0.0833} \quad (1), (2)$$

We prepare to add two columns to the previous table. Using the Gerber fatigue criterion, Eq. (6-47), p. 298, with  $S_e = S_f$ , and  $n = 1$ , we can write

$$S_f = \begin{cases} \frac{\sigma_a}{1 - (\sigma_m/S_{ut})^2} & \sigma_m > 0 \\ S_e & \sigma_m \leq 0 \end{cases} \quad (3)$$

Cycle 1:  $r = \sigma_a/\sigma_m = 70/10 = 7$ , and the strength amplitude from Table 6-7, p. 299, is

$$S_a = \frac{7^2 151^2}{2(67.5)} \left\{ -1 + \sqrt{1 + \left[ \frac{2(67.5)}{7(151)} \right]^2} \right\} = 67.2 \text{ kpsi}$$

Since  $\sigma_a > S_a$ , that is,  $70 > 67.2$ , life is reduced. From Eq. (3),

$$S_f = \frac{70}{1 - (10/151)^2} = 70.3 \text{ kpsi}$$

and from Eq. (2)

$$N = \left( \frac{70.3}{213.5} \right)^{-1/0.0833} = 619(10^3) \text{ cycles}$$

Cycle 2:  $r = 10/50 = 0.2$ , and the strength amplitude is

$$S_a = \frac{0.2^2 151^2}{2(67.5)} \left\{ -1 + \sqrt{1 + \left[ \frac{2(67.5)}{0.2(151)} \right]^2} \right\} = 24.2 \text{ kpsi}$$

Since  $\sigma_a < S_a$ , that is  $10 < 24.2$ , then  $S_f = S_e$  and indefinite life follows. Thus,  $N \rightarrow \infty$ .

Cycle 3:  $r = 10/-30 = -0.333$ , and since  $\sigma_m < 0$ ,  $S_f = S_e$ , indefinite life follows and  $N \rightarrow \infty$

Cycle Number	$S_f$ , kpsi	$N$ , cycles
1	70.3	$619(10^3)$
2	67.5	$\infty$
3	67.5	$\infty$

From Eq. (6-58) the damage per block is

$$D = \sum \frac{n_i}{N_i} = N \left[ \frac{1}{619(10^3)} + \frac{1}{\infty} + \frac{1}{\infty} \right] = \frac{N}{619(10^3)}$$

**Answer** Setting  $D = 1$  yields  $N = 619(10^3)$  cycles.

To further illustrate the use of the Miner rule, let us choose a steel having the properties  $S_{ut} = 80$  kpsi,  $S'_{e,0} = 40$  kpsi, and  $f = 0.9$ , where we have used the designation  $S'_{e,0}$  instead of the more usual  $S'_e$  to indicate the endurance limit of the *virgin*, or *undamaged*, material. The log  $S$ -log  $N$  diagram for this material is shown in Fig. 6-34 by the heavy solid line. Now apply, say, a reversed stress  $\sigma_1 = 60$  kpsi for  $n_1 = 3000$  cycles. Since  $\sigma_1 > S'_{e,0}$ , the endurance limit will be damaged, and we wish to find the new endurance limit  $S'_{e,1}$  of the damaged material using the Miner rule. The equation of the virgin material failure line in Fig. 6-34 in the  $10^3$  to  $10^6$  cycle range is

$$S_f = aN^b = 129.6N^{-0.085\ 091}$$

The cycles to failure at stress level  $\sigma_1 = 60$  kpsi are

$$N_1 = \left( \frac{\sigma_1}{129.6} \right)^{-1/0.085\ 091} = \left( \frac{60}{129.6} \right)^{-1/0.085\ 091} = 8520 \text{ cycles}$$

**Figure 6-34**

Use of the Miner rule to predict the endurance limit of a material that has been overstressed for a finite number of cycles.

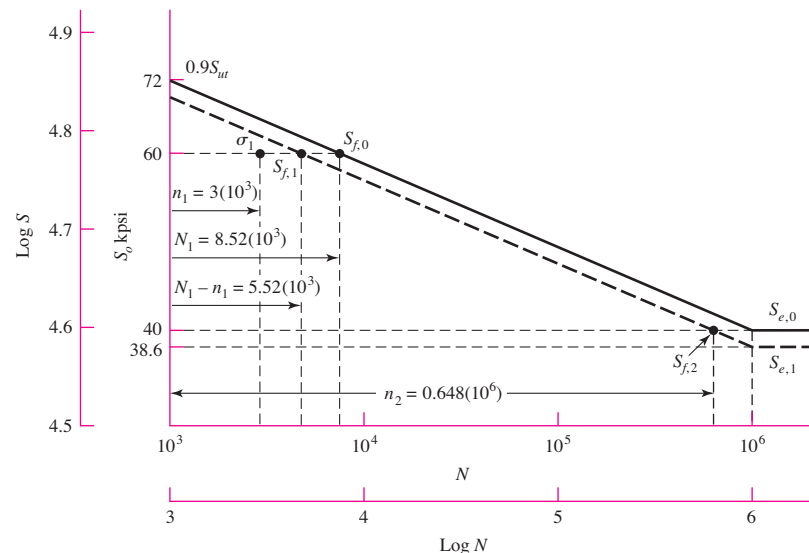


Figure 6–34 shows that the material has a life  $N_1 = 8520$  cycles at 60 kpsi, and consequently, after the application of  $\sigma_1$  for 3000 cycles, there are  $N_1 - n_1 = 5520$  cycles of life remaining at  $\sigma_1$ . This locates the finite-life strength  $S_{f,1}$  of the damaged material, as shown in Fig. 6–34. To get a second point, we ask the question: With  $n_1$  and  $N_1$  given, how many cycles of stress  $\sigma_2 = S'_{e,0}$  can be applied before the damaged material fails?

This corresponds to  $n_2$  cycles of stress reversal, and hence, from Eq. (6–58), we have

$$\frac{n_1}{N_1} + \frac{n_2}{N_2} = 1 \quad (a)$$

or

$$n_2 = \left(1 - \frac{n_1}{N_1}\right) N_2 \quad (b)$$

Then

$$n_2 = \left[1 - \frac{3(10)^3}{8.52(10)^3}\right] (10^6) = 0.648(10^6) \text{ cycles}$$

This corresponds to the finite-life strength  $S_{f,2}$  in Fig. 6–34. A line through  $S_{f,1}$  and  $S_{f,2}$  is the log  $S$ –log  $N$  diagram of the damaged material according to the Miner rule. The new endurance limit is  $S_{e,1} = 38.6$  kpsi.

We could leave it at this, but a little more investigation can be helpful. We have two points on the new fatigue locus,  $N_1 - n_1$ ,  $\sigma_1$  and  $n_2$ ,  $\sigma_2$ . It is useful to prove that the slope of the new line is still  $b$ . For the equation  $S_f = a'N^{b'}$ , where the values of  $a'$  and  $b'$  are established by two points  $\alpha$  and  $\beta$ . The equation for  $b'$  is

$$b' = \frac{\log \sigma_\alpha / \sigma_\beta}{\log N_\alpha / N_\beta} \quad (c)$$

Examine the denominator of Eq. (c):

$$\begin{aligned} \log \frac{N_\alpha}{N_\beta} &= \log \frac{N_1 - n_1}{n_2} = \log \frac{N_1 - n_1}{(1 - n_1/N_1)N_2} = \log \frac{N_1}{N_2} \\ &= \log \frac{(\sigma_1/a)^{1/b}}{(\sigma_2/a)^{1/b}} = \log \left(\frac{\sigma_1}{\sigma_2}\right)^{1/b} = \frac{1}{b} \log \left(\frac{\sigma_1}{\sigma_2}\right) \end{aligned}$$

Substituting this into Eq. (c) with  $\sigma_\alpha/\sigma_\beta = \sigma_1/\sigma_2$  gives

$$b' = \frac{\log(\sigma_1/\sigma_2)}{(1/b) \log(\sigma_1/\sigma_2)} = b$$

which means the damaged material line has the same slope as the virgin material line; therefore, the lines are parallel. This information can be helpful in writing a computer program for the Palmgren-Miner hypothesis.

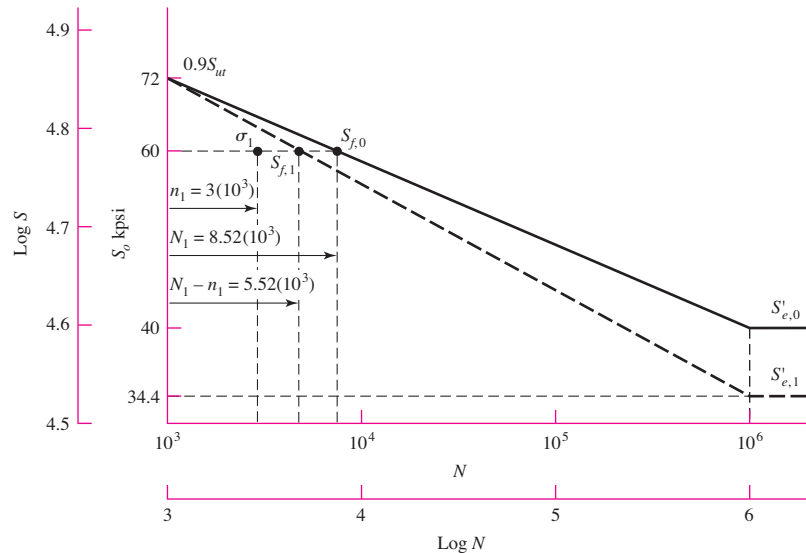
Though the Miner rule is quite generally used, it fails in two ways to agree with experiment. First, note that this theory states that the static strength  $S_{ut}$  is damaged, that is, decreased, because of the application of  $\sigma_1$ ; see Fig. 6–34 at  $N = 10^3$  cycles. Experiments fail to verify this prediction.

The Miner rule, as given by Eq. (6–58), does not account for the order in which the stresses are applied, and hence ignores any stresses less than  $S'_{e,0}$ . But it can be seen in Fig. 6–34 that a stress  $\sigma_3$  in the range  $S'_{e,1} < \sigma_3 < S'_{e,0}$  would cause damage if applied after the endurance limit had been damaged by the application of  $\sigma_1$ .



**Figure 6-35**

Use of the Manson method to predict the endurance limit of a material that has been overstressed for a finite number of cycles.



Manson's<sup>25</sup> approach overcomes both of the deficiencies noted for the Palmgren-Miner method; historically it is a much more recent approach, and it is just as easy to use. Except for a slight change, we shall use and recommend the Manson method in this book. Manson plotted the  $S$ - $\log N$  diagram instead of a  $\log S$ - $\log N$  plot as is recommended here. Manson also resorted to experiment to find the point of convergence of the  $S$ - $\log N$  lines corresponding to the static strength, instead of arbitrarily selecting the intersection of  $N = 10^3$  cycles with  $S = 0.9S_{ut}$  as is done here. Of course, it is always better to use experiment, but our purpose in this book has been to use the simple test data to learn as much as possible about fatigue failure.

The method of Manson, as presented here, consists in having all  $\log S$ - $\log N$  lines, that is, lines for both the damaged and the virgin material, converge to the same point,  $0.9S_{ut}$  at  $10^3$  cycles. In addition, the  $\log S$ - $\log N$  lines must be constructed in the same historical order in which the stresses occur.

The data from the preceding example are used for illustrative purposes. The results are shown in Fig. 6-35. Note that the strength  $S_{f,1}$  corresponding to  $N_1 - n_1 = 5.52(10^3)$  cycles is found in the same manner as before. Through this point and through  $0.9S_{ut}$  at  $10^3$  cycles, draw the heavy dashed line to meet  $N = 10^6$  cycles and define the endurance limit  $S'_{e,1}$  of the damaged material. In this case the new endurance limit is 34.4 kpsi, somewhat less than that found by the Miner method.

It is now easy to see from Fig. 6-35 that a reversed stress  $\sigma = 36$  kpsi, say, would not harm the endurance limit of the virgin material, no matter how many cycles it might be applied. However, if  $\sigma = 36$  kpsi should be applied *after* the material was damaged by  $\sigma_1 = 60$  kpsi, then additional damage would be done.

Both these rules involve a number of computations, which are repeated every time damage is estimated. For complicated stress-time traces, this might be every cycle. Clearly a computer program is useful to perform the tasks, including scanning the trace and identifying the cycles.

<sup>25</sup>S. S. Manson, A. J. Nachtigall, C. R. Ensign, and J. C. Fresche, "Further Investigation of a Relation for Cumulative Fatigue Damage in Bending," *Trans. ASME, J. Eng. Ind.*, ser. B, vol. 87, No. 1, pp. 25-35, February 1965.

Collins said it well: “In spite of all the problems cited, the Palmgren linear damage rule is frequently used because of its simplicity and the experimental fact that other more complex damage theories do not always yield a significant improvement in failure prediction reliability.”<sup>26</sup>

## 6-16 Surface Fatigue Strength

The surface fatigue mechanism is not definitively understood. The contact-affected zone, in the absence of surface shearing tractions, entertains compressive principal stresses. Rotary fatigue has its cracks grown at or near the surface in the presence of tensile stresses that are associated with crack propagation, to catastrophic failure. There are shear stresses in the zone, which are largest just below the surface. Cracks seem to grow from this stratum until small pieces of material are expelled, leaving pits on the surface. Because engineers had to design durable machinery before the surface fatigue phenomenon was understood in detail, they had taken the posture of conducting tests, observing pits on the surface, and declaring failure at an arbitrary projected area of hole, and they related this to the Hertzian contact pressure. This compressive stress did not produce the failure directly, but whatever the failure mechanism, whatever the stress type that was instrumental in the failure, the contact stress was an *index* to its magnitude.

Buckingham<sup>27</sup> conducted a number of tests relating the fatigue at  $10^8$  cycles to endurance strength (Hertzian contact pressure). While there is evidence of an endurance limit at about  $3(10^7)$  cycles for cast materials, hardened steel rollers showed no endurance limit up to  $4(10^8)$  cycles. Subsequent testing on hard steel shows no endurance limit. Hardened steel exhibits such high fatigue strengths that its use in resisting surface fatigue is widespread.

Our studies thus far have dealt with the failure of a machine element by yielding, by fracture, and by fatigue. The endurance limit obtained by the rotating-beam test is frequently called the *flexural endurance limit*, because it is a test of a rotating beam. In this section we shall study a property of *mating materials* called the *surface endurance shear*. The design engineer must frequently solve problems in which two machine elements mate with one another by rolling, sliding, or a combination of rolling and sliding contact. Obvious examples of such combinations are the mating teeth of a pair of gears, a cam and follower, a wheel and rail, and a chain and sprocket. A knowledge of the surface strength of materials is necessary if the designer is to create machines having a long and satisfactory life.

When two surfaces roll or roll and slide against one another with sufficient force, a pitting failure will occur after a certain number of cycles of operation. Authorities are not in complete agreement on the exact mechanism of the pitting; although the subject is quite complicated, they do agree that the Hertz stresses, the number of cycles, the surface finish, the hardness, the degree of lubrication, and the temperature all influence the strength. In Sec. 3-19 it was learned that, when two surfaces are pressed together, a maximum shear stress is developed slightly below the contacting surface. It is postulated by some authorities that a surface fatigue failure is initiated by this maximum shear stress and then is propagated rapidly to the surface. The lubricant then enters the crack that is formed and, under pressure, eventually wedges the chip loose.

<sup>26</sup>J. A. Collins, *Failure of Materials in Mechanical Design*, John Wiley & Sons, New York, 1981, p. 243.

<sup>27</sup>Earle Buckingham, *Analytical Mechanics of Gears*, McGraw-Hill, New York, 1949.

To determine the surface fatigue strength of mating materials, Buckingham designed a simple machine for testing a pair of contacting rolling surfaces in connection with his investigation of the wear of gear teeth. Buckingham and, later, Talbourdet gathered large numbers of data from many tests so that considerable design information is now available. To make the results useful for designers, Buckingham defined a *load-stress factor*, also called a *wear factor*, which is derived from the Hertz equations. Equations (3–73) and (3–74), pp. 118–119, for contacting cylinders are found to be

$$b = \sqrt{\frac{2F}{\pi l} \frac{(1 - \nu_1^2)/E_1 + (1 - \nu_2^2)/E_2}{(1/d_1) + (1/d_2)}} \quad (6-59)$$

$$p_{\max} = \frac{2F}{\pi bl} \quad (6-60)$$

where  $b$  = half width of rectangular contact area

$F$  = contact force

$l$  = length of cylinders

$\nu$  = Poisson's ratio

$E$  = modulus of elasticity

$d$  = cylinder diameter

It is more convenient to use the cylinder radius, so let  $2r = d$ . If we then designate the length of the cylinders as  $w$  (for width of gear, bearing, cam, etc.) instead of  $l$  and remove the square root sign, Eq. (6–59) becomes

$$b^2 = \frac{4F}{\pi w} \frac{(1 - \nu_1^2)/E_1 + (1 - \nu_2^2)/E_2}{1/r_1 + 1/r_2} \quad (6-61)$$

We can define a *surface endurance strength*  $S_C$  using

$$p_{\max} = \frac{2F}{\pi bw} \quad (6-62)$$

as

$$S_C = \frac{2F}{\pi bw} \quad (6-63)$$

which may also be called *contact strength*, the *contact fatigue strength*, or the *Hertzian endurance strength*. The strength is the contacting pressure which, after a specified number of cycles, will cause failure of the surface. Such failures are often called *wear* because they occur over a very long time. They should not be confused with abrasive wear, however. By squaring Eq. (6–63), substituting  $b^2$  from Eq. (6–61), and rearranging, we obtain

$$\frac{F}{w} \left( \frac{1}{r_1} + \frac{1}{r_2} \right) = \pi S_C^2 \left[ \frac{1 - \nu_1^2}{E_1} + \frac{1 - \nu_2^2}{E_2} \right] = K_1 \quad (6-64)$$

The left expression consists of parameters a designer may seek to control independently. The central expression consists of material properties that come with the material and condition specification. The third expression is the parameter  $K_1$ , Buckingham's load-stress factor, determined by a test fixture with values  $F$ ,  $w$ ,  $r_1$ ,  $r_2$  and the number of

cycles associated with the first tangible evidence of fatigue. In gear studies a similar  $K$  factor is used:

$$K_g = \frac{K_1}{4} \sin \phi \quad (6-65)$$

where  $\phi$  is the tooth pressure angle, and the term  $[(1 - \nu_1^2)/E_1 + (1 - \nu_2^2)/E_2]$  is defined as  $1/(\pi C_P^2)$ , so that

$$S_C = C_P \sqrt{\frac{F}{w} \left( \frac{1}{r_1} + \frac{1}{r_2} \right)} \quad (6-66)$$

Buckingham and others reported  $K_1$  for  $10^8$  cycles and nothing else. This gives only one point on the  $S_C N$  curve. For cast metals this may be sufficient, but for wrought steels, heat-treated, some idea of the slope is useful in meeting design goals of other than  $10^8$  cycles.

Experiments show that  $K_1$  versus  $N$ ,  $K_g$  versus  $N$ , and  $S_C$  versus  $N$  data are rectified by loglog transformation. This suggests that

$$K_1 = \alpha_1 N^{\beta_1} \quad K_g = a N^b \quad S_C = \alpha N^\beta$$

The three exponents are given by

$$\beta_1 = \frac{\log(K_1/K_2)}{\log(N_1/N_2)} \quad b = \frac{\log(K_{g1}/K_{g2})}{\log(N_1/N_2)} \quad \beta = \frac{\log(S_{C1}/S_{C2})}{\log(N_1/N_2)} \quad (6-67)$$

Data on induction-hardened steel on steel give  $(S_C)_{10^7} = 271$  kpsi and  $(S_C)_{10^8} = 239$  kpsi, so  $\beta$ , from Eq. (6-67), is

$$\beta = \frac{\log(271/239)}{\log(10^7/10^8)} = -0.055$$

It may be of interest that the American Gear Manufacturers Association (AGMA) uses  $\beta = -0.056$  between  $10^4 < N < 10^{10}$  if the designer has no data to the contrary beyond  $10^7$  cycles.

A longstanding correlation in steels between  $S_C$  and  $H_B$  at  $10^8$  cycles is

$$(S_C)_{10^8} = \begin{cases} 0.4H_B - 10 \text{ kpsi} \\ 2.76H_B - 70 \text{ MPa} \end{cases} \quad (6-68)$$

AGMA uses

$$0.99(S_C)_{10^7} = 0.327H_B + 26 \text{ kpsi} \quad (6-69)$$

Equation (6-66) can be used in design to find an allowable surface stress by using a design factor. Since this equation is nonlinear in its stress-load transformation, the designer must decide if loss of function denotes inability to carry the load. If so, then to find the allowable stress, one divides the load  $F$  by the design factor  $n_d$ :

$$\sigma_C = C_P \sqrt{\frac{F}{w n_d} \left( \frac{1}{r_1} + \frac{1}{r_2} \right)} = \frac{C_P}{\sqrt{n_d}} \sqrt{\frac{F}{w} \left( \frac{1}{r_1} + \frac{1}{r_2} \right)} = \frac{S_C}{\sqrt{n_d}}$$

and  $n_d = (S_C/\sigma_C)^2$ . If the loss of function is focused on stress, then  $n_d = S_C/\sigma_C$ . It is recommended that an engineer

- Decide whether loss of function is failure to carry load or stress.
- Define the design factor and factor of safety accordingly.
- Announce what he or she is using and why.
- Be prepared to defend his or her position.

In this way everyone who is party to the communication knows what a design factor (or factor of safety) of 2 means and adjusts, if necessary, the judgmental perspective.

## 6-17 Stochastic Analysis<sup>28</sup>

As already demonstrated in this chapter, there are a great many factors to consider in a fatigue analysis, much more so than in a static analysis. So far, each factor has been treated in a deterministic manner, and if not obvious, these factors are subject to variability and control the overall reliability of the results. When reliability is important, then fatigue testing must certainly be undertaken. There is no other way. Consequently, the methods of stochastic analysis presented here and in other sections of this book constitute guidelines that enable the designer to obtain a good understanding of the various issues involved and help in the development of a safe and reliable design.

In this section, key stochastic modifications to the deterministic features and equations described in earlier sections are provided in the same order of presentation.

### Endurance Limit

To begin, a method for estimating endurance limits, the *tensile strength correlation method*, is presented. The ratio  $\Phi = S'_e / \bar{S}_{ut}$  is called the *fatigue ratio*.<sup>29</sup> For ferrous metals, most of which exhibit an endurance limit, the endurance limit is used as a numerator. For materials that do not show an endurance limit, an endurance strength at a specified number of cycles to failure is used and noted. Gough<sup>30</sup> reported the stochastic nature of the fatigue ratio  $\Phi$  for several classes of metals, and this is shown in Fig. 6-36. The first item to note is that the coefficient of variation is of the order 0.10 to 0.15, and the distribution varies for classes of metals. The second item to note is that Gough's data include materials of no interest to engineers. In the absence of testing, engineers use the correlation that  $\Phi$  represents to estimate the endurance limit  $S'_e$  from the mean ultimate strength  $\bar{S}_{ut}$ .

Gough's data are for ensembles of metals, some chosen for metallurgical interest, and include materials that are not commonly selected for machine parts. Mischke<sup>31</sup> analyzed data for 133 common steels and treatments in varying diameters in rotating bending,<sup>32</sup> and the result was

$$\Phi = 0.445d^{-0.107} \mathbf{LN}(1, 0.138)$$

where  $d$  is the specimen diameter in inches and  $\mathbf{LN}(1, 0.138)$  is a unit lognormal variate with a mean of 1 and a standard deviation (and coefficient of variation) of 0.138. For the standard R. R. Moore specimen,

$$\Phi_{0.30} = 0.445(0.30)^{-0.107} \mathbf{LN}(1, 0.138) = 0.506 \mathbf{LN}(1, 0.138)$$

<sup>28</sup>Review Chap. 20 before reading this section.

<sup>29</sup>From this point, since we will be dealing with statistical distributions in terms of means, standard deviations, etc. A key quantity, the ultimate strength, will here be presented by its mean value,  $\bar{S}_{ut}$ . This means that certain terms that were defined earlier in terms of the minimum value of  $S_{ut}$  will change slightly.

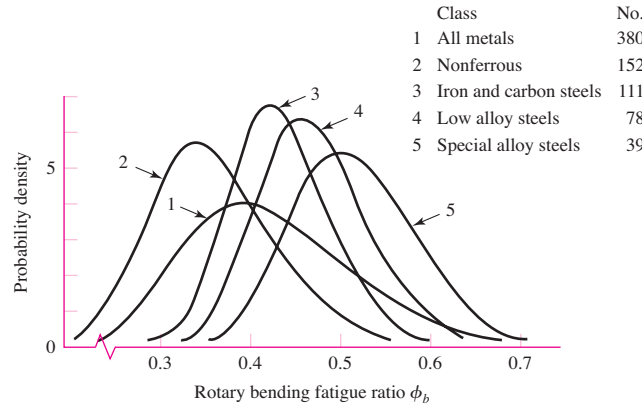
<sup>30</sup>In J. A. Pope, *Metal Fatigue*, Chapman and Hall, London, 1959.

<sup>31</sup>Charles R. Mischke, "Prediction of Stochastic Endurance Strength," *Trans. ASME, Journal of Vibration, Acoustics, Stress, and Reliability in Design*, vol. 109, no. 1, January 1987, pp. 113-122.

<sup>32</sup>Data from H. J. Grover, S. A. Gordon, and L. R. Jackson, *Fatigue of Metals and Structures*, Bureau of Naval Weapons, Document NAVWEPS 00-2500435, 1960.

**Figure 6-36**

The lognormal probability density PDF of the fatigue ratio  $\phi_b$  of Gough.



Also, 25 plain carbon and low-alloy steels with  $S_{ut} > 212$  kpsi are described by

$$S'_e = 107\text{LN}(1, 0.139) \text{ kpsi}$$

In summary, for the rotating-beam specimen,

$$S'_e = \begin{cases} 0.506\bar{S}_{ut}\text{LN}(1, 0.138) \text{ kpsi or MPa} & \bar{S}_{ut} \leq 212 \text{ kpsi (1460 MPa)} \\ 107\text{LN}(1, 0.139) \text{ kpsi} & \bar{S}_{ut} > 212 \text{ kpsi} \\ 740\text{LN}(1, 0.139) \text{ MPa} & \bar{S}_{ut} > 1460 \text{ MPa} \end{cases} \quad (6-70)$$

where  $\bar{S}_{ut}$  is the *mean* ultimate tensile strength.

Equations (6-70) represent the state of information before an engineer has chosen a material. In choosing, the designer has made a random choice from the ensemble of possibilities, and the statistics can give the odds of disappointment. If the testing is limited to finding an estimate of the ultimate tensile strength mean  $\bar{S}_{ut}$  with the chosen material, Eqs. (6-70) are directly helpful. If there is to be rotary-beam fatigue testing, then statistical information on the endurance limit is gathered and there is no need for the correlation above.

Table 6-9 compares approximate mean values of the fatigue ratio  $\bar{\phi}_{0.30}$  for several classes of ferrous materials.

### Endurance Limit Modifying Factors

A Marin equation can be written as

$$S_e = k_a k_b k_c k_d k_f S'_e \quad (6-71)$$

where the size factor  $k_b$  is deterministic and remains unchanged from that given in Sec. 6-9. Also, since we are performing a stochastic analysis, the “reliability factor”  $k_e$  is unnecessary here.

The surface factor  $k_a$  cited earlier in deterministic form as Eq. (6-20), p. 280, is now given in stochastic form by

$$k_a = a\bar{S}_{ut}^b \text{LN}(1, C) \quad (\bar{S}_{ut} \text{ in kpsi or MPa}) \quad (6-72)$$

where Table 6-10 gives values of  $a$ ,  $b$ , and  $C$  for various surface conditions.

**Table 6-9**

Comparison of  
Approximate Values of  
Mean Fatigue Ratio for  
Some Classes of Metals

Material Class	$\bar{\phi}_{0.30}$
Wrought steels	0.50
Cast steels	0.40
Powdered steels	0.38
Gray cast iron	0.35
Malleable cast iron	0.40
Normalized nodular cast iron	0.33

**Table 6-10**

Parameters in Marin  
Surface Condition  
Factor

Surface Finish	$k_a = aS_{ut}^b \text{LN}(1, C)$			Coefficient of Variation, $C$
	kpsi	MPa	$b$	
Ground*	1.34	1.58	-0.086	0.120
Machined or Cold-rolled	2.67	4.45	-0.265	0.058
Hot-rolled	14.5	58.1	-0.719	0.110
As-forged	39.8	271	-0.995	0.145

\*Due to the wide scatter in ground surface data, an alternate function is  $k_a = 0.878 \text{LN}(1, 0.120)$ . Note:  $S_{ut}$  in kpsi or MPa.

**EXAMPLE 6-16**

A steel has a mean ultimate strength of 520 MPa and a machined surface. Estimate  $k_a$ .

**Solution**

From Table 6-10,

$$k_a = 4.45(520)^{-0.265} \text{LN}(1, 0.058)$$

$$\bar{k}_a = 4.45(520)^{-0.265}(1) = 0.848$$

$$\hat{\sigma}_{ka} = C\bar{k}_a = (0.058)4.45(520)^{-0.265} = 0.049$$

**Answer**

so  $k_a = \text{LN}(0.848, 0.049)$ .

The load factor  $k_c$  for axial and torsional loading is given by

$$(k_c)_{\text{axial}} = 1.23\bar{S}_{ut}^{-0.0778} \text{LN}(1, 0.125) \quad (6-73)$$

$$(k_c)_{\text{torsion}} = 0.328\bar{S}_{ut}^{0.125} \text{LN}(1, 0.125) \quad (6-74)$$

where  $\bar{S}_{ut}$  is in kpsi. There are fewer data to study for axial fatigue. Equation (6-73) was deduced from the data of Landgraf and of Grover, Gordon, and Jackson (as cited earlier).

Torsional data are sparser, and Eq. (6-74) is deduced from data in Grover et al. Notice the mild sensitivity to strength in the axial and torsional load factor, so  $k_c$  in these cases is not constant. Average values are shown in the last column of Table 6-11, and as footnotes to Tables 6-12 and 6-13. Table 6-14 shows the influence of material classes on the load factor  $k_c$ . Distortion energy theory predicts  $(k_c)_{\text{torsion}} = 0.577$  for materials to which the distortion-energy theory applies. For bending,  $k_c = \text{LN}(1, 0)$ .



**Table 6-11**

Parameters in Marin Loading Factor

Mode of Loading	$k_c = \alpha \bar{S}_{ut}^\beta \text{LN}(1, C)$				Average $k_c$
	kpsi	MPa	$\beta$	C	
Bending	1	1	0	0	1
Axial	1.23	1.43	-0.078	0.125	0.85
Torsion	0.328	0.258	0.125	0.125	0.59

**Table 6-12**

Average Marin Loading Factor for Axial Load

$\bar{S}_{ut}$ , kpsi	$k_c^*$
50	0.907
100	0.860
150	0.832
200	0.814

\*Average entry 0.85.

**Table 6-13**

Average Marin Loading Factor for Torsional Load

$\bar{S}_{ut}$ , kpsi	$k_c^*$
50	0.535
100	0.583
150	0.614
200	0.636

\*Average entry 0.59.

**Table 6-14**Average Marin Torsional Loading Factor  $k_c$  for Several Materials

Material	Range	n	$\bar{k}_c$	$\hat{\sigma}_{k_c}$
Wrought steels	0.52–0.69	31	0.60	0.03
Wrought Al	0.43–0.74	13	0.55	0.09
Wrought Cu and alloy	0.41–0.67	7	0.56	0.10
Wrought Mg and alloy	0.49–0.60	2	0.54	0.08
Titanium	0.37–0.57	3	0.48	0.12
Cast iron	0.79–1.01	9	0.90	0.07
Cast Al, Mg, and alloy	0.71–0.91	5	0.85	0.09

Source: The table is an extension of P. G. Forrest, *Fatigue of Metals*, Pergamon Press, London, 1962, Table 17, p. 110, with standard deviations estimated from range and sample size using Table A-1 in J. B. Kennedy and A. M. Neville, *Basic Statistical Methods for Engineers and Scientists*, 3rd ed., Harper & Row, New York, 1986, pp. 54–55.

**EXAMPLE 6-17**

Estimate the Marin loading factor  $k_c$  for a 1-in-diameter bar that is used as follows.

(a) In bending. It is made of steel with  $S_{ut} = 100\text{LN}(1, 0.035)$  kpsi, and the designer intends to use the correlation  $S'_e = \Phi_{0.30}\bar{S}_{ut}$  to predict  $S'_e$ .

(b) In bending, but endurance testing gave  $S'_e = 55\text{LN}(1, 0.081)$  kpsi.

(c) In push-pull (axial) fatigue,  $S_{ut} = \text{LN}(86.2, 3.92)$  kpsi, and the designer intended to use the correlation  $S'_e = \Phi_{0.30}\bar{S}_{ut}$ .

(d) In torsional fatigue. The material is cast iron, and  $S'_e$  is known by test.

**Solution** (a) Since the bar is in bending,

**Answer**  $k_c = (1, 0)$

(b) Since the test is in bending and use is in bending,

**Answer**  $k_c = (1, 0)$

(c) From Eq. (6-73),

**Answer**  $(k_c)_{ax} = 1.23(86.2)^{-0.0778}\text{LN}(1, 0.125)$

$$\bar{k}_c = 1.23(86.2)^{-0.0778}(1) = 0.870$$

$$\hat{\sigma}_{kc} = C\bar{k}_c = 0.125(0.870) = 0.109$$

(d) From Table 6-15,  $\bar{k}_c = 0.90$ ,  $\hat{\sigma}_{kc} = 0.07$ , and

**Answer**  $C_{kc} = \frac{0.07}{0.90} = 0.08$

The temperature factor  $k_d$  is

$$k_d = \bar{k}_d\text{LN}(1, 0.11) \quad (6-75)$$

where  $\bar{k}_d = k_d$ , given by Eq. (6-27), p. 283.

Finally,  $k_f$  is, as before, the miscellaneous factor that can come about from a great many considerations, as discussed in Sec. 6-9, where now statistical distributions, possibly from testing, are considered.

### Stress Concentration and Notch Sensitivity

Notch sensitivity  $q$  was defined by Eq. (6-31), p. 287. The stochastic equivalent is

$$q = \frac{K_f - 1}{K_t - 1} \quad (6-76)$$

where  $K_t$  is the theoretical (or geometric) stress-concentration factor, a deterministic quantity. A study of lines 3 and 4 of Table 20-6, will reveal that adding a scalar to (or subtracting one from) a variate  $x$  will affect only the mean. Also, multiplying (or dividing) by a scalar affects both the mean and standard deviation. With this in mind, we can

**Table 6-15**

Heywood's Parameter  $\sqrt{a}$  and coefficients of variation  $C_{Kf}$  for steels

Notch Type	$\sqrt{a}(\sqrt{\text{in}})$ , $S_{ut}$ in kpsi	$\sqrt{a}(\sqrt{\text{mm}})$ , $S_{ut}$ in MPa	Coefficient of Variation $C_{kf}$
Transverse hole	$5/S_{ut}$	$174/S_{ut}$	0.10
Shoulder	$4/S_{ut}$	$139/S_{ut}$	0.11
Groove	$3/S_{ut}$	$104/S_{ut}$	0.15

relate the statistical parameters of the fatigue stress-concentration factor  $\mathbf{K}_f$  to those of notch sensitivity  $\mathbf{q}$ . It follows that

$$\mathbf{q} = \text{LN} \left( \frac{\bar{K}_f - 1}{K_t - 1}, \frac{C \bar{K}_f}{K_t - 1} \right)$$

where  $C = C_{Kf}$  and

$$\begin{aligned} \bar{q} &= \frac{\bar{K}_f - 1}{K_t - 1} \\ \hat{\sigma}_q &= \frac{C \bar{K}_f}{K_t - 1} \\ C_q &= \frac{C \bar{K}_f}{\bar{K}_f - 1} \end{aligned} \quad (6-77)$$

The fatigue stress-concentration factor  $\mathbf{K}_f$  has been investigated more in England than in the United States. For  $\bar{K}_f$ , consider a modified Neuber equation (after Heywood<sup>33</sup>), where the fatigue stress-concentration factor is given by

$$\bar{K}_f = \frac{K_t}{1 + \frac{2(K_t - 1)}{K_t} \frac{\sqrt{a}}{\sqrt{r}}} \quad (6-78)$$

where Table 6-15 gives values of  $\sqrt{a}$  and  $C_{Kf}$  for steels with transverse holes, shoulders, or grooves. Once  $\mathbf{K}_f$  is described,  $\mathbf{q}$  can also be quantified using the set Eqs. (6-77).

The modified Neuber equation gives the fatigue stress concentration factor as

$$\mathbf{K}_f = \bar{K}_f \text{LN} (1, C_{Kf}) \quad (6-79)$$

<sup>33</sup>R. B. Heywood, *Designing Against Fatigue*, Chapman & Hall, London, 1962.

### EXAMPLE 6-18

Estimate  $\mathbf{K}_f$  and  $\mathbf{q}$  for the steel shaft given in Ex. 6-6, p. 288.

#### Solution

From Ex. 6-6, a steel shaft with  $S_{ut} = 690$  Mpa and a shoulder with a fillet of 3 mm was found to have a theoretical stress-concentration-factor of  $K_t \doteq 1.65$ . From Table 6-15,

$$\sqrt{a} = \frac{139}{S_{ut}} = \frac{139}{690} = 0.2014\sqrt{\text{mm}}$$

From Eq. (6-78),

$$K_f = \frac{K_t}{1 + \frac{2(K_t - 1)\sqrt{a}}{K_t\sqrt{r}}} = \frac{1.65}{1 + \frac{2(1.65 - 1)0.2014}{1.65\sqrt{3}}} = 1.51$$

which is 2.5 percent lower than what was found in Ex. 6-6.

From Table 6-15,  $C_{Kf} = 0.11$ . Thus from Eq. (6-79),

**Answer**  $\mathbf{K}_f = 1.51 \text{ LN}(1, 0.11)$

From Eq. (6-77), with  $K_t = 1.65$

$$\bar{q} = \frac{1.51 - 1}{1.65 - 1} = 0.785$$

$$C_q = \frac{C_{Kf}\bar{K}_f}{\bar{K}_f - 1} = \frac{0.11(1.51)}{1.51 - 1} = 0.326$$

$$\hat{\sigma}_q = C_q\bar{q} = 0.326(0.785) = 0.256$$

So,

**Answer**  $\mathbf{q} = \text{LN}(0.785, 0.256)$

### EXAMPLE 6-19

The bar shown in Fig. 6-37 is machined from a cold-rolled flat having an ultimate strength of  $\mathbf{S}_{ut} = \text{LN}(87.6, 5.74)$  kpsi. The axial load shown is completely reversed. The load amplitude is  $\mathbf{F}_a = \text{LN}(1000, 120)$  lbf.

(a) Estimate the reliability.

(b) Reestimate the reliability when a rotating bending endurance test shows that  $\mathbf{S}'_e = \text{LN}(40, 2)$  kpsi.

**Solution** (a) From Eq. (6-70),  $\mathbf{S}'_e = 0.506\bar{S}_{ut}\text{LN}(1, 0.138) = 0.506(87.6)\text{LN}(1, 0.138)$   
 $= 44.3\text{LN}(1, 0.138)$  kpsi

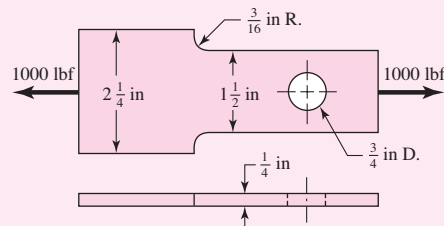
From Eq. (6-72) and Table 6-10,

$$\mathbf{k}_a = 2.67\bar{S}_{ut}^{-0.265}\text{LN}(1, 0.058) = 2.67(87.6)^{-0.265}\text{LN}(1, 0.058)$$

$$= 0.816\text{LN}(1, 0.058)$$

$$k_b = 1 \quad (\text{axial loading})$$

| Figure 6-37



From Eq. (6-73),

$$\mathbf{k}_c = 1.23 \bar{S}_{ut}^{-0.0778} \mathbf{LN}(1, 0.125) = 1.23(87.6)^{-0.0778} \mathbf{LN}(1, 0.125) \\ = 0.869 \mathbf{LN}(1, 0.125)$$

$$\mathbf{k}_d = \mathbf{k}_f = (1, 0)$$

The endurance strength, from Eq. (6-71), is

$$\mathbf{S}_e = \mathbf{k}_a \mathbf{k}_b \mathbf{k}_c \mathbf{k}_d \mathbf{k}_f \mathbf{S}'_e$$

$$\mathbf{S}_e = 0.816 \mathbf{LN}(1, 0.058)(1)0.869 \mathbf{LN}(1, 0.125)(1)(1)44.3 \mathbf{LN}(1, 0.138)$$

The parameters of  $\mathbf{S}_e$  are

$$\bar{S}_e = 0.816(0.869)44.3 = 31.4 \text{ kpsi}$$

$$C_{S_e} = (0.058^2 + 0.125^2 + 0.138^2)^{1/2} = 0.195$$

so  $\mathbf{S}_e = 31.4 \mathbf{LN}(1, 0.195)$  kpsi.

In computing the stress, the section at the hole governs. Using the terminology of Table A-15-1 we find  $d/w = 0.50$ , therefore  $K_t \doteq 2.18$ . From Table 6-15,  $\sqrt{a} = 5/S_{ut} = 5/87.6 = 0.0571$  and  $C_{kf} = 0.10$ . From Eqs. (6-78) and (6-79) with  $r = 0.375$  in,

$$\mathbf{K}_f = \frac{K_t}{1 + \frac{2(K_t - 1)}{K_t} \frac{\sqrt{a}}{\sqrt{r}}} \mathbf{LN}(1, C_{K_f}) = \frac{2.18}{1 + \frac{2(2.18 - 1)}{2.18} \frac{0.0571}{\sqrt{0.375}}} \mathbf{LN}(1, 0.10) \\ = 1.98 \mathbf{LN}(1, 0.10)$$

The stress at the hole is

$$\boldsymbol{\sigma} = \mathbf{K}_f \frac{\mathbf{F}}{A} = 1.98 \mathbf{LN}(1, 0.10) \frac{1000 \mathbf{LN}(1, 0.12)}{0.25(0.75)}$$

$$\bar{\sigma} = 1.98 \frac{1000}{0.25(0.75)} 10^{-3} = 10.56 \text{ kpsi}$$

$$C_{\sigma} = (0.10^2 + 0.12^2)^{1/2} = 0.156$$

so stress can be expressed as  $\boldsymbol{\sigma} = 10.56 \mathbf{LN}(1, 0.156)$  kpsi.<sup>34</sup>

The endurance limit is considerably greater than the load-induced stress, indicating that finite life is not a problem. For interfering lognormal-lognormal distributions, Eq. (5-43), p. 242, gives

$$z = -\frac{\ln\left(\frac{\bar{S}_e}{\bar{\sigma}} \sqrt{\frac{1 + C_{\sigma}^2}{1 + C_{S_e}^2}}\right)}{\sqrt{\ln[(1 + C_{S_e}^2)(1 + C_{\sigma}^2)]}} = -\frac{\ln\left(\frac{31.4}{10.56} \sqrt{\frac{1 + 0.156^2}{1 + 0.195^2}}\right)}{\sqrt{\ln[(1 + 0.195^2)(1 + 0.156^2)]}} = -4.37$$

From Table A-10 the probability of failure  $p_f = \Phi(-4.37) = .000\,006\,35$ , and the reliability is

**Answer**

$$R = 1 - 0.000\,006\,35 = 0.999\,993\,65$$

<sup>34</sup>Note that there is a simplification here. The area is *not* a deterministic quantity. It will have a statistical distribution also. However no information was given here, and so it was treated as being deterministic.

(b) The rotary endurance tests are described by  $\mathbf{S}'_e = 40\mathbf{LN}(1, 0.05)$  kpsi whose mean is *less* than the predicted mean in part *a*. The mean endurance strength  $\bar{S}_e$  is

$$\bar{S}_e = 0.816(0.869)40 = 28.4 \text{ kpsi}$$

$$C_{Se} = (0.058^2 + 0.125^2 + 0.05^2)^{1/2} = 0.147$$

so the endurance strength can be expressed as  $\mathbf{S}_e = 28.3\mathbf{LN}(1, 0.147)$  kpsi. From Eq. (5-43),

$$z = -\frac{\ln\left(\frac{28.4}{10.56}\sqrt{\frac{1+0.156^2}{1+0.147^2}}\right)}{\sqrt{\ln[(1+0.147^2)(1+0.156^2)]}} = -4.65$$

Using Table A-10, we see the probability of failure  $p_f = \Phi(-4.65) = 0.000\,001\,71$ , and

$$R = 1 - 0.000\,001\,71 = 0.999\,998\,29$$

*an increase!* The reduction in the probability of failure is  $(0.000\,001\,71 - 0.000\,006\,35)/0.000\,006\,35 = -0.73$ , a reduction of 73 percent. We are analyzing an existing design, so in part (a) the factor of safety was  $\bar{n} = \bar{S}/\bar{\sigma} = 31.4/10.56 = 2.97$ . In part (b)  $\bar{n} = 28.4/10.56 = 2.69$ , a *decrease*. This example gives you the opportunity to see the role of the design factor. Given knowledge of  $\bar{S}$ ,  $C_S$ ,  $\bar{\sigma}$ ,  $C_\sigma$ , and reliability (through  $z$ ), the mean factor of safety (as a design factor) separates  $\bar{S}$  and  $\bar{\sigma}$  so that the reliability goal is achieved. Knowing  $\bar{n}$  alone *says nothing about the probability of failure*. Looking at  $\bar{n} = 2.97$  and  $\bar{n} = 2.69$  says nothing about the respective probabilities of failure. The tests did not reduce  $\bar{S}_e$  significantly, but reduced the variation  $C_S$  such that the reliability was *increased*.

When a mean design factor (or mean factor of safety) defined as  $\bar{S}_e/\bar{\sigma}$  is said to be *silent* on matters of frequency of failures, it means that a scalar factor of safety by itself does not offer any information about probability of failure. Nevertheless, some engineers let the factor of safety speak up, and they can be wrong in their conclusions.

As revealing as Ex. 6-19 is concerning the meaning (and lack of meaning) of a design factor or factor of safety, let us remember that the rotary testing associated with part (b) changed *nothing* about the part, but only our knowledge about the part. The mean endurance limit was 40 kpsi all the time, and our adequacy assessment had to move with what was known.

### Fluctuating Stresses

Deterministic failure curves that lie among the data are candidates for regression models. Included among these are the Gerber and ASME-elliptic for ductile materials, and, for brittle materials, Smith-Dolan models, which use mean values in their presentation. Just as the deterministic failure curves are located by endurance strength and ultimate tensile (or yield) strength, so too are stochastic failure curves located by  $\mathbf{S}_e$  and by  $\mathbf{S}_{ut}$  or  $\mathbf{S}_y$ . Figure 6-32, p. 312, shows the parabolic Gerber mean curve. We also need to establish a contour located one standard deviation from the mean. Since stochastic

curves are most likely to be used with a radial load line we will use the equation given in Table 6–7, p. 299, expressed in terms of the strength means as

$$\bar{S}_a = \frac{r^2 \bar{S}_{ut}^2}{2 \bar{S}_e} \left[ -1 + \sqrt{1 + \left( \frac{2 \bar{S}_e}{r \bar{S}_{ut}} \right)^2} \right] \quad (6-80)$$

Because of the positive correlation between  $\mathbf{S}_e$  and  $\mathbf{S}_{ut}$ , we increment  $\bar{S}_e$  by  $C_{Se} \bar{S}_e$ ,  $\bar{S}_{ut}$  by  $C_{Sut} \bar{S}_{ut}$ , and  $\bar{S}_a$  by  $C_{Sa} \bar{S}_a$ , substitute into Eq. (6–80), and solve for  $C_{Sa}$  to obtain

$$C_{Sa} = \frac{(1 + C_{Sut})^2}{1 + C_{Se}} \frac{\left\{ -1 + \sqrt{1 + \left[ \frac{2 \bar{S}_e (1 + C_{Se})}{r \bar{S}_{ut} (1 + C_{Sut})} \right]^2} \right\}}{\left[ -1 + \sqrt{1 + \left( \frac{2 \bar{S}_e}{r \bar{S}_{ut}} \right)^2} \right]} - 1 \quad (6-81)$$

Equation (6–81) can be viewed as an interpolation formula for  $C_{Sa}$ , which falls between  $C_{Se}$  and  $C_{Sut}$  depending on load line slope  $r$ . Note that  $\mathbf{S}_a = \bar{S}_a \mathbf{LN}(1, C_{Sa})$ .

Similarly, the ASME-elliptic criterion of Table 6–8, p. 300, expressed in terms of its means is

$$\bar{S}_a = \frac{r \bar{S}_y \bar{S}_e}{\sqrt{r^2 \bar{S}_y^2 + \bar{S}_e^2}} \quad (6-82)$$

Similarly, we increment  $\bar{S}_e$  by  $C_{Se} \bar{S}_e$ ,  $\bar{S}_y$  by  $C_{Sy} \bar{S}_y$ , and  $\bar{S}_a$  by  $C_{Sa} \bar{S}_a$ , substitute into Eq. (6–82), and solve for  $C_{Sa}$ :

$$C_{Sa} = (1 + C_{Sy})(1 + C_{Se}) \sqrt{\frac{r^2 \bar{S}_y^2 + \bar{S}_e^2}{r^2 \bar{S}_y^2 (1 + C_{Sy})^2 + \bar{S}_e^2 (1 + C_{Se})^2}} - 1 \quad (6-83)$$

Many *brittle* materials follow a Smith-Dolan failure criterion, written deterministically as

$$\frac{n \sigma_a}{S_e} = \frac{1 - n \sigma_m / S_{ut}}{1 + n \sigma_m / S_{ut}} \quad (6-84)$$

Expressed in terms of its means,

$$\frac{\bar{S}_a}{\bar{S}_e} = \frac{1 - \bar{S}_m / \bar{S}_{ut}}{1 + \bar{S}_m / \bar{S}_{ut}} \quad (6-85)$$

For a radial load line slope of  $r$ , we substitute  $\bar{S}_a / r$  for  $\bar{S}_m$  and solve for  $\bar{S}_a$ , obtaining

$$\bar{S}_a = \frac{r \bar{S}_{ut} + \bar{S}_e}{2} \left[ -1 + \sqrt{1 + \frac{4r \bar{S}_{ut} \bar{S}_e}{(r \bar{S}_{ut} + \bar{S}_e)^2}} \right] \quad (6-86)$$

and the expression for  $C_{Sa}$  is

$$C_{Sa} = \frac{r \bar{S}_{ut} (1 + C_{Sut}) + \bar{S}_e (1 + C_{Se})}{2 \bar{S}_a} \cdot \left\{ -1 + \sqrt{1 + \frac{4r \bar{S}_{ut} \bar{S}_e (1 + C_{Se}) (1 + C_{Sut})}{[r \bar{S}_{ut} (1 + C_{Sut}) + \bar{S}_e (1 + C_{Se})]^2}} \right\} - 1 \quad (6-87)$$

**EXAMPLE 6-20**

A rotating shaft experiences a steady torque  $\mathbf{T} = 1360\mathbf{LN}(1, 0.05)$  lbf · in, and at a shoulder with a 1.1-in small diameter, a fatigue stress-concentration factor  $\mathbf{K}_f = 1.50\mathbf{LN}(1, 0.11)$ ,  $\mathbf{K}_{fs} = 1.28\mathbf{LN}(1, 0.11)$ , and at that location a bending moment of  $\mathbf{M} = 1260\mathbf{LN}(1, 0.05)$  lbf · in. The material of which the shaft is machined is hot-rolled 1035 with  $\mathbf{S}_{ut} = 86.2\mathbf{LN}(1, 0.045)$  kpsi and  $\mathbf{S}_y = 56.0\mathbf{LN}(1, 0.077)$  kpsi. Estimate the reliability using a stochastic Gerber failure zone.

**Solution**

Establish the endurance strength. From Eqs. (6–70) to (6–72) and Eq. (6–20), p. 280,

$$\mathbf{S}'_e = 0.506(86.2)\mathbf{LN}(1, 0.138) = 43.6\mathbf{LN}(1, 0.138) \text{ kpsi}$$

$$\mathbf{k}_a = 2.67(86.2)^{-0.265}\mathbf{LN}(1, 0.058) = 0.820\mathbf{LN}(1, 0.058)$$

$$k_b = (1.1/0.30)^{-0.107} = 0.870$$

$$\mathbf{k}_c = \mathbf{k}_d = \mathbf{k}_f = \mathbf{LN}(1, 0)$$

$$\mathbf{S}_e = 0.820\mathbf{LN}(1, 0.058)0.870(43.6)\mathbf{LN}(1, 0.138)$$

$$\bar{S}_e = 0.820(0.870)43.6 = 31.1 \text{ kpsi}$$

$$C_{Se} = (0.058^2 + 0.138^2)^{1/2} = 0.150$$

and so  $\mathbf{S}_e = 31.1\mathbf{LN}(1, 0.150)$  kpsi.

Stress (in kpsi):

$$\sigma_a = \frac{32\mathbf{K}_f\mathbf{M}_a}{\pi d^3} = \frac{32(1.50)\mathbf{LN}(1, 0.11)1.26\mathbf{LN}(1, 0.05)}{\pi(1.1)^3}$$

$$\bar{\sigma}_a = \frac{32(1.50)1.26}{\pi(1.1)^3} = 14.5 \text{ kpsi}$$

$$C_{\sigma a} = (0.11^2 + 0.05^2)^{1/2} = 0.121$$

$$\tau_m = \frac{16\mathbf{K}_{fs}\mathbf{T}_m}{\pi d^3} = \frac{16(1.28)\mathbf{LN}(1, 0.11)1.36\mathbf{LN}(1, 0.05)}{\pi(1.1)^3}$$

$$\bar{\tau}_m = \frac{16(1.28)1.36}{\pi(1.1)^3} = 6.66 \text{ kpsi}$$

$$C_{\tau m} = (0.11^2 + 0.05^2)^{1/2} = 0.121$$

$$\bar{\sigma}'_a = (\bar{\sigma}_a^2 + 3\bar{\tau}_a^2)^{1/2} = [14.5^2 + 3(0)^2]^{1/2} = 14.5 \text{ kpsi}$$

$$\bar{\sigma}'_m = (\bar{\sigma}_m^2 + 3\bar{\tau}_m^2)^{1/2} = [0 + 3(6.66)^2]^{1/2} = 11.54 \text{ kpsi}$$

$$r = \frac{\bar{\sigma}'_a}{\bar{\sigma}'_m} = \frac{14.5}{11.54} = 1.26$$

Strength: From Eqs. (6–80) and (6–81),

$$\bar{S}_a = \frac{1.26^2 86.2^2}{2(31.1)} \left\{ -1 + \sqrt{1 + \left[ \frac{2(31.1)}{1.26(86.2)} \right]^2} \right\} = 28.9 \text{ kpsi}$$



$$C_{Sa} = \frac{(1 + 0.045)^2}{1 + 0.150} \frac{-1 + \sqrt{1 + \left[ \frac{2(31.1)(1 + 0.15)}{1.26(86.2)(1 + 0.045)} \right]^2}}{-1 + \sqrt{1 + \left[ \frac{2(31.1)}{1.26(86.2)} \right]^2}} - 1 = 0.134$$

*Reliability:* Since  $S_a = 28.9\text{LN}(1, 0.134)$  kpsi and  $\sigma'_a = 14.5\text{LN}(1, 0.121)$  kpsi, Eq. (5-44), p. 242, gives

$$z = -\frac{\ln\left(\frac{\bar{S}_a}{\bar{\sigma}_a} \sqrt{\frac{1 + C_{\sigma_a}^2}{1 + C_{S_a}^2}}\right)}{\sqrt{\ln[(1 + C_{S_a}^2)(1 + C_{\sigma_a}^2)]}} = -\frac{\ln\left(\frac{28.9}{14.5} \sqrt{\frac{1 + 0.121^2}{1 + 0.134^2}}\right)}{\sqrt{\ln[(1 + 0.134^2)(1 + 0.121^2)]}} = -3.83$$

From Table A-10 the probability of failure is  $p_f = 0.000\,065$ , and the reliability is, against fatigue,

**Answer**

$$R = 1 - p_f = 1 - 0.000\,065 = 0.999\,935$$

The chance of first-cycle yielding is estimated by interfering  $S_y$  with  $\sigma'_{\max}$ . The quantity  $\sigma'_{\max}$  is formed from  $\sigma'_a + \sigma'_m$ . The mean of  $\sigma'_{\max}$  is  $\bar{\sigma}'_a + \bar{\sigma}'_m = 14.5 + 11.54 = 26.04$  kpsi. The coefficient of variation of the sum is 0.121, since both COVs are 0.121, thus  $C_{\sigma_{\max}} = 0.121$ . We interfere  $S_y = 56\text{LN}(1, 0.077)$  kpsi with  $\sigma'_{\max} = 26.04\text{LN}(1, 0.121)$  kpsi. The corresponding  $z$  variable is

$$z = -\frac{\ln\left(\frac{56}{26.04} \sqrt{\frac{1 + 0.121^2}{1 + 0.077^2}}\right)}{\sqrt{\ln[(1 + 0.077^2)(1 + 0.121^2)]}} = -5.39$$

which represents, from Table A-10, a probability of failure of approximately  $0.07358$  [which represents  $3.58(10^{-8})$ ] of first-cycle yield in the fillet.

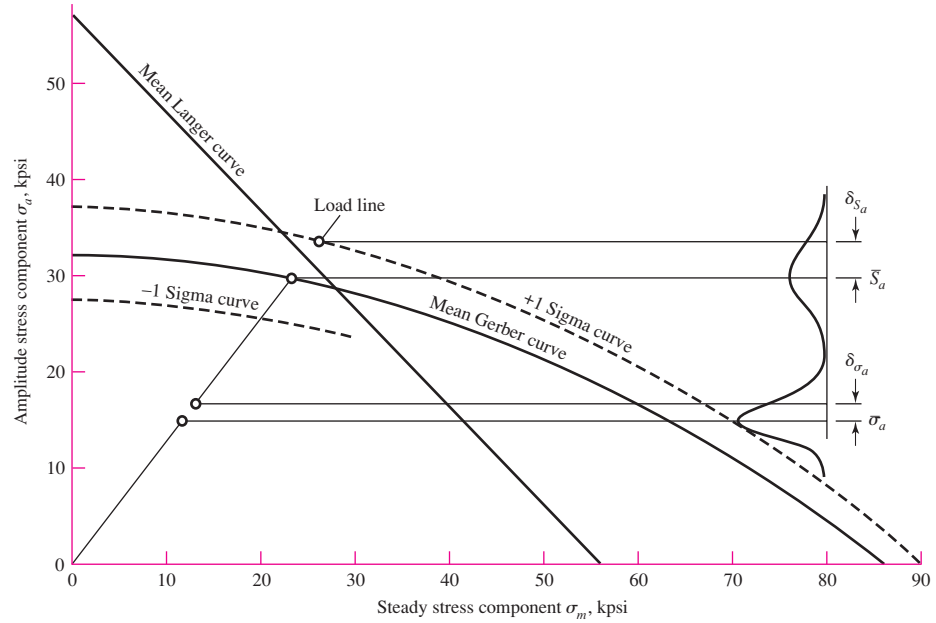
The probability of observing a fatigue failure exceeds the probability of a yield failure, something a deterministic analysis does not foresee and in fact could lead one to expect a yield failure should a failure occur. Look at the  $\sigma'_a S_a$  interference and the  $\sigma'_{\max} S_y$  interference and examine the  $z$  expressions. These control the relative probabilities. A deterministic analysis is oblivious to this and can mislead. Check your statistics text for events that are not mutually exclusive, but are independent, to quantify the probability of failure:

$$\begin{aligned} p_f &= p(\text{yield}) + p(\text{fatigue}) - p(\text{yield and fatigue}) \\ &= p(\text{yield}) + p(\text{fatigue}) - p(\text{yield})p(\text{fatigue}) \\ &= 0.358(10^{-7}) + 0.65(10^{-4}) - 0.358(10^{-7})0.65(10^{-4}) = 0.650(10^{-4}) \\ R &= 1 - 0.650(10^{-4}) = 0.999\,935 \end{aligned}$$

against either or both modes of failure.

**Figure 6-38**

Designer's fatigue diagram  
for Ex. 6-20.



Examine Fig. 6-38, which depicts the results of Ex. 6-20. The problem distribution of  $S_e$  was compounded of historical experience with  $S'_e$  and the uncertainty manifestations due to features requiring Marin considerations. The Gerber “failure zone” displays this. The interference with load-induced stress predicts the risk of failure. If additional information is known (R. R. Moore testing, with or without Marin features), the stochastic Gerber can accommodate to the information. Usually, the accommodation to additional test information is movement and contraction of the failure zone. In its own way the stochastic failure model accomplishes more precisely what the deterministic models and conservative postures intend. Additionally, stochastic models can estimate the probability of failure, something a deterministic approach cannot address.

### The Design Factor in Fatigue

The designer, in envisioning how to execute the geometry of a part subject to the imposed constraints, can begin making a priori decisions without realizing the impact on the design task. Now is the time to note how these things are related to the reliability goal.

The mean value of the design factor is given by Eq. (5-45), repeated here as

$$\bar{n} = \exp \left[ -z \sqrt{\ln(1 + C_n^2)} + \ln \sqrt{1 + C_n^2} \right] \doteq \exp[C_n(-z + C_n/2)] \quad (6-88)$$

in which, from Table 20-6 for the quotient  $\mathbf{n} = \mathbf{S}/\boldsymbol{\sigma}$ ,

$$C_n = \sqrt{\frac{C_S^2 + C_\sigma^2}{1 + C_\sigma^2}}$$

where  $C_S$  is the COV of the significant strength and  $C_\sigma$  is the COV of the significant stress at the critical location. Note that  $\bar{n}$  is a function of the reliability goal (through  $z$ ) and the COVs of the strength and stress. There are no means present, just measures of variability. The nature of  $C_S$  in a fatigue situation may be  $C_{Se}$  for fully reversed loading, or  $C_{Sa}$  otherwise. Also, experience shows  $C_{Se} > C_{Sa} > C_{Sut}$ , so  $C_{Se}$  can be used as a conservative estimate of  $C_{Sa}$ . If the loading is bending or axial, the form of

$\sigma'_a$  might be

$$\sigma'_a = K_f \frac{M_a c}{I} \quad \text{or} \quad \sigma'_a = K_f \frac{F}{A}$$

respectively. This makes the COV of  $\sigma'_a$ , namely  $C_{\sigma'_a}$ , expressible as

$$C_{\sigma'_a} = (C_{K_f}^2 + C_F^2)^{1/2}$$

again a function of variabilities. The COV of  $S_e$ , namely  $C_{S_e}$ , is

$$C_{S_e} = (C_{k_a}^2 + C_{k_c}^2 + C_{k_d}^2 + C_{k_f}^2 + C_{S_e'}^2)^{1/2}$$

again, a function of variabilities. An example will be useful.

### EXAMPLE 6-21

A strap to be made from a cold-drawn steel strip workpiece is to carry a fully reversed axial load  $F = \text{LN}(1000, 120)$  lbf as shown in Fig. 6-39. Consideration of adjacent parts established the geometry as shown in the figure, except for the thickness  $t$ . Make a decision as to the magnitude of the design factor if the reliability goal is to be 0.999 95, then make a decision as to the workpiece thickness  $t$ .

#### Solution

Let us take each a priori decision and note the consequence:

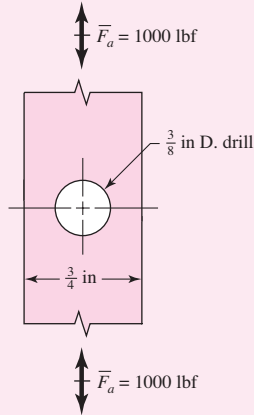


**Figure 6-39**

A strap with a thickness  $t$  is subjected to a fully reversed axial load of 1000 lbf. Example 6-21 considers the thickness necessary to attain a reliability of 0.999 95 against a fatigue failure.

#### A Priori Decision

#### Consequence

Use 1018 CD steel

$$\bar{S}_{ut} = 87.6 \text{ kpsi}, C_{S_{ut}} = 0.0655$$

Function:

Carry axial load

$$C_F = 0.12, C_{k_c} = 0.125$$

$R \geq 0.999\ 95$

$$z = -3.891$$

Machined surfaces

$$C_{k_a} = 0.058$$

Hole critical

$$C_{K_f} = 0.10, C_{\sigma'_a} = (0.10^2 + 0.12^2)^{1/2} = 0.156$$

Ambient temperature

$$C_{k_d} = 0$$

Correlation method

$$C_{S_e} = 0.138$$

Hole drilled

$$C_{S_e} = (0.058^2 + 0.125^2 + 0.138^2)^{1/2} = 0.195$$

$$C_n = \sqrt{\frac{C_{S_e}^2 + C_{\sigma'_a}^2}{1 + C_{\sigma'_a}^2}} = \sqrt{\frac{0.195^2 + 0.156^2}{1 + 0.156^2}} = 0.2467$$

$$\bar{n} = \exp \left[ -(-3.891) \sqrt{\ln(1 + 0.2467^2)} + \ln \sqrt{1 + 0.2467^2} \right] = 2.65$$

These eight a priori decisions have quantified the mean design factor as  $\bar{n} = 2.65$ . Proceeding deterministically hereafter we write

$$\sigma'_a = \frac{\bar{S}_e}{\bar{n}} = \bar{K}_f \frac{\bar{F}}{(w - d)t}$$

from which

$$t = \frac{\bar{K}_f \bar{n} \bar{F}}{(w - d) \bar{S}_e} \quad (1)$$

To evaluate the preceding equation we need  $\bar{S}_e$  and  $\bar{K}_f$ . The Marin factors are

$$\mathbf{k}_a = 2.67\bar{S}_{ut}^{-0.265}\mathbf{LN}(1, 0.058) = 2.67(87.6)^{-0.265}\mathbf{LN}(1, 0.058)$$

$$\bar{k}_a = 0.816$$

$$k_b = 1$$

$$\mathbf{k}_c = 1.23\bar{S}_{ut}^{-0.078}\mathbf{LN}(1, 0.125) = 0.868\mathbf{LN}(1, 0.125)$$

$$\bar{k}_c = 0.868$$

$$\bar{k}_d = \bar{k}_f = 1$$

and the endurance strength is

$$\bar{S}_e = 0.816(1)(0.868)(1)(1)0.506(87.6) = 31.4 \text{ kpsi}$$

The hole governs. From Table A-15-1 we find  $d/w = 0.50$ , therefore  $K_t = 2.18$ . From Table 6-15  $\sqrt{a} = 5/\bar{S}_{ut} = 5/87.6 = 0.0571$ ,  $r = 0.1875$  in. From Eq. (6-78) the fatigue stress concentration factor is

$$\bar{K}_f = \frac{2.18}{1 + \frac{2(2.18 - 1)}{2.18} \frac{0.0571}{\sqrt{0.1875}}} = 1.91$$

The thickness  $t$  can now be determined from Eq. (1)

$$t \geq \frac{\bar{K}_f \bar{n} \bar{F}}{(w - d)S_e} = \frac{1.91(2.65)1000}{(0.75 - 0.375)31\,400} = 0.430 \text{ in}$$

Use  $\frac{1}{2}$ -in-thick strap for the workpiece. The  $\frac{1}{2}$ -in thickness attains and, in the rounding to available nominal size, exceeds the reliability goal.

The example demonstrates that, for a given reliability goal, the fatigue design factor that facilitates its attainment is decided by the variabilities of the situation. Furthermore, the necessary design factor is not a constant independent of the way the concept unfolds. Rather, it is a function of a number of seemingly unrelated a priori decisions that are made in giving definition to the concept. The involvement of stochastic methodology can be limited to defining the necessary design factor. In particular, in the example, the design factor is not a function of the design variable  $t$ ; rather,  $t$  follows from the design factor.

## 6-18 Road Maps and Important Design Equations for the Stress-Life Method

As stated in Sec. 6-15, there are three categories of fatigue problems. The important procedures and equations for deterministic stress-life problems are presented here.

### Completely Reversing Simple Loading

- 1 Determine  $S'_e$  either from test data or

$$\text{p. 274} \quad S'_e = \begin{cases} 0.5S_{ut} & S_{ut} \leq 200 \text{ kpsi (1400 MPa)} \\ 100 \text{ kpsi} & S_{ut} > 200 \text{ kpsi} \\ 700 \text{ MPa} & S_{ut} > 1400 \text{ MPa} \end{cases} \quad (6-8)$$

2 Modify  $S'_e$  to determine  $S_e$ .

p. 279 
$$S_e = k_a k_b k_c k_d k_e k_f S'_e \quad (6-18)$$

$$k_a = a S_{ut}^b \quad (6-19)$$

**Table 6-2**

Parameters for Marin  
Surface Modification  
Factor, Eq. (6-19)

Surface Finish	Factor $a$		Exponent $b$
	$S_{ut}$ , kpsi	$S_{ut}$ , MPa	
Ground	1.34	1.58	-0.085
Machined or cold-drawn	2.70	4.51	-0.265
Hot-rolled	14.4	57.7	-0.718
As-forged	39.9	272.	-0.995

**Rotating shaft.** For bending or torsion,

p. 280 
$$k_b = \begin{cases} (d/0.3)^{-0.107} = 0.879d^{-0.107} & 0.11 \leq d \leq 2 \text{ in} \\ 0.91d^{-0.157} & 2 < d \leq 10 \text{ in} \\ (d/7.62)^{-0.107} = 1.24d^{-0.107} & 2.79 \leq d \leq 51 \text{ mm} \\ 1.51d^{-0.157} & 51 < 254 \text{ mm} \end{cases} \quad (6-20)$$

For axial,

$$k_b = 1 \quad (6-21)$$

**Nonrotating member.** Use Table 6-3, p. 282, for  $d_e$  and substitute into Eq. (6-20) for  $d$ .

p. 282 
$$k_c = \begin{cases} 1 & \text{bending} \\ 0.85 & \text{axial} \\ 0.59 & \text{torsion} \end{cases} \quad (6-26)$$

p. 283 Use Table 6-4 or

$$k_d = 0.975 + 0.432(10^{-3})T_F - 0.115(10^{-5})T_F^2 \\ + 0.104(10^{-8})T_F^3 - 0.595(10^{-12})T_F^4 \quad (6-27)$$

pp. 284-285,  $k_e$

**Table 6-5**

Reliability Factors  $k_e$   
Corresponding to  
8 Percent Standard  
Deviation of the  
Endurance Limit

Reliability, %	Transformation Variate $z_a$	Reliability Factor $k_e$
50	0	1.000
90	1.288	0.897
95	1.645	0.868
99	2.326	0.814
99.9	3.091	0.753
99.99	3.719	0.702
99.999	4.265	0.659
99.9999	4.753	0.620

pp. 285–286,  $k_f$

- 3** Determine fatigue stress-concentration factor,  $K_f$  or  $K_{fs}$ . First, find  $K_t$  or  $K_{ts}$  from Table A–15.

p. 287 
$$K_f = 1 + q(K_t - 1) \quad \text{or} \quad K_{fs} = 1 + q(K_{ts} - 1) \quad (6-32)$$

Obtain  $q$  from either Fig. 6–20 or 6–21, pp. 287–288.

Alternatively, for reversed bending or axial loads,

p. 288 
$$K_f = 1 + \frac{K_t - 1}{1 + \sqrt{a/r}} \quad (6-33)$$

For  $S_{ut}$  in kpsi,

$$\begin{aligned} \sqrt{a} = & 0.245\,799 - 0.307\,794(10^{-2})S_{ut} \\ & + 0.150\,874(10^{-4})S_{ut}^2 - 0.266\,978(10^{-7})S_{ut}^3 \end{aligned} \quad (6-35)$$

For torsion for low-alloy steels, increase  $S_{ut}$  by 20 kpsi and apply to Eq. (6–35).

- 4** Apply  $K_f$  or  $K_{fs}$  by *either* dividing  $S_e$  by it *or* multiplying it with the purely reversing stress *not* both.

- 5** Determine fatigue life constants  $a$  and  $b$ . If  $S_{ut} \geq 70$  kpsi, determine  $f$  from Fig. 6–18, p. 277. If  $S_{ut} < 70$  kpsi, let  $f = 0.9$ .

p. 277 
$$a = (f S_{ut})^2 / S_e \quad (6-14)$$

$$b = -[\log(f S_{ut}/S_e)]/3 \quad (6-15)$$

- 6** Determine fatigue strength  $S_f$  at  $N$  cycles, or,  $N$  cycles to failure at a reversing stress  $\sigma_a$

(Note: this only applies to purely reversing stresses where  $\sigma_m = 0$ ).

p. 277 
$$S_f = aN^b \quad (6-13)$$

$$N = (\sigma_a/a)^{1/b} \quad (6-16)$$

### Fluctuating Simple Loading

For  $S_e$ ,  $K_f$  or  $K_{fs}$ , see previous subsection.

- 1** Calculate  $\sigma_m$  and  $\sigma_a$ . Apply  $K_f$  to both stresses.

p. 293 
$$\sigma_m = (\sigma_{\max} + \sigma_{\min})/2 \quad \sigma_a = |\sigma_{\max} - \sigma_{\min}|/2 \quad (6-36)$$

- 2** Apply to a fatigue failure criterion, p. 298

$$\sigma_m \geq 0$$

**Soderburg** 
$$\sigma_a/S_e + \sigma_m/S_y = 1/n \quad (6-45)$$

**mod-Goodman** 
$$\sigma_a/S_e + \sigma_m/S_{ut} = 1/n \quad (6-46)$$

**Gerber** 
$$n\sigma_a/S_e + (n\sigma_m/S_{ut})^2 = 1 \quad (6-47)$$

**ASME-elliptic** 
$$(\sigma_a/S_e)^2 + (\sigma_m/S_{ut})^2 = 1/n^2 \quad (6-48)$$

$$\sigma_m < 0$$

p. 297 
$$\sigma_a = S_e/n$$

**Torsion.** Use the same equations as apply for  $\sigma_m \geq 0$ , except replace  $\sigma_m$  and  $\sigma_a$  with  $\tau_m$  and  $\tau_a$ , use  $k_c = 0.59$  for  $S_e$ , replace  $S_{ut}$  with  $S_{su} = 0.67S_{ut}$  [Eq. (6-54), p. 309], and replace  $S_y$  with  $S_{sy} = 0.577S_y$  [Eq. (5-21), p. 217]

**3** Check for localized yielding.

p. 296  $\sigma_a + \sigma_m = S_y/n$  (6-49)

or, for torsion,  $\tau_a + \tau_m = 0.577S_y/n$

**4** For finite-life fatigue strength (see Ex. 6-12, pp. 305-306),

$$\text{mod-Goodman} \quad S_f = \frac{\sigma_a}{1 - (\sigma_m/S_{ut})}$$

$$\text{Gerber} \quad S_f = \frac{\sigma_a}{1 - (\sigma_m/S_{ut})^2}$$

If determining the finite life  $N$  with a factor of safety  $n$ , substitute  $S_f/n$  for  $\sigma_a$  in Eq. (6-16). That is,

$$N = \left( \frac{S_f/n}{a} \right)^{1/b}$$

### Combination of Loading Modes

See previous subsections for earlier definitions.

- 1** Calculate von Mises stresses for alternating and midrange stress states,  $\sigma'_a$  and  $\sigma'_m$ . When determining  $S_e$ , do not use  $k_c$  nor divide by  $K_f$  or  $K_{fs}$ . Apply  $K_f$  and/or  $K_{fs}$  directly to each specific alternating and midrange stress. If axial stress is present divide the alternating axial stress by  $k_c = 0.85$ . For the special case of combined bending, torsional shear, and axial stresses

p. 310

$$\sigma'_a = \left\{ \left[ (K_f)_{bending}(\sigma_a)_{bending} + (K_f)_{axial} \frac{(\sigma_a)_{axial}}{0.85} \right]^2 + 3 \left[ (K_{fs})_{torsion}(\tau_a)_{torsion} \right]^2 \right\}^{1/2} \quad (6-55)$$

$$\sigma'_m = \left\{ \left[ (K_f)_{bending}(\sigma_m)_{bending} + (K_f)_{axial}(\sigma_m)_{axial} \right]^2 + 3 \left[ (K_{fs})_{torsion}(\tau_m)_{torsion} \right]^2 \right\}^{1/2} \quad (6-56)$$

- 2** Apply stresses to fatigue criterion [see Eq. (6-45) to (6-48), p. 338 in previous subsection].

- 3** Conservative check for localized yielding using von Mises stresses.

p. 298  $\sigma'_a + \sigma'_m = S_y/n$  (6-49)

## PROBLEMS

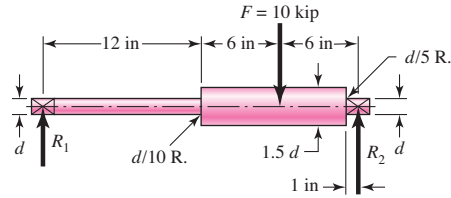
Problems 6–1 to 6–31 are to be solved by deterministic methods. Problems 6–32 to 6–38 are to be solved by stochastic methods. Problems 6–39 to 6–46 are computer problems.

### Deterministic Problems

- 6–1** A  $\frac{1}{4}$ -in drill rod was heat-treated and ground. The measured hardness was found to be 490 Brinell. Estimate the endurance strength if the rod is used in rotating bending.
- 6–2** Estimate  $S'_e$  for the following materials:  
 (a) AISI 1020 CD steel.  
 (b) AISI 1080 HR steel.  
 (c) 2024 T3 aluminum.  
 (d) AISI 4340 steel heat-treated to a tensile strength of 250 kpsi.
- 6–3** Estimate the fatigue strength of a rotating-beam specimen made of AISI 1020 hot-rolled steel corresponding to a life of 12.5 kilocycles of stress reversal. Also, estimate the life of the specimen corresponding to a stress amplitude of 36 kpsi. The known properties are  $S_{ut} = 66.2$  kpsi,  $\sigma_0 = 115$  kpsi,  $m = 0.22$ , and  $\varepsilon_f = 0.90$ .
- 6–4** Derive Eq. (6–17). For the specimen of Prob. 6–3, estimate the strength corresponding to 500 cycles.
- 6–5** For the interval  $10^3 \leq N \leq 10^6$  cycles, develop an expression for the axial fatigue strength  $(S'_f)_{ax}$  for the polished specimens of 4130 used to obtain Fig. 6–10. The ultimate strength is  $S_{ut} = 125$  kpsi and the endurance limit is  $(S'_e)_{ax} = 50$  kpsi.
- 6–6** Estimate the endurance strength of a 32-mm-diameter rod of AISI 1035 steel having a machined finish and heat-treated to a tensile strength of 710 MPa.
- 6–7** Two steels are being considered for manufacture of as-forged connecting rods. One is AISI 4340 Cr-Mo-Ni steel capable of being heat-treated to a tensile strength of 260 kpsi. The other is a plain carbon steel AISI 1040 with an attainable  $S_{ut}$  of 113 kpsi. If each rod is to have a size giving an equivalent diameter  $d_e$  of 0.75 in, is there any advantage to using the alloy steel for this fatigue application?
- 6–8** A solid round bar, 25 mm in diameter, has a groove 2.5-mm deep with a 2.5-mm radius machined into it. The bar is made of AISI 1018 CD steel and is subjected to a purely reversing torque of  $200 \text{ N} \cdot \text{m}$ . For the  $S$ - $N$  curve of this material, let  $f = 0.9$ .  
 (a) Estimate the number of cycles to failure.  
 (b) If the bar is also placed in an environment with a temperature of  $450^\circ\text{C}$ , estimate the number of cycles to failure.
- 6–9** A solid square rod is cantilevered at one end. The rod is 0.8 m long and supports a completely reversing transverse load at the other end of  $\pm 1$  kN. The material is AISI 1045 hot-rolled steel. If the rod must support this load for  $10^4$  cycles with a factor of safety of 1.5, what dimension should the square cross section have? Neglect any stress concentrations at the support end and assume that  $f = 0.9$ .
- 6–10** A rectangular bar is cut from an AISI 1018 cold-drawn steel flat. The bar is 60 mm wide by 10 mm thick and has a 12-mm hole drilled through the center as depicted in Table A–15–1. The bar is concentrically loaded in push-pull fatigue by axial forces  $F_a$ , uniformly distributed across the width. Using a design factor of  $n_d = 1.8$ , estimate the largest force  $F_a$  that can be applied ignoring column action.
- 6–11** Bearing reactions  $R_1$  and  $R_2$  are exerted on the shaft shown in the figure, which rotates at 1150 rev/min and supports a 10-kip bending force. Use a 1095 HR steel. Specify a diameter  $d$  using a design factor of  $n_d = 1.6$  for a life of 3 min. The surfaces are machined.



Problem 6-11



- 6-12** A bar of steel has the minimum properties  $S_e = 276$  MPa,  $S_y = 413$  MPa, and  $S_{ut} = 551$  MPa. The bar is subjected to a steady torsional stress of 103 MPa and an alternating bending stress of 172 MPa. Find the factor of safety guarding against a static failure, and either the factor of safety guarding against a fatigue failure or the expected life of the part. For the fatigue analysis use:
- Modified Goodman criterion.
  - Gerber criterion.
  - ASME-elliptic criterion.

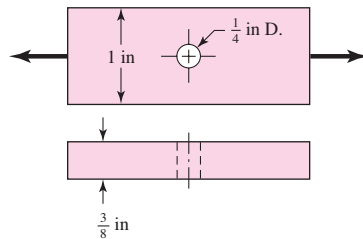
- 6-13** Repeat Prob. 6-12 but with a steady torsional stress of 138 MPa and an alternating bending stress of 69 MPa.

- 6-14** Repeat Prob. 6-12 but with a steady torsional stress of 103 MPa, an alternating torsional stress of 69 MPa, and an alternating bending stress of 83 MPa.

- 6-15** Repeat Prob. 6-12 but with an alternating torsional stress of 207 MPa.

- 6-16** Repeat Prob. 6-12 but with an alternating torsional stress of 103 MPa and a steady bending stress of 103 MPa.

- 6-17** The cold-drawn AISI 1018 steel bar shown in the figure is subjected to an axial load fluctuating between 800 and 3000 lbf. Estimate the factors of safety  $n_y$  and  $n_f$  using (a) a Gerber fatigue failure criterion as part of the designer's fatigue diagram, and (b) an ASME-elliptic fatigue failure criterion as part of the designer's fatigue diagram.



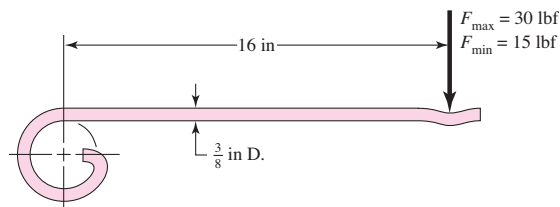
Problem 6-17

- 6-18** Repeat Prob. 6-17, with the load fluctuating between  $-800$  and  $3000$  lbf. Assume no buckling.

- 6-19** Repeat Prob. 6-17, with the load fluctuating between  $800$  and  $-3000$  lbf. Assume no buckling.

- 6-20** The figure shows a formed round-wire cantilever spring subjected to a varying force. The hardness tests made on 25 springs gave a minimum hardness of 380 Brinell. It is apparent from the mounting details that there is no stress concentration. A visual inspection of the springs indicates

Problem 6-20



that the surface finish corresponds closely to a hot-rolled finish. What number of applications is likely to cause failure? Solve using:

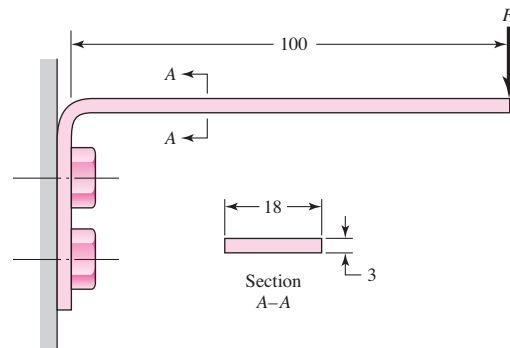
- Modified Goodman criterion.
- Gerber criterion.

### 6-21

The figure is a drawing of a 3- by 18-mm latching spring. A preload is obtained during assembly by shimming under the bolts to obtain an estimated initial deflection of 2 mm. The latching operation itself requires an additional deflection of exactly 4 mm. The material is ground high-carbon steel, bent then hardened and tempered to a minimum hardness of 490 Bhn. The radius of the bend is 3 mm. Estimate the yield strength to be 90 percent of the ultimate strength.

- Find the maximum and minimum latching forces.
- Is it likely the spring will fail in fatigue? Use the Gerber criterion.

Problem 6-21  
Dimensions in millimeters



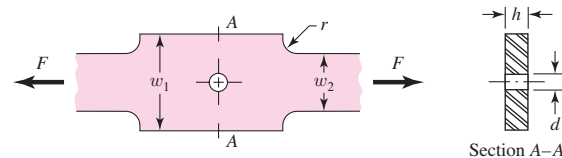
### 6-22

Repeat Prob. 6-21, part *b*, using the modified Goodman criterion.

### 6-23

The figure shows the free-body diagram of a connecting-link portion having stress concentration at three sections. The dimensions are  $r = 0.25$  in,  $d = 0.75$  in,  $h = 0.50$  in,  $w_1 = 3.75$  in, and  $w_2 = 2.5$  in. The forces  $F$  fluctuate between a tension of 4 kip and a compression of 16 kip. Neglect column action and find the least factor of safety if the material is cold-drawn AISI 1018 steel.

Problem 6-23

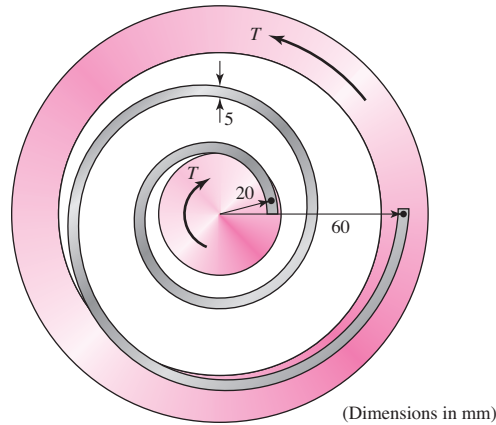


### 6-24

The torsional coupling in the figure is composed of a curved beam of square cross section that is welded to an input shaft and output plate. A torque is applied to the shaft and cycles from zero to  $T$ . The cross section of the beam has dimensions of 5 by 5 mm, and the centroidal axis of the beam describes a curve of the form  $r = 20 + 10\theta/\pi$ , where  $r$  and  $\theta$  are in mm and radians, respectively ( $0 \leq \theta \leq 4\pi$ ). The curved beam has a machined surface with yield and ultimate strength values of 420 and 770 MPa, respectively.

- Determine the maximum allowable value of  $T$  such that the coupling will have an infinite life with a factor of safety,  $n = 3$ , using the modified Goodman criterion.
- Repeat part (a) using the Gerber criterion.
- Using  $T$  found in part (b), determine the factor of safety guarding against yield.

Problem 6–24

**6–25**

Repeat Prob. 6–24 ignoring curvature effects on the bending stress.

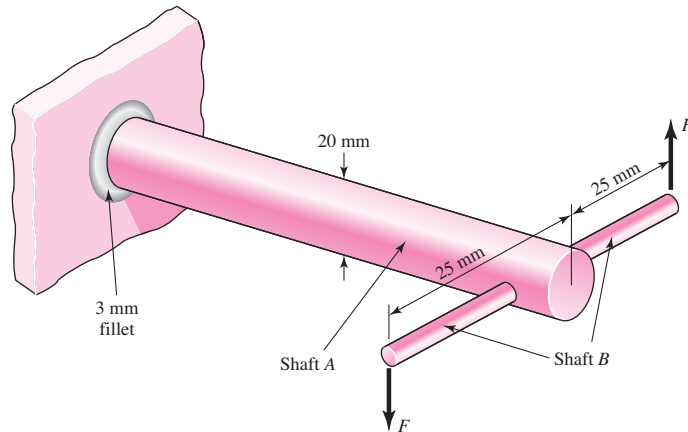
**6–26**

In the figure shown, shaft A, made of AISI 1010 hot-rolled steel, is welded to a fixed support and is subjected to loading by equal and opposite forces  $F$  via shaft B. A theoretical stress concentration  $K_{ts}$  of 1.6 is induced by the 3-mm fillet. The length of shaft A from the fixed support to the connection at shaft B is 1 m. The load  $F$  cycles from 0.5 to 2 kN.

(a) For shaft A, find the factor of safety for infinite life using the modified Goodman fatigue failure criterion.

(b) Repeat part (a) using the Gerber fatigue failure criterion.

Problem 6–26

**6–27**

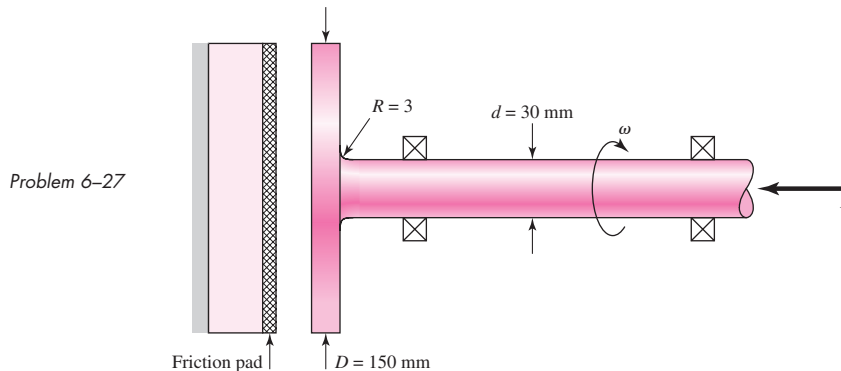
A schematic of a clutch-testing machine is shown. The steel shaft rotates at a constant speed  $\omega$ . An axial load is applied to the shaft and is cycled from zero to  $P$ . The torque  $T$  induced by the clutch face onto the shaft is given by

$$T = \frac{fP(D+d)}{4}$$

where  $D$  and  $d$  are defined in the figure and  $f$  is the coefficient of friction of the clutch face. The shaft is machined with  $S_y = 800$  MPa and  $S_{ut} = 1000$  MPa. The theoretical stress concentration factors for the fillet are 3.0 and 1.8 for the axial and torsional loading, respectively.

(a) Assume the load variation  $P$  is synchronous with shaft rotation. With  $f = 0.3$ , find the maximum allowable load  $P$  such that the shaft will survive a minimum of  $10^6$  cycles with a factor of safety of 3. Use the modified Goodman criterion. Determine the corresponding factor of safety guarding against yielding.

- (b) Suppose the shaft is not rotating, but the load  $P$  is cycled as shown. With  $f = 0.3$ , find the maximum allowable load  $P$  so that the shaft will survive a minimum of  $10^6$  cycles with a factor of safety of 3. Use the modified Goodman criterion. Determine the corresponding factor of safety guarding against yielding.



- 6-28** For the clutch of Prob. 6-27, the external load  $P$  is cycled between 20 kN and 80 kN. Assuming that the shaft is rotating synchronous with the external load cycle, estimate the number of cycles to failure. Use the modified Goodman fatigue failure criteria.
- 6-29** A flat leaf spring has fluctuating stress of  $\sigma_{\max} = 420$  MPa and  $\sigma_{\min} = 140$  MPa applied for  $5 (10^4)$  cycles. If the load changes to  $\sigma_{\max} = 350$  MPa and  $\sigma_{\min} = -200$  MPa, how many cycles should the spring survive? The material is AISI 1040 CD and has a fully corrected endurance strength of  $S_e = 200$  MPa. Assume that  $f = 0.9$ .
- (a) Use Miner's method.  
(b) Use Manson's method.
- 6-30** A machine part will be cycled at  $\pm 48$  kpsi for  $4 (10^3)$  cycles. Then the loading will be changed to  $\pm 38$  kpsi for  $6 (10^4)$  cycles. Finally, the load will be changed to  $\pm 32$  kpsi. How many cycles of operation can be expected at this stress level? For the part,  $S_{ut} = 76$  kpsi,  $f = 0.9$ , and has a fully corrected endurance strength of  $S_e = 30$  kpsi.
- (a) Use Miner's method.  
(b) Use Manson's method.
- 6-31** A rotating-beam specimen with an endurance limit of 50 kpsi and an ultimate strength of 100 kpsi is cycled 20 percent of the time at 70 kpsi, 50 percent at 55 kpsi, and 30 percent at 40 kpsi. Let  $f = 0.9$  and estimate the number of cycles to failure.

### Stochastic Problems

- 6-32** Solve Prob. 6-1 if the ultimate strength of production pieces is found to be  $S_{ut} = 245\text{LN}(1, 0.0508)$  kpsi.
- 6-33** The situation is similar to that of Prob. 6-10 wherein the imposed completely reversed axial load  $F_a = 15\text{LN}(1, 0.20)$  kN is to be carried by the link with a thickness to be specified by you, the designer. Use the 1018 cold-drawn steel of Prob. 6-10 with  $S_{ut} = 440\text{LN}(1, 0.30)$  MPa and  $S_{yt} = 370\text{LN}(1, 0.061)$ . The reliability goal must exceed 0.999. Using the correlation method, specify the thickness  $t$ .
- 6-34** A solid round steel bar is machined to a diameter of 1.25 in. A groove  $\frac{1}{8}$  in deep with a radius of  $\frac{1}{8}$  in is cut into the bar. The material has a mean tensile strength of 110 kpsi. A completely reversed bending moment  $M = 1400$  lbf · in is applied. Estimate the reliability. The size factor should be based on the gross diameter. The bar rotates.

- 6-35** Repeat Prob. 6-34, with a completely reversed torsional moment of  $T = 1400 \text{ lbf} \cdot \text{in}$  applied.
- 6-36** A  $1\frac{1}{4}$ -in-diameter hot-rolled steel bar has a  $\frac{1}{8}$ -in diameter hole drilled transversely through it. The bar is nonrotating and is subject to a completely reversed bending moment of  $M = 1600 \text{ lbf} \cdot \text{in}$  in the same plane as the axis of the transverse hole. The material has a mean tensile strength of 58 kpsi. Estimate the reliability. The size factor should be based on the gross size. Use Table A-16 for  $K_t$ .
- 6-37** Repeat Prob. 6-36, with the bar subject to a completely reversed torsional moment of  $2400 \text{ lbf} \cdot \text{in}$ .
- 6-38** The plan view of a link is the same as in Prob. 6-23; however, the forces  $F$  are completely reversed, the reliability goal is 0.998, and the material properties are  $S_{ut} = 64\text{LN}(1, 0.045)$  kpsi and  $S_y = 54\text{LN}(1, 0.077)$  kpsi. Treat  $F_a$  as deterministic, and specify the thickness  $h$ .

### Computer Problems

- 6-39** A  $\frac{1}{4}$  by  $1\frac{1}{2}$ -in steel bar has a  $\frac{3}{4}$ -in drilled hole located in the center, much as is shown in Table A-15-1. The bar is subjected to a completely reversed axial load with a deterministic load of 1200 lbf. The material has a mean ultimate tensile strength of  $\bar{S}_{ut} = 80$  kpsi.
- Estimate the reliability.
  - Conduct a computer simulation to confirm your answer to part *a*.
- 6-40** From your experience with Prob. 6-39 and Ex. 6-19, you observed that for completely reversed axial and bending fatigue, it is possible to
- Observe the COVs associated with a priori design considerations.
  - Note the reliability goal.
  - Find the mean design factor  $\bar{n}_d$  which will permit making a geometric design decision that will attain the goal using deterministic methods in conjunction with  $\bar{n}_d$ .
- Formulate an interactive computer program that will enable the user to find  $\bar{n}_d$ . While the material properties  $S_{ut}$ ,  $S_y$ , and the load COV must be input by the user, all of the COVs associated with  $\Phi_{0.30}$ ,  $k_a$ ,  $k_c$ ,  $k_d$ , and  $K_f$  can be internal, and answers to questions will allow  $C_\sigma$  and  $C_S$ , as well as  $C_n$  and  $\bar{n}_d$ , to be calculated. Later you can add improvements. Test your program with problems you have already solved.
- 6-41** When using the Gerber fatigue failure criterion in a stochastic problem, Eqs. (6-80) and (6-81) are useful. They are also computationally complicated. It is helpful to have a computer subroutine or procedure that performs these calculations. When writing an executive program, and it is appropriate to find  $S_a$  and  $C_{Sa}$ , a simple call to the subroutine does this with a minimum of effort. Also, once the subroutine is tested, it is always ready to perform. Write and test such a program.
- 6-42** Repeat Problem. 6-41 for the ASME-elliptic fatigue failure locus, implementing Eqs. (6-82) and (6-83).
- 6-43** Repeat Prob. 6-41 for the Smith-Dolan fatigue failure locus, implementing Eqs. (6-86) and (6-87).
- 6-44** Write and test computer subroutines or procedures that will implement
- Table 6-2, returning  $a$ ,  $b$ ,  $C$ , and  $\bar{k}_a$ .
  - Equation (6-20) using Table 6-4, returning  $k_b$ .
  - Table 6-11, returning  $\alpha$ ,  $\beta$ ,  $C$ , and  $\bar{k}_c$ .
  - Equations (6-27) and (6-75), returning  $\bar{k}_d$  and  $C_{kd}$ .
- 6-45** Write and test a computer subroutine or procedure that implements Eqs. (6-76) and (6-77), returning  $\bar{q}$ ,  $\hat{\sigma}_q$ , and  $C_q$ .
- 6-46** Write and test a computer subroutine or procedure that implements Eq. (6-78) and Table 6-15, returning  $\sqrt{a}$ ,  $C_{Kf}$ , and  $\bar{K}_f$ .